A STUDY ON THE INTERACTION OF ALZHEIMER'S DISEASE ß AMYLOID PROTEIN WITH CULTURED MOUSE NEUROBLASTOMA CELL LINE NB41A3

A

THESIS

Presented to the Faculty
of the University of Alaska Fairbanks
in Partial Fulfillment of the Requirements
for the Degree of

DOCTOR OF PHILOSOPHY

By

Xiaohong Zhao, B.S., M.S.

Fairbanks, Alaska

December 1994

A STUDY ON THE INTERACTION OF ALZHEIMER'S DISEASE ß AMYLOID PROTEIN WITH CULTURED MOUSE NEUROBLASTOMA CELL LINE NB41A3

By

Xiaohong Zhao

RECOMMENDED:

Advisory Committee Chair

Department Head

APPROVED:

Dean, College of Natural Sciences

Dean, Graduate School

Dec. 20, 1994

Date

ABSTRACT

The ß amyloid protein is the primary constituent of amyloid plaques in the brains of Alzheimer's disease patients. The generation of ß amyloid protein from ß amyloid precursor protein and its interaction with neuronal cells were studied in the mouse neuroblastoma cell line NB41A3. Immunoreactivity to the carboxyl terminal of the precursor protein was detected among the membrane proteins of these cells, indicating that ß amyloid precursor protein is produced by NB41A3 cells. Also amyloid precursor protein carboxyl terminal immunoreactivity was observed in the conditioned medium of the cells, demonstrating various cytosolic peptide fragments are secreted during the cellular processing of the ß amyloid precursor protein. Synthetic ß amyloid peptide was shown to negatively affect NB41A3 neuroblastoma cells as judged by decreasing cell numbers, decreasing amount of cell protein, and release of the cytosolic enzyme, lactic dehydrogenase, into the medium. At the ultrastructural level, internal damage to the nucleus could be observed. Synthetic ß pepide showed specific binding with neuroblastoma cells. The internalization of the ß peptide into the cells suggest a direct mechanism for ß amyloid protein toxicity *in vivo*. This research contributes to the knowledge of the processing of Alzheimer's disease ß amyloid precursor protein in NB41A3 cells and demonstrates that NB41A3 cell provides a practical *in vitro* model for studying the mechanism of Alzheimer's disease and amyloid toxicity.

TABLE OF CONTENTS

LIST OF FIGURES

LIST OF TABLES

ACKNOWLEDGEMENT

I would like to express my great appreciation to my advisor, Dr. Lawrence K. Duffy. Without his constant support and encouragement, this dissertation would be impossible. I would also like to thank my committee members, Dr. Scott Smiley, Dr. F. Gerald Plumley, Dr. Edward J. Brown, and Dr. Joan Braddock for their help in my study and research. I am grateful to Kerry Irons for her help in the studies of electron microscopy and immunocytochemistry.

I would like to extend my thanks to other people in the Chemistry Department: Sheila Chapman, Marlys Schneider, and Linnea Delatour. Among my many helpful friends are my fellow students, Sandip Vyas and Sherry Smith, who offered me constant assistance in the lab and valuable discussions on the research. My thanks also go to Arthur Clark and Dr. Patricia Clark, who patiently smoothed the language of the dissertation and helped me to become comfortable with life in this society.

Chapter 1.

Introduction

Alzheimer's disease (AD) is the most common form of cerebral degeneration leading to dementia in elderly people. It is a late onset neurodegenerative disorder disease causing widespread functional disturbance of the human brain. The typical clinical presentation of AD is quite characteristic, with deficits in short term memory present early in the course of the disease. Eventually, the dementia spreads to affect language skills, abstract thinking, judgment, and visual-spatial orientation.

Alzheimer's disease occurs in two to four million individuals in the United States. It is estimated that AD afflicts 5 to 11 percent of the population over the age of 65 and as much as 47 percent of the population over the age of 85 (Yankner & Mesulam, 1991). The obvious impact of this fact on health care has stimulated interest in research aimed at understanding the etiology and pathogenesis of this disease.

Alzheimer's disease was first reported by Alzheimer in 1907. The abnormal amyloid deposits or amyloid plaques in certain areas of the brain of a

diseased patient have become the histopathological characteristic of Alzheimer's disease. Definitive diagnosis of Alzheimer's disease requires the confirmation of insoluble proteinaceous deposits in the brain by either autopsy or biopsy. There are two general types of deposits: 1) extracellular amyloid deposits in senile plaques and in cerebral blood vessels; and 2) intracellular neurofibrillary tangles in the cytoplasm of neurons (Terry & Katzman 1983; Glenner & Wong 1984). The reduction in the number of neurons and synapses, as well as the gradual accumulation of amyloid plaques and neurofibrillary tangles, occur predominantly in the frontal, temporal and parietal lobes, and in the amygdala and thalamus (Masliah *et al.*, 1989; Masliah *et al.*, 1991; Terry *et al.*, 1983; Hamos *et al.*, 1989). The observation that a reduction in the number of neurons accompanies a gradual accumulation of amyloid plaques in AD brains suggests a correlation between the degree of dementia and the number of plaques.

The extracellular amyloid plaque is composed of an amyloid core surrounded by dysfunctional neurites. Though many proteins are associated with these extracellular amyloid deposits, the primary constituent

of the plaque core that accounts for its fibrillar properties is a 4 kilodalton (Kd) protein, called ß amyloid protein (ßAP) or ß protein. Using a synthetic fragment of ß amyloid protein, ß1-40, and a cultured mouse neuroblastoma cell line NB41A3 as an experimental model, this research project investigates the interaction between individual cells and the ß amyloid protein. Will ß1-40 have a biological effect on cultured neuroblastoma cells? Does amyloid ß peptide interact with cells by binding to the cell surface? Or could amyloid ß peptide be internalized by cells?

This research will be described in six chapters. Chapter 2 will review the current research on ß amyloid protein and its role in neurodegeneration hypothesis in Alzheimer's disease. Chapters 3 - 5 each address a different aspect of this research project. Chapter 3 describes the process of the ß peptide synthesis and its purification. Chapter 4 shows the anti - ß amyloid precursor protein (ßAPP) immunoreactivities in cultured neuroblastoma cells, using antibodies raised against synthesized peptides. Chapter 5 reports on investigations involving the neurotoxic effects of ß1-40 and the mechanism of ß peptide - neuroblastoma interaction. Chapter 6 introduces the initial

experimental data of an ultrastructural study on cultured neuroblastoma cells. Chapter 7 summarizes the findings in this research project.

Chapter 2

ß Amyloid Protein, ß Amyloid Precursor Protein, and Alzheimer's Disease: a Review

The characteristic lesions in the brains of AD patients are intracellular as well as extracellular insoluble proteinaceous fibers called amyloid. Intracellular amyloid deposits are named neurofibrillary tangles, which consist of paired 10 nm filaments as seen under the electron microscope. The principle protein subunit in neuorofibrillary tangles is the microtubule-associated protein *tau*. On the other hand, extracellular amyloid deposits are called amyloid plaques or senile plaques, which contain amyloid cores surrounded by dysfunctional neurites. The major protein component of the amyloid core is identified as ß amyloid protein (ßAP).

2-1. Identification of ß amyloid protein and ß amyloid precursor protein

The major proteinaceous component of extracellular amyloid deposit in the AD brain was first identified in 1984. From cerebrovascular amyloid of an AD brain, Glenner and Wong (1984) isolated a 4200-dalton protein

which, studies indicated, was a major component of amyloid plaque. Monoclonal antibodies against this protein label both cerebrovascular and extracellular plaque amyloid, leaving little doubt that this protein is an intrinsic fibril component of amyloid deposits. This protein has been named ß amyloid protein or ß protein (ßAP). Amino acid sequencing data indicate that ßAP is a short peptide containing 42 to 43 amino acid residues. It is highly insoluble under physiological conditions, which accounts for amyloid deposits' fibrillar properties (Masters *et al.*, 1985a; 1985b). Knowledge of the amino acid sequence of ßAP has provided a means to isolate a full-length cDNA clone encoding a large ß amyloid protein precursor (ßAPP). Further sequencing studies indicate that this cDNA encodes a protein of 695 amino acid residues; therefore, it is referred as $ßAPP_{695}$. Near the carboxyl terminus of ßAPP is the ß amyloid protein region (Kang *et al.*, 1987).

2-2. ßAPP domain structure and ßAPP function

Soon after the ßAPP-encoding cDNA was isolated, Kang and colleagues proposed a domain structure of this protein based on its deduced amino acid sequence (Kang

et al., 1987). Assuming that translation starts at the first AUG of the cDNA clone, this ßAPP would contain 695 amino acid residues. As shown in Figure 2-1, the $ßAPP_{695}$ begins with a signal sequence of 17 amino acid residues for transporting the protein through the endoplasmic reticulum membrane (Dyrks *et al.*, 1988). Following the signal sequence is a cysteine-rich region, which might help stabilize the protein by forming disulfide bonds. The next hundred residues are extremely rich in negatively charged amino acids; this region contains 28 glutamic acids and 17 aspartic acids, but only one lysine and two arginines. The region from residue 290 to residue 597, the N-terminus of ßAP, contains two potential N-glycosylation sites. The amyloid ß protein sequence starts at residue 597 of the precursor, and terminates at residue 639, containing 42 to 43 amino acid residues. The first 28 amino acids at the N-terminus of ßAP are located in the extracellular domain of the precursor, while the last 15 residues are embedded within the cell membrane. The C-terminal cleavage of mature precursor during amyloidogenesis would have to occur within the membrane. The hydrophobic membrane spanning region

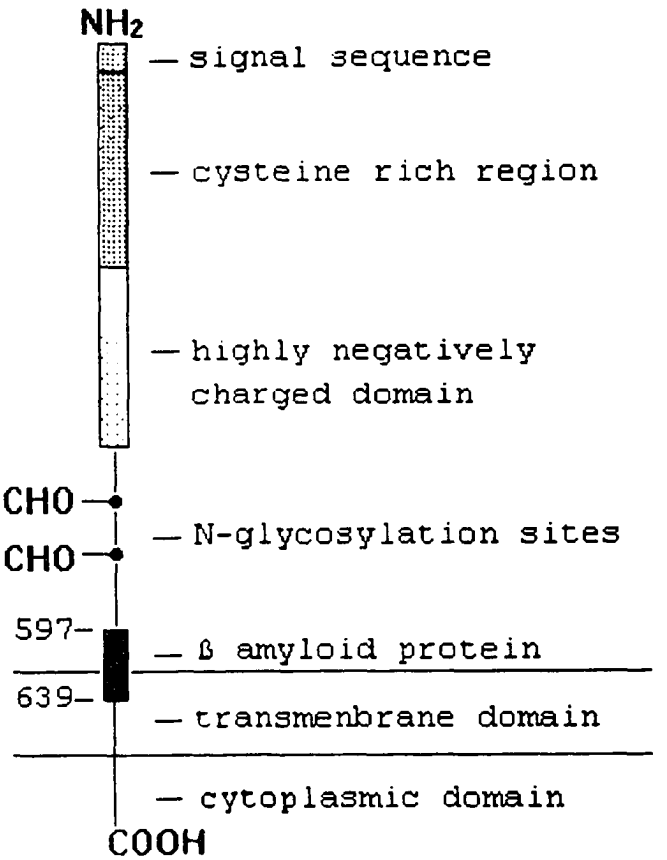

Figure 2-1. Domain structure of ßAPP695

starts at residue 624 and ends at residue 648, spanning the membrane once. The three lysines after the membrane spanning region are characteristic features of the junction between membrane and cytoplasmic domains of cell-surface receptors, and interact with the phospholipid head groups in the membrane. The cytoplasmic domain of ßAPP contains the last 47 amino acid residues.

Amyloid ß protein precursor is found in both cultured cells as well as in a variety of tissues. Currently, the normal physiological function of ßAPP is still unknown. There are reports that suggest ßAPP is involved in the regulation of cell growth and in the regulation of cell - cell or cell - surface adhesion (Saitoh *et al.*, 1989; Breen *et al.*, 1991; Brenda *et al.*, 1988). Recently, Nishimoto *et al.* (1993) reported that ßAPP forms a complex with G_0, a major ATP binding protein in neuronal membranes. A cytoplasmic ßAPP sequence, histidine 657 - lysine 676 in $ßAPP_{695}$, has been shown to have a specific G_0-activating function, and the immunoreactive α- and ß- subunits of G_0 from solubilized brain membranes were co-precipitated with ßAPP by an anti-ßAPP monoclonal antibody. This suggests that ßAPP may be a receptor protein coupled to G_0.

2-3. ßAPP mRNA isoforms expressed in various tissues

Almost at the same time as $ßAPP_{695}$ was isolated, several other research groups independently identified two ßAPP mRNAs encoding proteins of 770 or 751 amino acid residues, respectively. The ßAPP mRNA identified by Tanzi *et al.*, (1988) and Ponteet *al.*, (1988) contained a sequence identical to that of the previously reported $ßAPP_{695}$, except for a 168 base pair insertion within the codon for valine 289 of ßAPP. The insertion preserved the reading frame of the ßAPP message, contained no termination codon, and would introduce 56 amino acids C-terminal to arginine 288 of the ßAPP. It would also convert valine 289 to an isoleucine. A group of polypeptides with sequences similar to that of the ßAPP insert are members of a family of Kunitz-type serine protease inhibitors. This insert-containing mRNA encoded 751 amino acid residues. Thus it was referred to as $ßAPP_{751}$. In the same year, Kitaguchi *et al.* (1988) isolated the third ßAPP mRNA, encoding a $ßAPP_{770}$, which contained a 225 base pair nucleotide insert introducing 75 additional amino acid residues. The 56 amino acid at the N-terminal of the 75 residue insert was highly homologous to the Kunitz

protease inhibitor. The insert of βAPP_{770} occurred in the same position as it did in βAPP_{751}, with valine 289 replaced by glutamic acid.

The isolation of βAPP-encoding cDNA clones reveals that this protein is derived from a much larger precursor protein. The precursor protein is synthesized in three major forms containing 695, 751, and 770 amino acid residues, respectively. All three forms have an identical amino acid sequence, except that the two longer forms contain a conserved sequence found in the family of Kunitz protease inhibitors. It was subsequently shown that these isoforms of βAPP mRNA are transcripts of alternative splicing of one βAPP gene, which was localized to the long arm of chromosome 21 in humans. (Goldgaber *et al.*, 1987; Zabel *et al.*, 1987; Patterson *et al.*, 1988; Kang *et al.*, 1987).

Kitaguchi *et al.* (1988) has reported that the βAPP Kunitz protease inhibitor domain has protease inhibitor activity *in vitro*. In their experiments, COS-1 cells were transfected either with an insert-containing βAPP_{695} or with an insert-lacking βAPP_{770}. An increase in trypsin activity inhibition was observed in βAPP_{770} transfected cell lysates.

The mRNAs of ßAPP, which result from alternative splicing, have been detected in a variety of tissues including muscle, spleen, kidney, and epithelial cells. Thus, the amyloid precursor protein gene is expressed in the brain as well as in other peripheral tissues. Ponte *et al.* (1988) investigated the expression of $ßAPP_{695}$ and the insert-containing $ßAPP_{751}$ in various tissues, and found that $ßAPP_{751}$ mRNA appeared to be ubiquitous, whereas APP_{695} mRNA had a restricted pattern of expression. When searching cDNA libraries prepared from a human SV40 transformed fibroblast cell line, lymphocytes, and normal or AD brain, the insert-positive clones were identified in all libraries, and only the brain libraries contained $ßAPP_{695}$. This suggests that the ßAPP transcripts might be differentially regulated and the insert-lacking $ßAPP_{695}$ could be specifically expressed in the brain. Meanwhile, other reports indicated $ßAPP_{751}$ and $ßAPP_{770}$ levels were significantly increased in AD brain, suggesting the possible role of insert-containing ßAPP in AD (Tanaka *et al.*, 1988; Johnson *et al.*, 1990). Though the subject is still controversial, the fact that the relative proportion of these alternative forms of the ßAPP message varies from tissue to tissue has

been confirmed. The balance among ßAPP isoforms might be one of the factors in AD development.

2-4. Familial Alzheimer's disease and mutation of the ßAPP gene

Although in most cases Alzheimer's disease is a late-onset neurodegenerative disease, some people do develop AD in their early 50's or even in their late 40's. The fact that early-onset AD shows familial inheritance suggests that the disease has some genetic components. The ßAPP has been a suspect gene because: 1) ßAP is a major component of amyloid deposits in the AD brain; 2) Down's syndrome, which also shows the amyloid deposits in the brain similar to AD, has an extra copy of chromosome 21, and the ßAPP gene is also located on the human chromosome 21.

In 1987, St. George-Hyslop *et al.* (1987) first showed that Alzheimer's disease was linked to two small marker sections of DNA in a band of chromosome 21, called q21; one of these two sections has in turn been linked with the ßAPP gene. However, very soon, other research groups (Tanzi *et al.*, 1987; Schellenberg *et al.*, 1988) reported that they did not find an association between the chromosome 21 site and

Alzheimer's disease in the families they were studying; making the case much more complicated.

In 1991, John Hardy's group directly detected mutations in the ßAPP gene from patients in some AD families (Goate *et al.*, 1991). The point mutation involved conversion of valine 717 on $ßAPP_{770}$ to isoleucine. In other AD families, the valine 717 was also reported to be replaced by glycine (Chartier-Harlin et al, 1991) or phenylalanine (Murrell *et al.*, 1991). These mutations occur within the transmembrane domain two residues from the carboxyl terminus of the ß protein. Computer analysis predicts that these substitutions would make the transmembrane domain more hydrophobic and could influence the stability of the deposited peptide. Up to now, about a dozen mutations in the ßAPP gene have been reported in familial inherited Alzheimer's disease. From all these studies, Hardy concludes that the aberrations in the ß amyloid precursor protein are sufficient, if not necessary, for the development of Alzheimer's disease. However, it is clear that mutations in the ßAPP gene are relatively rare and the defect in the ßAPP gene probably accounts for, at most, only 20% of the cases of Alzheimer's disease.

Later, Schellenberg *et al.*, (1992) showed that chromosome 14 was also linked to an inherited form of AD that develops unusually early, at about 45 years of age. As yet the gene responsible for AD on chromosome 14 has not been identified, but it is suspected to be connected with ßAPP synthesis and processing.

Meanwhile, previous evidence of the involvement of chromosome 19 in late onset AD (Pericak-Vance *et al.*, 1991) has been recently confirmed by the finding of an association between AD and the apolipoprotein E (apoE) locus on chromosome 19 (Corder *et al.*, 1993; Schmechel *et al.*, 1993). ApoE is important in lipid metabolism and to nerve regeneration. It is also reported that apoE has high affinity binding to ßAP (Strittmatter *et al.*, 1993). Therefore, Alzheimer's disease is genetically heterogeneous and more than one gene is involved.

As of now, the major amino acid residues reported to be involved in the ßAPP mutations include (Goate *et al.*, 1991; Chartier-Harlin *et al.*, 1991; Murrell *et al.*, 1991):

(1) Lysine 670 of $ßAPP_{770}$ mutates to asparagine.

(2) Methionine 671 mutates to leucine.

(3) Glutamate 693 mutates to glutamine.

(4) Valine 717 mutates to isoleucine.

(5) Valine 717 mutates to phenylalanine.

(6) Valine 717 mutates to glycine.

As shown in Figure 2-2, all these mutations are located either within or immediately flanking the ßAP region of ßAPP. The lysine 670 and methionine 671 mutations are right at the amino end of ßAP. The glutamate 693 mutation is within the ßAP sequence, while the valine 717 mutation is within the transmembrane domain of ßAPP, and is only two residues away from the C-terminus of ßAP. The locations of these mutations suggest that they may cause AD by altering ßAPP processing.

To further investigate the consequences of the mutations within the ßAPP gene, the mutated ßAPP genes have been introduced to various cell culture systems. Martin Citron *et al.* (1992) introduced into the human kidney 293 cell a ßAPP cDNA bearing a double mutation, lysine 670 in $ßAPP_{770}$ to asparagine plus methionine 671 to leucine. They detected six to eight times more ßAP in these cells than in cells transfected with DNA constructs expressing wild type ßAPP. They suggest that a methionine to leucine mutation was principally

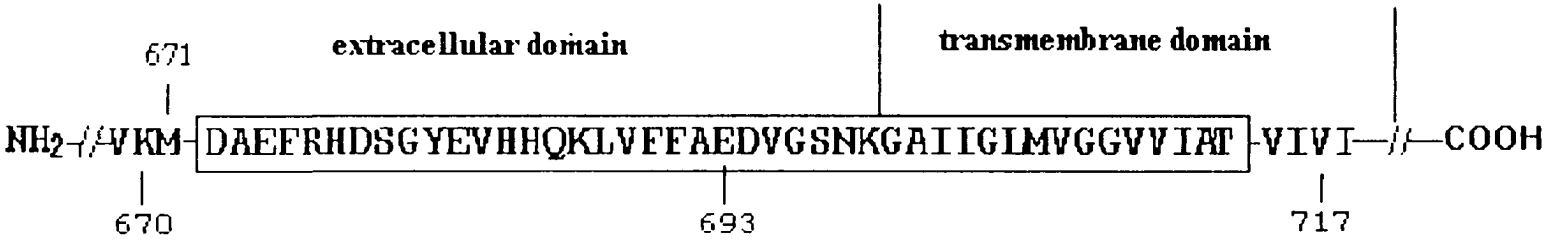

Figure 2-2. Demonstration of ßAPP mutations found in familial Alzheimer's disease. Open box indicates ßAP region. Lysine-670, methionine-671, glutamate-693, and valine-717 are amino acids involved in the ßAPP mutations in familial Alzheimer's disease. These positions are either within or immediately flanking the ßAP region.

responsible for the ßAP increase. The fact that familial AD mutations increase ßAP production was further confirmed when Cai *et al.* (1993) published a similar observation in human neuroblastoma cells. Cells carrying a mutated ßAPP gene produced five times more ßAP-bearing, carboxyl terminal ßAPP derivatives than cells expressing wild type ßAPP. Besides, they also released six times more ßAP into the cell culture medium. These findings suggested a correlation between the amount of released ß-amyloid protein and the mutations within a ßAPP gene.

2-5. Animal models of Alzheimer's disease

Most of the early biochemical evidence linking ßamyloid deposits to AD had come from studies on human brains obtained at autopsies. The big disadvantage of this approach is that the pathological lesions are the end stage of the disease. Only rarely do scientists get to see what early or intermediate-stage lesions look like. While aged nonhuman primates also develop amyloid plaques and the other characteristic symptoms of AD, including memory deficits, similar to those of Alzheimer's disease, the plaques are less frequent and

the animals are too expensive to be used for routine research.

One investigative approach for overcoming this difficulty was to develop an animal model of human AD. By inducing mice to overproduce ß amyloid protein, researchers attempted to reproduce neuropathologies and behavioral symptoms similar to those of the human Alzheimer's disease. If this strategy is successful, it would not only confirm the role of ßAPP in disease pathogenesis, but would also provide an animal model which permits researchers to test highly experimental drugs against AD and to perform other studies not appropriate or possible on humans.

By December 1991, three such transgenic mouse models had been reported, of which two showed apparent ßAP deposits, and a third developed neurofibrillary tangles and neurodegeneration (Quon *et al.*, 1991; Kawabata *et al.*, 1991; Wirak *et al.*, 1991). All these groups used similar genetic engineering approaches. They injected genes encoding human ß amyloid protein precursor into newly fertilized mouse eggs, which were then implanted in foster mothers to develop. However they chose different isoforms of the ßAPP gene.

In July, 1991, Cordell and her group (Quon *et al.*, 1991) first reported the extracellular amyloid deposits in their transgenic mice expressing additional ßAPP$_{751}$. These amyloid deposits were primarily in the cortex and in the hippocampus, two of the principal brain areas affected by Alzheimer's disease. However, the amyloid deposits in their mice did not have the same morphology as observed in humans AD.

At about the same time, Wirak *et al.* (1991) reported ßAP deposits in the central nervous system of their transgenic mice. The Wirak-Underbeck mice model also showed ßAP immunoreactive deposits in brain neurons, particularly in the hippocampus. However, the deposits were later found to occur occasionally in normal mice of that strain. Later work showed that the deposits were also stained nonspecifically by several different antibody preparations. This indicated that the deposits had a high non-specific affinity for antibodies and might not contain ß amyloid protein.

In December, another transgenic mouse model was reported by Kawabata *et al.* (1991). The Kawabata-Higgins-Gordon model reported all the major pathological features of AD in the transgenic animals, and showed the full range of AD's pathology, including

well-developed plaques, tangles, and degenerating neurons. However, the failure to reproduce the results in other transgenic mice in later studies made them finally retract their paper in March, 1992.

In July, 1992, Kammesheidt *et al.* (1992) reported another transgenic mouse model for human AD. They expressed the C-terminal 100 amino acids peptide of ßAPP in transgenic mice. Using an anti-ßAPP-antibody, the accumulation of ßAPP immunoreactivity in the brains of 4- and 6-month-old transgenic mice were studied. Only light cytoplasmic staining with antibody was visible in control mice, while darker punctuate accumulations of immunoreactive stain throughout the hippocampus were unique to the transgenic mice. In addition, the immunocytochemical analysis using an antibody against the carboxyl terminus of ßAPP revealed aggregation of this epitope of ßAPP in neurites with abnormal appearing in the area of the hippocampus of transgenic mice, similar to its aggregation in the cells of AD brains. They suggested the expression of abnormal carboxyl terminal subfragments of ßAPP *in vivo* may cause amyloidogenesis and specific neuropathology.

2-6. ßAPP processing and ßAP release

The amyloid ß precursor protein is a glycosylated membrane protein with a ß amyloid protein sequence partially embedded in the membrane. Studies on cultured cells documented that ßAPP has a short intracellular half-life of 20 to 30 minutes with a molecular weight ranging from 90 to 135 Kd, depending on the extent of glycosylation. During the proteolytic processing, breakdown fragments of ßAPP appeared both intracellularly and extracellularly. The carboxyl-terminal truncated ßAPP fragments were found to be secreted into the cell culture medium. Dewji *et al.* (1990) reported that the intracellular form of ßAPP appears to undergo amino-terminal processing, yielding many smaller fragments, whereas the secreted form does not show any further proteolytic cleavage after its release from the cell surface.

In addition to the finding of the ßAP-region-lacking ßAPP in cell culture medium, the similar ßAPP forms lacking ßAP region were also detected in the human cerebrospinal fluid (Weidemann *et al.*, 1989; Palmert *et al.*, 1989). This evidence indicated that in normal ßAPP processing, the cleavage of ßAPP is a membrane-associated event that occurs within the ßAP

sequence, thus preventing amyloid formation in the brain (Sisodia *et al.*, 1990). Sisdoia *et al.* (1990) also showed that the cleavage site on ßAPP was close to the interface between the extracellular and transmembrane domains within the ßAP region. Thus, an intact amyloidogenic ßAP fragment was not generated during normal ßAPP catabolism. The detection of the same ßAPP form in human cerebrospinal fluid showed that similar events occurred *in vivo* (Palmert *et al.*, 1989). Therefore, an altered ßAPP processing may occur in the release and subsequent deposit of the intact ßAP region.

In a cell culture study, the protein kinase C stimulator, phorbol 12,13-dibutyrate, was reported to increase the turn-over and processing of ßAPP as measured by a high level of ßAPP degradation fragments (Buxbaum *et al.*, 1990). Protein kinase C activators were also shown to inhibit ßAP production by altering its precursor's processing (Gabuzda *et al.*, 1993). Alternatively, because the ßAP sequence is partially embedded within the membrane, the production of ßAP could require membrane damage that exposes the embedded ßAP sequence to a protease, and results in the release of ßAP by abnormal cleavage of precursor protein within

the cell membrane. The ß protein then presumably accumulates in the brain because of its low solubility under physiological conditions. Thus Pettegrew hypothesized that the aberrations in the synthesis and degradation of membrane phospholipids were early events in the pathogenesis of AD (Pettegrew *et al.*, 1988a; 1988b). Phospholipid abnormalities in AD brain have been reported by several other research groups (Nitsch *et al.*, 1992; Blusztajn *et al.*, 1990; Barany *et al.*, 1985) since then.

2-7. Neurotoxicity of ß amyloid protein

Several *in vivo* studies have reported brain damage after the injection of ßAP into animals. Frautschy *et al.* (1991) injected SDS isolated AD amyloid cores into rat hippocampus. The similarly isolated lipofuscin fractions from human brains were injected on the contralateral side of the brain as control. One month after injection, the AD-related antigen Alz-50, ubiquitin, and silver positive structures were observed only in response to amyloid, suggesting that the injection of ß amyloid caused neuronal damages and induced AD-associated antigens in the animals' brains. In a similar experiment using a

synthetic ßAP fragment, the neurodegeneration and Alz-50 antigen induction were also observed in rat and in primate cortices (Kowall *et al.*, 1991; 1992), indicating neuronal responses to ßAP.

However, several other studies reported that ß protein failed to produce neurotoxicity after injection into rat and monkey brains (Podlisny *et al.*, 1992; Games *et al.*, 1992). While conflicting observations have been reported regarding the direct *in vivo* and *in vitro* neurotoxicity of ßAP, May *et al.* (1992) pointed out there were marked lot-to-lot differences in the neurotoxic properties of ßAP in primary rat hippocampal cultures. Attempting to find an explanation, the ß amyloid peptide preparations with differential neurotoxicity were studied extensively. Amino acid sequencing, HPLC, and mass spectroscopy provided evidences that these peptides were all synthesized correctly and were free of contamination. Rather, the important difference appeared to be related to peptide confirmation or aggregation state (Yankner 1992). Pike *et al.* (1991; 1993) has reported that the prolonged incubation of synthetic ß peptide in solution resulted in increases of peptide aggregation and neurotoxicity, while newly solubilized ß amyloid peptide was

predominantly monomeric and was not as toxic to neurons.

The neurotoxicity of ßAP was also reported in many *in vitro* studies on primary neuronal cultures (Loo *et al.*, 1993; Forloni *et al.*, 1993; Pike *et al.*, 1992; Busciglio *et al.*, 1993). Yankner *et al.* (1990a; 1990b) showed that ßAP could either be trophic or toxic to neuronal cells, depending on the stage of the neuronal cells and the concentrations of ßAP. Based on the observations of a primary culture from the rat brain at embryonic day 18, they showed that ß amyloid protein is neurotoxic to mature neurons and also neurotrophic to undifferentiated neurons. The ßAP toxicity was also reported to be dose-dependent and reversible at low doses (Roher *et al.*, 1991). These facts suggest that the deposit of amyloid in the AD brain may be partly responsible for the destruction of neurites, thereby contributing to the formation of neuritic plaques and to neuronal death.

Chapter 3

Amyloid ß peptide Synthesis, Purification, and Identification

In order to study the biological effect of ß amyloid protein and its interaction with a mouse neuroblastoma cell line, a synthetic fragment of ßAP, ß1-40, was needed. This peptide was synthesized using an automated solid phase peptide synthesizer. This chapter briefly describes the synthesis, purification, and identification of ß1-40.

3-1. The general scheme of peptide synthesis

There are two ways to chemically synthesize a peptide: solution synthesis or solid phase synthesis. In solution synthesis, a peptide is assembled from its amino terminus to its carboxyl terminus. One amino acid at a time is added and separation procedures are needed after each step in the synthesis to remove excess reagents and by-products. In solid phase peptide synthesis, the carboxyl terminal amino acid is covalently attached to an insoluble support by its carboxyl group, and therefore immobilized. Peptide chains are assembled from the carboxyl terminus,

working towards the amino terminus. The development of solid phase peptide synthesis procedures greatly simplifies the process of peptide synthesis because all intermediate purification steps are essentially eliminated. Excess reagents and reaction by-products are washed away from the support-bound synthesizing peptide. Solid phase synthesis also avoids some of the problems that might be created by peptide insolubility.

The commercially available solid supports for peptide synthesis include polystyrene and polyamide-Kieselguhr supports. For this study, the ß1-40 was synthesized on PepSyn K (MilliGen/Biosearch, Burlington, MA, USA), which is a polyamide-Kieselguhr type peptide synthesis support consisting of a polyacrylamide gel polymerized within the pores of rigid macroporous kieselguhr particles (diatomaceous earth). The rigid framework of the kieselguhr particles provides a noncompressible support that retains the open channels necessary for rapid diffusion of reactants throughout the matrix. There is also no significant change in bed volume when reagents are changed during synthesis, and a continuous flow process is allowed. The polyacrylamide gel within the pores of Kieselguhr particles is formed by copolymerization of

dimethylacrylamide with cross-linking monomers and functionalizing compounds. The latter, sarcosine methyl ester, react with linker molecules to form primary amines, and provide the sites of attachment for the growing peptide.

In solid phase peptide synthesis, when the first C-terminal amino acid is attached to an immobilized support via its carboxyl group, its α-amino group is temporarily protected to prevent unwanted side reactions during amino acid-support coupling. After the coupling reaction, the amino terminus of support-bound amino acid is deprotected by basic cleavage of the protecting group. Next, after washing, the second amino acid with an activated carboxyl group and protected amino group is added. The deblocked amino terminus of a support-bound amino acid reacts with the activated carboxyl group of the incoming amino acid, resulting in the formation of a peptide bond. The peptide elongates by one amino acid. In each of the peptide synthesis cycles, the α-amino group of the incoming amino acid is temporarily protected at addition, to avoid side reactions during peptide bond formation. After this amino acid is assembled to the synthesizing peptide, its α-amino group protection is removed, the

deprotected N-terminus of support-bound synthesizing peptide is then ready for the reaction with the next amino acid. Figure 3-1 shows the general scheme of peptide synthesis. The process of deprotecting the amino terminus of support-bound peptide, activating the carboxyl terminus of incoming amino acid, and performing the coupling reaction with the next amino acid, is repeated until the peptide is completed.

If the amino acid has a chemically active side chain group, It will also need to be protected in order to avoid participation of the reactive group during chain assembly. At the completion of peptide synthesis, the side chain protecting groups are removed and the synthesized peptide is cleaved from the support. The peptide is then subjected to further purification and identification.

3-2. Fmoc strategy of peptide synthesis: α-amino group protection

During peptide synthesis, the protection for α-amino groups and side-chain amino groups need to be distinguishable, so that the α-amino protection can be selectively removed before the coupling reaction in each peptide synthesis cycle, while keeping the side

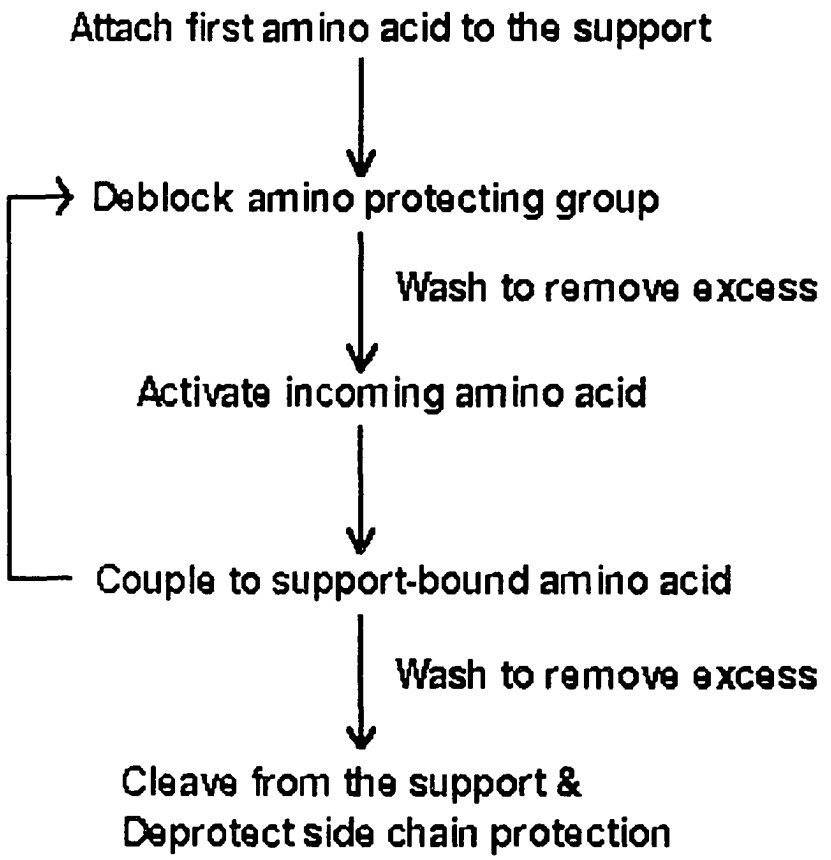

Figure 3-1.General peptide synthesis scheme

chain protection intact. The two most widely used methods of protecting an α-amino group in solid phase peptide synthesis are the Boc-benzyl strategy and the Fmoc-tBu strategy.

The framework for the solid-phase peptide synthesis using the Boc-benzyl strategy originated more than 30 years ago (Merrifield, 1963). The method is based on the differential acid lability of an α-amino protecting group and the side chain protecting groups. The acid labile t-butyloxy carbonyl group (Boc) is used in α-amino protection, and benzyl derivatives are used for side chain protection. The Boc-benzyl strategy uses the differential strength of acids to selectively remove the temporary α-amino protection during the repetitive synthesis cycles and the final side-chain deprotection at the completion of synthesis. Usually trifluoroacetic acid (TFA) is used in removing α-amino protection and HF is used to deblock side chain groups when peptide synthesis is completed.

The Fmoc-tBu synthetic strategy in solid phase peptide synthesis was introduced simultaneously by two groups (Chang and Meienhofer 1978; Artherton *et al.*, 1978). A clear distinction between the Fmoc-tBu strategy and the Boc-benzyl strategy is the adoption of

the base-labile 9-fluorenyl methoxy carbonyl (Fmoc) group as the α-amino protecting group. The acid labile tertiary-butyl (tBu) derivatives are used for side chain protection. The amino Fmoc protecting group can be rapidly removed by ß-elimination with secondary amines such as piperidine or other nucleophilic bases. The side chain protecting groups and peptide-support links, which are acid labile, are totally stable to peperidine during peptide synthesis. Amino acid side chain protecting groups are cleaved by 25-90% TFA when peptide assembly is completed.

3-3. Carboxyl group activation and side chain protection in Fmoc peptide synthesis

The activation of an amino acid is an essential step in the assembly of peptide chains because simple alkyl esters on the incoming amino acid undergo aminolysis at too slow a rate to be generally useful for peptide bond synthesis. Phenyl esters of amino acids are more active leaving groups, especially if electronegative substitutes are present on the aromatic ring. Examples of phenyl esters are -OPfp (penta-fluorophenyl) ester derivatives and -ODhbt (1-oxo-2-hydroxy-dihydrobenzo-triazine) ester derivatives. In

the process of activation, the electron density around the carboxylate carbon is altered, making it susceptible to nucleophilic addition by the amino terminus of the support-bound peptide chain. After the amino protecting Fmoc group is removed by piperidine from the amino terminus of support-bound synthesizing peptide, the incoming amino acid with an activated ester group is added. Most amino acids are used as the solid -OPfp derivatives. Threonine and serine, however, are used in the -ODhbt form, since it is impractical to handle their -OPfp derivatives which are viscous oils. HOBt (1-hydroxybenzotriazole hydrate) is commonly used as a catalyst in acylation reaction to increase the efficiency of peptide bond formation (MilliGen/Biosearch 1991).

Side chain protection is employed to avoid unwanted side reactions during peptide synthesis. Tertiary-butyl ether (tBu) and tertiary butyl ester (OtBu) are typical protecting groups for threonine, tyrosine, serine, asparate, and glutamate. The tertiary-butyloxycarbonyl (tBoc) protection group is used for the routine protection of lysine and histidine. Figure 3-2 shows a general structure of Fmoc - amino acid - OPfp, an amino acid with its α-amino

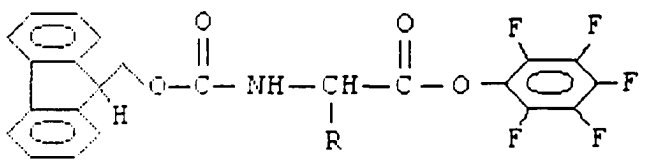

Fmoc - amino acid - OPfp

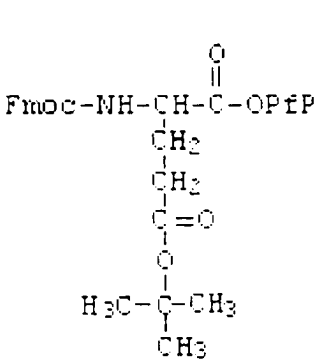

Fmoc-Glu (OtBu)-OPfp

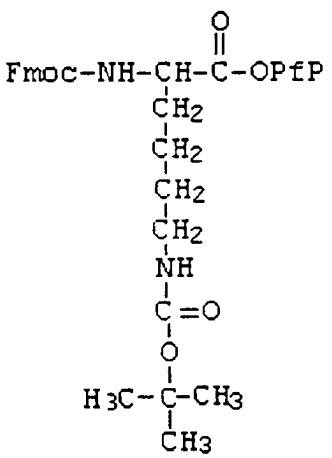

Fmoc-Lys (Boc)-OPfp

Figure 3-2. Structure of Fmoc-amino acid-OPfp. Structures of side-chain protected Fmoc-glutarate-OPfp and Fmoc-lysine -OPfp.

group in protected form and its carboxyl group in activated form. Side chain protecting groups -OtBu and -Boc are also shown in the examples of glutamic acid and lysine.

3-4. Amyloid ß1-40 synthesis, cleavage, and deprotection

In this study, amyloid ß1-40 peptide was synthesized on a MilliGen/Biosearch 9050 Peptide Synthesizer, using the solid phase Fmoc-tBu strategy. The amino acid sequence of ß1-40 is:

H_2N-Asp-Ala-Glu-Phe-Arg-His-Asp-Ser-Gly-Tyr-
Glu-Val-His-His-Gln-Lys-Leu-Val-Phe-Phe-Ala-
Glu-Asp-Val-Gly-Ser-Asn-Lys-Gly-Ala-Ile-Ile-
Gly-Leu-Met-Val-Gly-Gly-Val-Val-COOH

The PepSyn Valine-KA resin, all reagents, and all amino acids in their Fmoc -amino acid -OPfp or Fmoc -amino acid -ODhbt form with side chain protection were purchased from MilliGen/Biosearch, Division of Millipore (Burlington, MA, USA).

Since the solid phase peptide synthesis started from the C-terminus of the peptide, the first C-terminal amino acid of ß1-40, Fmoc-valine, was covalently attached to PepSyn KA resin via its carboxyl

group. About 1.5 gram of PepSyn Valine-KA 100 holding 0.1 mmole of valine was packed into a column and connected to the peptide synthesizer.

When 20% piperidine in DMF (dimethylformamide) was flushed through the column, the α-amino protecting Fmoc group of valine was cleaved. The excess piperidine was removed from the system by washing with DMF. The second amino acid at the C-terminus of ß1-40 in its N-protected and C-activated derivative, a Fmoc-valine-Opfp, was then dissolved in a solution containing 0.3 M HOBt as a catalyst. Four millimole amino acid derivative to each millimole support-bound valine was injected into the system in this step to guarantee efficient coupling. When the second amino acid was coupled to the α-amino group of support-bound valine, the peptide chain was elongated by one amino acid. The cycle was repeated until completion of synthesis of ß1-40 peptide.

During the entire synthesizing process, the on-line post-column detector enabled continuous spectrophotometric monitoring of the progress of peptide assembly. A typical post-column trace for one and a half cycles of amino acid addition and deprotection is shown in Figure 3-3. A sharp

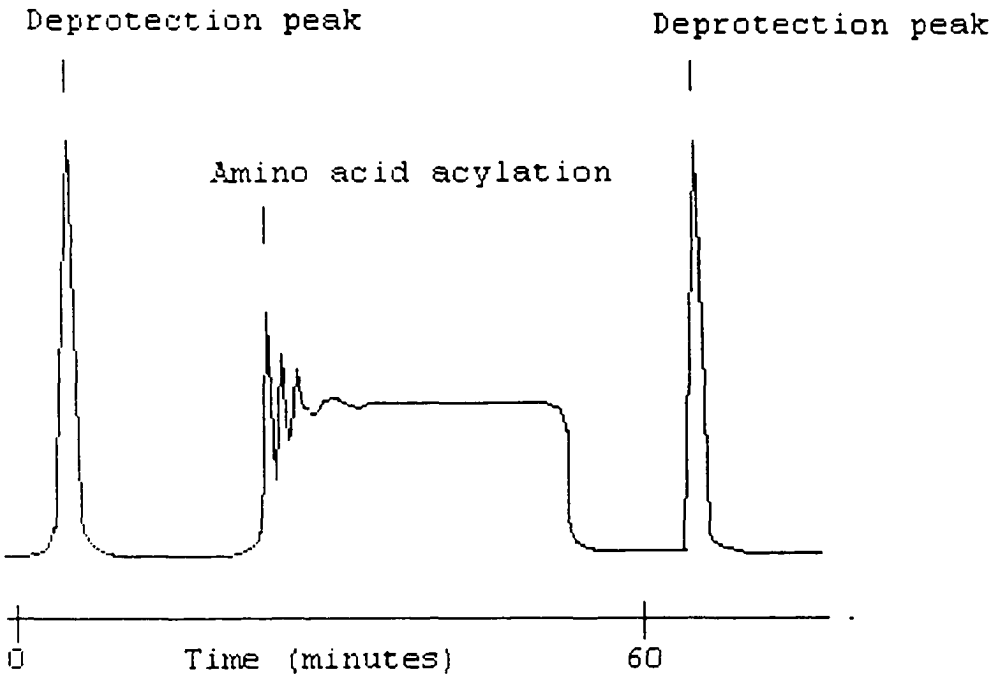

Figure 3-3. A typical peptide synthesis cycle monitored with the absorbance at 365 nm.

deprotection peak was observed when the Fmoc group was released from the amino terminus of the synthesizing peptide during the piperidine wash. After the deprotection peak, strong absorption was caused by the addition of the Fmoc-amino acid derivative, which was followed by a series of oscillating peaks as the reactant was recirculated until the column and the system reached a uniform concentration. The removal of extra free amino acid derivatives by washing the column with DMF and directing the flow to waste was observed by the sharp fall in absorbance. At this point, the N-terminal deprotection for the next cycle was ready to start. The consistent area of deprotection peaks indicated that the assembly was proceeding smoothly.

The total amyloid ß1-40 peptide contained 40 amino acid residues; and the synthesis took 39 cycles. The side chain deprotecion of Fmoc-tBu peptide was achieved using TFA. The Fmoc-tBu strategy limits exposure to acid to the last event of synthesis, i.e., the liberation of the tBu type of protecting groups from the side chain and the peptide from the support at the completion of the peptide assembly. A conventional deblocking protocol for a synthetic peptide without Arg, Trp, Cys, Met, or Tyr is achieved by incubating

the synthesized peptide with TFA: water (95:5 v/v) for one hour.

The ß1-40 sequence also includes amino acid residues of Arg, His, Tyr, and Met. Since it is difficult to remove the arginine side chain protecting group (4-methoxy-2,3,6-trimethylbenzenesulfonyl group), extended reaction time is required. On the other hand, methionine and histidine are readily deblocked of their side chain protecting groups in TFA, and are labile to free radical attack under acid conditions. To minimize side reactions, a low concentration of scavengers such as thiol (ethanedithiol and thiophenol) and sulfide (thioanisole or dimethylsulfide) were added to the deblocking reagent TFA.

After ß1-40 synthesis was complete, the peptide-support was taken from the synthesizer and unpacked from the column. The peptide-support was vacuum dried overnight and then incubated with cleavage reagent containing 90% TFA, 5% thioanisole, 3% ethanedithiol, and 0.01% methionine for 12 hours. The peptide-containing TFA solution was filtered and the filtrate was mixed with 7 times excess ethyl ether. A white precipitate was observed immediately, and the ether-peptide solution was incubated at $4^{0}C$ overnight to

allow complete precipitation. The precipitated peptide was collected by centrifugation, washed with ethyl ether and dried under vacuum for 6 hours.

3-5. Purification and identification of synthesized ß1-40 peptide

The precipitated ß1-40 was dissolved in 20 ml of 5% acetic acid and then lyophilyzed to remove traces of organic solvent. The peptide was redissolved in a small volume of 5% acetic acid, and desalted by passing through a Bio-Rad (Hercules, CA, USA) Econo-Pac 10 DG gel filtration column.

Amyloid ß1-40 peptide contains only one tyrosine and three phenylalanines in its sequence. Its absorption at 280 nm is relatively low compared with its absorption at 210 nm. However, 210 nm could not be used to detect the presence of synthesized ß peptide in gel filtration eluates, because the eluting buffer of acetic acid also absorbs strongly at wavelengths of 200 nm to 220nm. Figure 3-4 compares the absorbance of the eluating buffer and the absorbance of ß1-40 peptide over the wavelength range of 190 nm to 280 nm. The maximum absorption of acetic acid is at 215 nm. The absorbance drops very sharply and approaches zero at

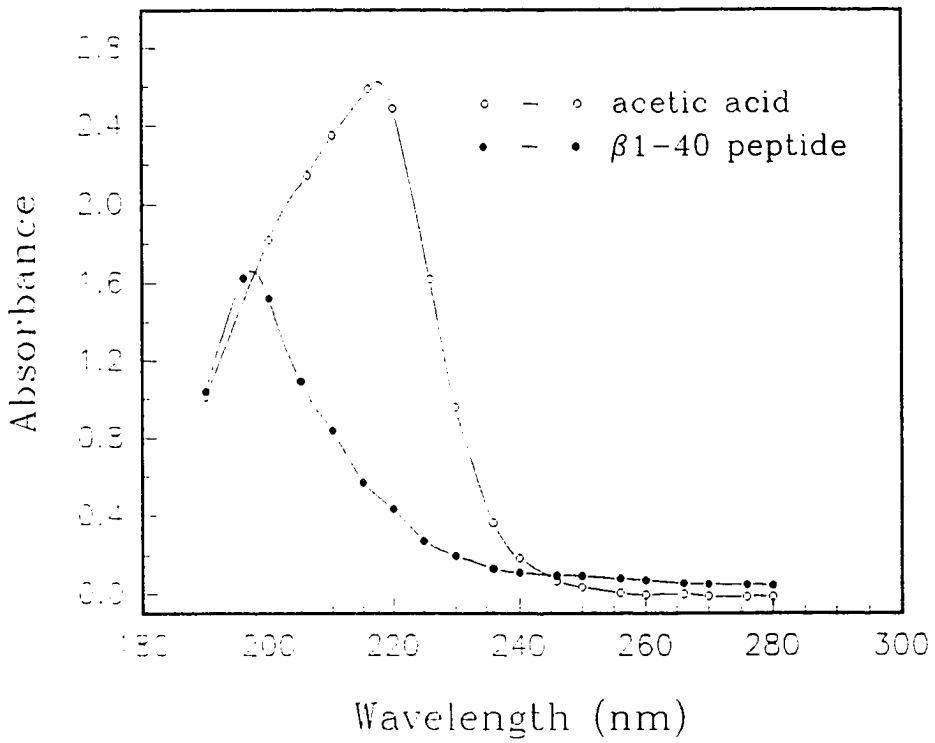

Figure 3-4. UV absorbances of acetic acid and β1-40 peptide.

255 nm. Amyloid ß1-40 peptide absorbs most strongly at 195 nm. The absorption then slowly decreases. Between 245 nm to 280 nm, the asbsorbance of ß1-40 peptide is greater than that of acetic acid. Therefore, 254 nm was chosen to detect the presence of ß1-40 peptide in the eluates from the gel filtration column.

When fractions from the gel filtration column were monitored for their absorbances at 254 nm, a large peak containing synthesized peptide was obtained (Figure 3-5). The fractions containing the peptide were pooled, lyophilyzed, and dissolved in 2 ml buffer containing 20% acetonitrile in 0.1% trifluoroacetic acid (TFA). After passing through a 0.5 μ filter to remove undissolved impurities, 5 μl of the synthetic peptide solution were injected into a 0.46x25cm reverse phase HPLC Vydac (The Separations Group, Hesperia, CA, USA) C4 column. The column was eluted by a gradient of acetonitrile using a mixture of buffer A and B at a flow rate of 1 ml/min. Buffer A contains 20% acetonitrile in 0.1% TFA while buffer B is 80% acetonitrile in 0.1% TFA. Elution of the peptide component was monitored by the UV absorbance at 214 nm. Figure 3-6 shows a major peak of synthesized peptide at a retention time of 22.6 minutes. Several HPLC runs

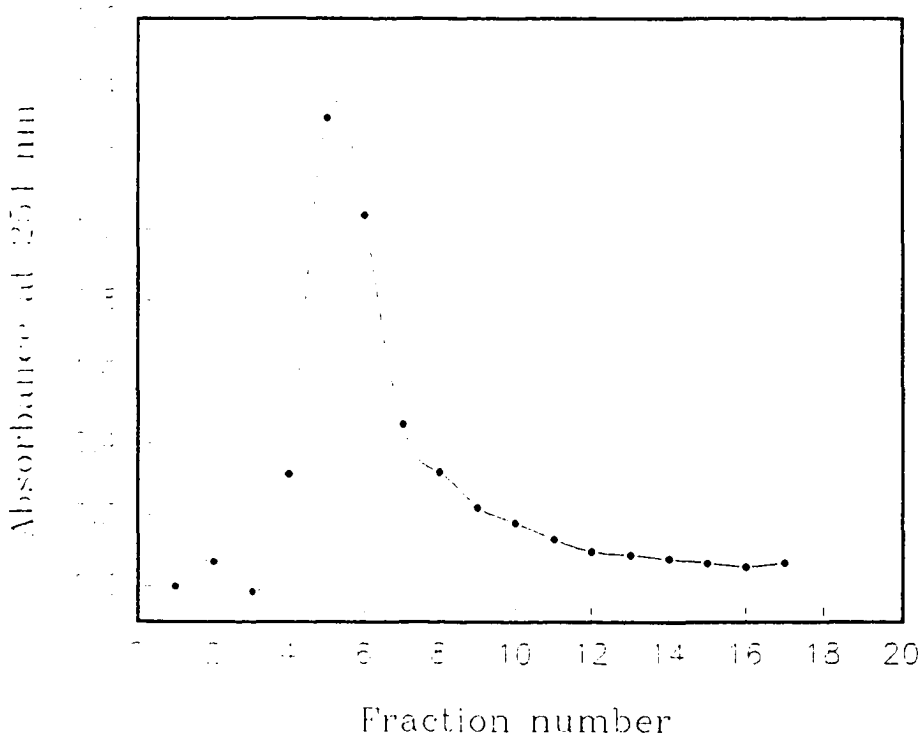

Figure 3.5 Gel filtration chromatograph of the synthesized β1-40 peptide on Bio-Rad Econo-Pac 10DG column.

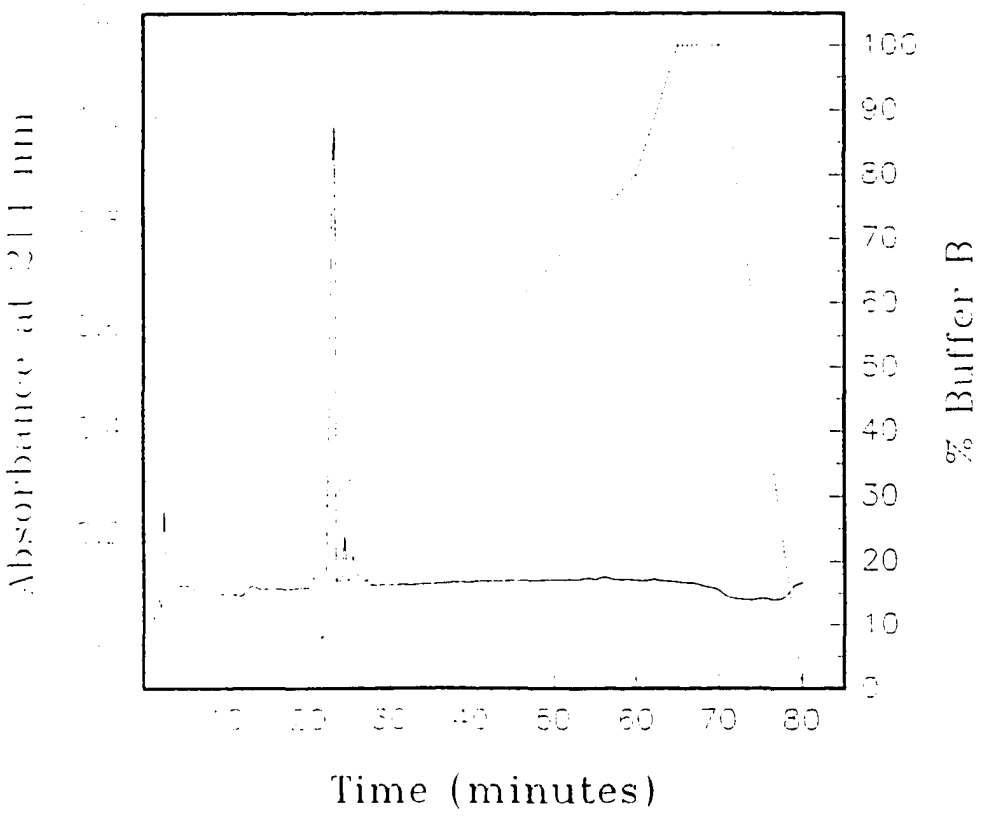

Figure 3-6. HPLC purification of the synthesized β1-40 peptide. Buffer A: 20% acetonitrile in 0.1% TFA, Buffer B: 80% acetonitrile in 0.1% TFA.

with 100 μl injections were performed to purify the synthesized ß1-40 peptide.

The synthesized ß1-40 peptide was further characterized by amino acid analysis. A 50 μl HPLC fraction of the peptide peak was hydrolyzed with 6 N HCl at 110^0C for 20 hours. The amino acid composition was analyzed using a Beckman 6300 Amino Acid Analyzer. Table 3-1 compares the amino acid composition of synthesized peptide with that expected from a ß1-40 sequence. The synthesized peptide has the correct amounts of alanine, phenylalanine, arginine, histidine, serine, valine, lysine, leucine, and methionine. Four aspartic acids are detected in the hydrolysis of synthesized peptide, matching the three aspartic acid and one asparagine residues in the ß1-40 sequence. This pattern is obtained because asparagine is hydrolyzed to aspartic acid during acid hydrolysis. The number of glutamic acids detected in the peptide hydrolysis matches the total of glutamic acid and glutamine in the ß1-40 sequence. Due to the destruction of tyrosine during acid hydrolysis, the tyrosine residue in the ß1-40 sequence is not seen in the hydrolysis products of synthesized peptide. A slightly low level of isoleucine in the synthesized peptide could be explained by

Table 3-1. Comparison of amino acid compositions between synthesized ß peptide and the ß1-40 sequence

Amino Acid	ß1-40 Sequence	Synthesized Peptide
Aspartic acid	3	4
Asparagine	1	0
Glutamic acid	3	4
Glutamine	1	0
Alanine	3	3
Phenylalanine	3	3
Arginine	1	1
Histidine	3	3
Serine	2	2
Glycine	6	7
Tyrosine	1	Trace
Valine	6	6
Lysine	2	2
Leucine	2	2
Isoleucine	2	1
Methionine	1	1

incomplete hydrolysis to the more resistant (hindered) peptide bound of Ile-Ile in ß1-40. Therefore, the amino acid compositions of the synthetic peptide and the ß1-40 sequence match very well, except for a slightly high level of glycine in the hydrolysis of synthesized peptide.

Immunochemistry studies also indicated that the synthesized ß1-40 peptide was recognized by an antibody against ßAP using a dot blot assay. The synthesized peptide was not cross-reactive with an antibody against the C-terminal of ßAPP. Thus, both amino acid composition analysis and immunoreactivity studies indicated the ß1-40 peptide was correctly synthesized.

Chapter 4

A Heparin-binding Protein from Mouse Neuroblastoma Cells Shows Immunoreactivity to Antibody Against the ß Amyloid Precursor Protein.

4-1. Introduction

Mammalian cell surfaces and the surrounding extracellular matrix are rich in a wide variety of glycoconjugates, including heparin (Hughes, 1983). Heparin interacts with a variety of proteins such as fibronectin (Hayashi *et al.*, 1980), endothelial cell growth factor (Klagsbrun and Shing, 1985), neural cell adhesion molecule (Cole and Glaser, 1986) and Alzheimer ß amyloid precursor protein (Schubert *et al.*, 1988; Snow and Wight, 1989). Heparin also binds to a class of low molecular weight proteins whose activity is more lectin-like (Eloumami *et al.*, 1990).

On the basis of its structure, it has been suggested that ß amyloid precursor protein is a transmembrane glycosylated protein (Schubert *et al.*, 1989; Weidemann *et al.*, 1989). Northern blot analysis indicates that ß amyloid precursor protein is present in a variety of tissues (Tanzi *et al.*, 1988). There are several isoforms of ß amyloid precursor protein,

generated by alternatively spliced RNA, leading to a membrane bound form (Dyrks *et al.*, 1988; Mita *et al.*, 1988), a form which is secreted by various cultured cells, and a form that has proteinase inhibitor activity (Castro *et al.*, 1990; Smith *et al.*, 1990). Different molecular weights have been described for these precursor isoforms based upon antibody recognition. These cross-reactive proteins have ranged in molecular weight from 135 to 90 Kd (Weidemann *et al.*, 1989; Selkoe *et al.*, 1988). Attempts to characterize the amyloid precursor protein in cultured cells have been limited to myelogenous leukemia (H562), lymphocytoma (U937) and monkey kidney cells as well as PC12 cells (Autilio-Gambetti *et al.*, 1988; Schubert *et al.*, 1988). In cultured human fibroblasts and a human neuroblastoma cell line, Dewji *et al.* (1990) reported that the cellular form of the precursor appears to undergo amino-terminal processing yielding many smaller fragments, whereas the secreted form does not show any proteolytic cleavage after its release from the cell surface. The study described in this chapter extended these works to include the mouse neuroblastoma cell line NB41A3 (Zhao *et al.*, 1991a).

4-2. ßAPP C-terminal peptide synthesis, purification, and identification

A ßAPP C-terminal peptide (C-peptide) was synthesized using the method described in Chapter 3. Figure 4-1 demonstrates the amino acid sequence of the C-peptide located in the cytoplasmic domain of ßAPP, containing residues 674-693 of $ßAPP_{695}$. Its amino acid sequence is: NH_2-Leu-Ser-Lys-Met-Gln-Gln-Asn-Gly-Tyr-Glu-Asn-Pro-Thr-Tyr-Lys-Phe-Phe-Glu-Gln-Met-COOH.

After peptide synthesis, the C-peptide was purified on a Bio-Rad Econo-Pac 10 DG gel filtration column (Bio-Rad Laboratories, Hercules, CA, USA). The first and also the major peak of the gel filtration chromatograph contains the synthesized C-peptide. The other two small peaks are fragments of synthetic peptide (Figure 4-2). Fractions 3 to 8 in the major peak were pooled together and subjected to amino acid analysis. When the amino acid composition of synthesized C-peptide is compared with that expected from its sequence, the synthetic C-peptide had the correct amount of threonine, serine, proline, glycine, leucine, phenylalanine, and lysine (Table 4-1). Due to the deamination of asparagine to aspartic acid in acid hydrolysis, the hydrolysis products of synthetic C-

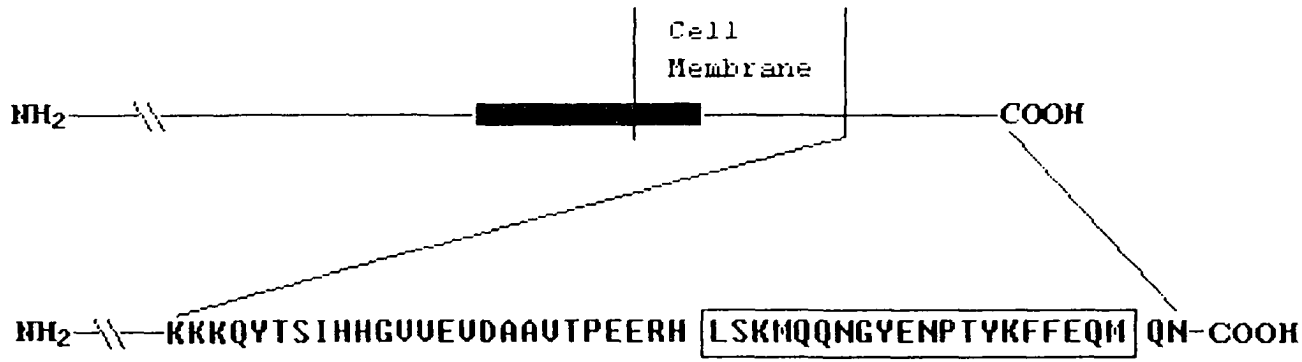

Figure 4-1. Demonstration of the βAPP C-terminal amino acid sequence. Black box indicates βAP region. Open box indicates the synthetic βAPP C-peptide sequence containing 20 amino acids. The amino acid sequence of the entire βAPP cytoplasmic domain is shown.

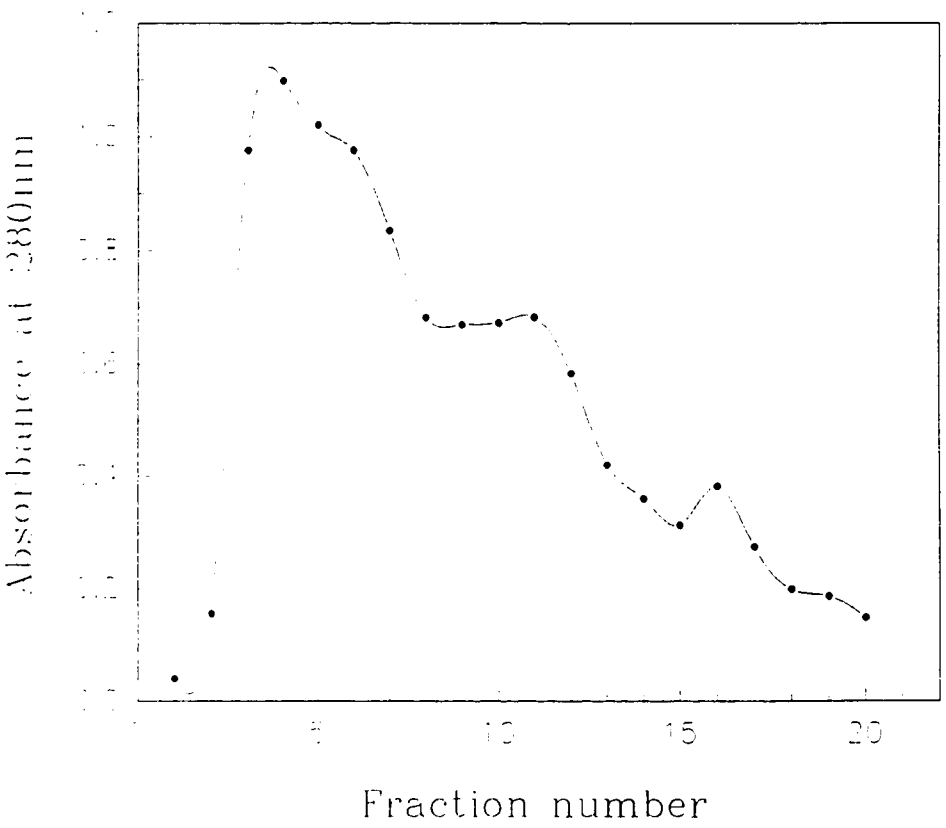

Figure 4-2.. Gel filtration purification of the synthesized βAPP C-terminal peptide on Bio Rad Econo-Pac 10 DG column. Fractions 3-8 were used in amino acid analysis and antibody produaction.

Table 4-1. Comparison of amino acid compositions between synthesized C-peptide and its native sequence.

Amino Acid	ßAPP C-Peptide Sequence	Synthesized C-Peptide
Aspartic acid		2
Asparagine	2	
Glutamic acid	2	4
Glutamine	3	
Phenylalanine	2	2
Serine	1	1
Glycine	1	1
Tyrosine	2	1
Lysine	2	2
Leucine	1	1
Methionine	2	1
Threonine	1	1
Proline	1	1

peptide showed two aspartic acids, matching the two residues of asparagine in the C-peptide sequence. The two glutamic acids and three glutamine residues in synthetic peptide should result in five glutamate residues after acid hydrolysis. Because of the large size of the glutamate peak compared to other amino acid residues, the integration of glutamic acid gave a relatively low value. The amino acid analysis indicated 4.37 glutamic acids in the hydrolysis products of synthetic C-peptide, slightly lower than the expected five glutamic acids from C-peptide sequence. The methionine and tyrosine were partially destroyed during acid hydrolysis, explaining their lower than expected values. Based on the amino acid analysis data, the ßAPP C-terminal peptide was judged to have the correct sequence.

4-3. Preparation of anti - C-peptide antibody and characterization of the antibody's specificity

The Imject SuperCarrier EDC System for Peptides (Pierce Chemical Co., Rockford, IL, USA) was used for antigen preparation. Two milligrams of synthesized C-peptide were reconstituted in 0.5 ml of conjugation buffer containing 0.1 M MES (2-(N-Morpholino)-

ethanesulfonic acid), 0.9 M NaCl, 0.02% sodium azide, pH 4.7. The peptide solution was then added to 0.2 ml of a carrier protein solution containing 2 mg of cationized BSA. The peptide - carrier protein conjugation reaction was carried out for 2 hours at room temperature. The reaction mixture was separated on a G-25 gel filtration column and the eluates were monitored at 280 nm on a UV spectrophotometer (Figure 4-3).

The adjuvant, Imject Alum (aluminum hydroxide; 45 mg/ml), was added drop-by-drop alternating with stirring to the conjugate solution to reach the final Alum concentration of 11.2-22.5 mg/ml. After stirring for 30 minutes, the mixture was filtered through a 0.2 μ sterile cellulose acetate membrane filter and 0.1 ml of immunogen filtrate (approximately 0.04 mg of peptide) was injected into several sites on the back of a rabbit. The rabbits were boosted again with an equivalent amount of antigen at day 14. Blood was drawn one month after the initial injection and allowed to clot for 18 hours at 4^0C. Serum was separated from the clot by centrifugation for 30 minutes at 2000xg.

The specificity of the anti-C antibody was tested in a dot blot experiment. About 40 μg synthetic ßAPP

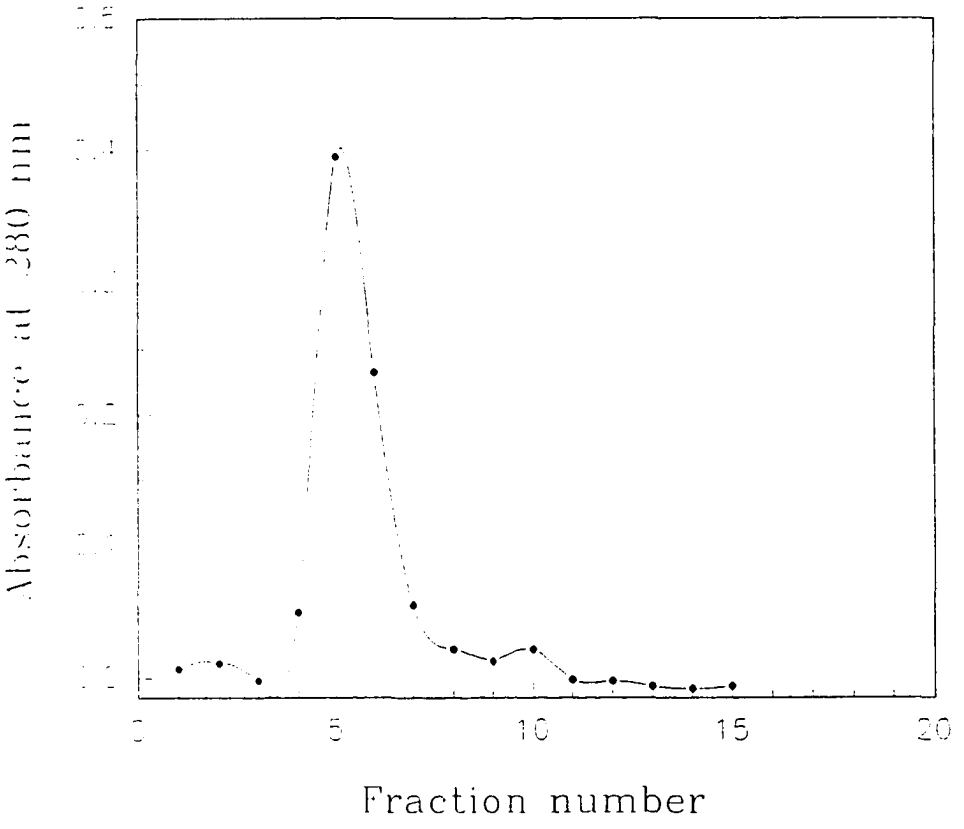

Figure 4-3. Gel filtration chromatograph of the C peptide - carrier protein conjugates.

C-terminal peptide and ß6-25 peptide, respectively, were dot blotted to Immobilon transfer membranes (Millipore Corp., Bedford, MA, USA) by applying a vacuum using a MilliBlot-S system (Millipore Corp.). Sections of the membrane were incubated either with anti - C-peptide antibody or with a pretreated anti-C antibody, which had been mixed with the synthetic C-peptide or ß6-25 peptide overnight and immuno-precipitates removed by centrifugation.

If the antibody recognizes the C-peptide specifically, the pretreatment of an antibody with synthetic C-peptide would block an antibody's binding sites and therefore inhibit its ability to bind C-peptide in the dot blot experiment. The results are shown in Table 4-2. The preparation of anti-C antibody recognized synthetic ßAPP C-terminal peptide. Preincubation of the antibody with synthetic C-peptide abolished the antibody's ability to recognize C-peptide on a dot blot test, indicating the antibody - C-peptide reaction was specific. The anti-C antibody did not recognize ß6-25 peptide and the preincubation of the antibody with synthetic ß6-25 peptide had no effect on the dot blot immunoreactivity. These results indicate that the anti - C-peptide antibody recognizes the C-

Table 4-2. Specificity test of anti-ßAPP C-peptide antibody.

Dot Blot	Site 1	Site 2	Site 3	Site 4
Sample:	C-peptide	C-peptide	C-peptide	ß6-25 peptide
Antibody:	Anti-C antibody	Anti-C antibody pretreated with C-peptide	Anti-C antibody pretreated with ß6-25 peptide	Anti-C antibody
Result:	(++++)	(+)	(++++)	(-)

terminal peptide of ßAPP and it does not cross react with the amyloid region of the precursor protein.

4-4. Anti-C immunoreactivity of neuroblastoma membrane extract and conditioned medium of cultured cells

Cultures of mouse neuroblastoma cells (NB41A3) were obtained from American Type Culture Collection (Rockville, MD, USA) and cultured at 37^0C in a 5% CO_2 humidified incubator in HL-1 medium (Ventrex Laboratories, Inc., Portland, ME, USA), which is a modified DME:F12 medium (See Appendix I), containing 2.5 mM Glutamine, 50 units/ml penicillin and 50 µg/ml streptomycin. Two groups of neuroblastoma cells were cultured in HL-1 medium either with or without a supplement of fetal calf serum (FCS). Conditioned medium (CM) was obtained by removing neuroblastoma cells via centrifugation, while neuroblastoma cell membrane proteins were extracted as described in section 4-5 using the modified protocol of Smith *et al.*, 1990.

Both the neuroblastoma membrane extract and the conditioned medium of cultured cells were blotted on an Immobilon transfer membrane and tested for their anti-C immunoreactivity as described previously. Synthetic C-

peptide was used as a positive control in this experiment. As shown in Table 4-3, the FCS-supplemented cell culture medium was slightly cross reactive with anti-C antibody; cell culture medium without FCS supplement was not recognized by the antibody. Therefore, any anti-C immunoreactivity present in FCS-free neuroblastoma conditioned medium should come from cultured neuroblastoma cells. The neuroblastoma cells released a small amount of anti-C immunoreactive ßAPP fragments into the cell culture medium.

The FCS-free neuroblastoma conditioned medium was also tested using a Mini-Protein II Multi Screen Apparatus (Bio-Rad Laboratories, Hercules, CA, USA) with anti-ß28 (Fraser *et al.*, 1991), anti-substance P (Sigma Chemical Co., St. Louis, MO, USA), and anti-Kunitz inhibitor antibodies (Sigma Chemical Co.). Only anti-ß28, which recognizes residues 1-28 of the ß amyloid region, showed a positive reaction. NB41A3 cells released fragments of ßAPP containing the C-peptide and ß1-28 sequences into the conditioned medium. However, most anti-C immunoreactivity was retained in the cell membrane fraction.

Table 4-3. Anti-C immunoreactivity of neuroblastoma membrane protein and conditioned medium

Dot Blot	Site 1	Site 2	Site 3
Sample: Antibody: Result:	C-peptide Anti-C Ab (++++)	HL-1 Medium w/o FCS Anti-C Ab (-)	HL-1 Medium w/ FCS Anti-C Ab (+)
	Site 4	Site 5	Site 6
Sample: Antibody: Result:	NB extraction Anti-C Ab (+++)	CM w/o FCS Anti-C Ab (+)	CM w/ FCS Anti-C Ab (+)

FCS: Fetal Calf Serum; CM: Conditioned Medium, NB: Neuroblastoma membrane extract; (+): Positive result; (-): Negative result.

4-5. Neuroblastoma membrane protein extraction and separation by heparin affinity chromatography

Neuroblastoma cells were grown for three days until confluent. The cells were scraped from the flask and washed free of medium with phosphate buffered saline (PBS) containing 10 mM phosphate and 150 mM NaCl, (pH 7.2). The cell pellet was homogenized in an extraction buffer containing 10 mM phosphate, 2.5 mM PMSF (phenylmethylsulfonyl fluoride) at pH 7.2 using a tight-fitting Dounce homogenizer. After centrifugation for two hours at 100,000xg, the soluble fraction was removed and the pellet was homogenized in PBS containing 1% Triton X-100 and 2.5 mM PMSF. The Triton X-100 homogenate was centrifuged at 20,000xg for 30 minutes. The soluble fraction contained neuroblastoma cell membrane-associated protein (Smith et al., 1990). Lipids in the Triton X-100 soluble fraction were removed by extraction with 5 volumes of hexane:isopropyl alcohol (3:2). The protein content in the neuroblastoma membrane extract was determined as 10 mg by the MicroBCA method (See Appendix II).

Five mg of neuroblastoma membrane protein extract were loaded on top of a 13x2.5cm column containing 50 ml of heparin-agrose (binding capacity = 800 μg

heparin/ml gel). The column was equilibrated with 0.01 M Tris-HCl (pH 7.0) containing 0.15 M NaCl (TBS) and unbound protein was washed out with TBS. The heparin-binding protein was eluted using a higher salt concentration, 1.0 M NaCl in 0.01 M Tris-HCl buffer (pH 7.0). The flow rate was 15 ml/hour. Figure 4-4 summarizes the neuroblastoma membrane protein separation procedure.

Collected fractions from heparin affinity chromatography were monitored for their absorbance at 280 nm (Figure 4-5). The large protein peak in Figure 4-5 was heparin-nonbinding and was washed through the column by 0.15 M NaCl in TBS. After the non-bound proteins passed through, the heparin-binding proteins eluted with 1.0 M NaCl were observed as a smaller peak. Fractions from each peak of heparin affinity chromatography were combined separately, desalted by concentrating on an ultrafiltration membrane PM 10 (Amicon, Inc., Beverly, MA, USA) and total protein concentration was determined. Thirty percent of the protein was recovered after heparin affinity chromatography (Table 4-4). The yield of heparin-binding proteins was 0.4 mg, which was 8.1% of the total membrane proteins loaded to the column.

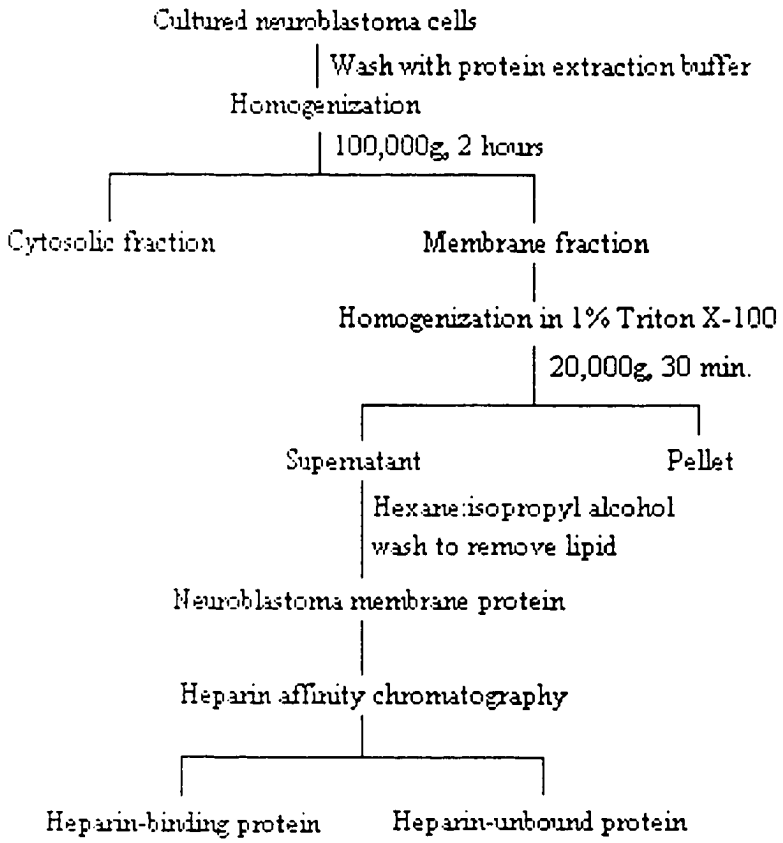

Figure 4-4. Neuroblastoma membrane protein extraction protocol.

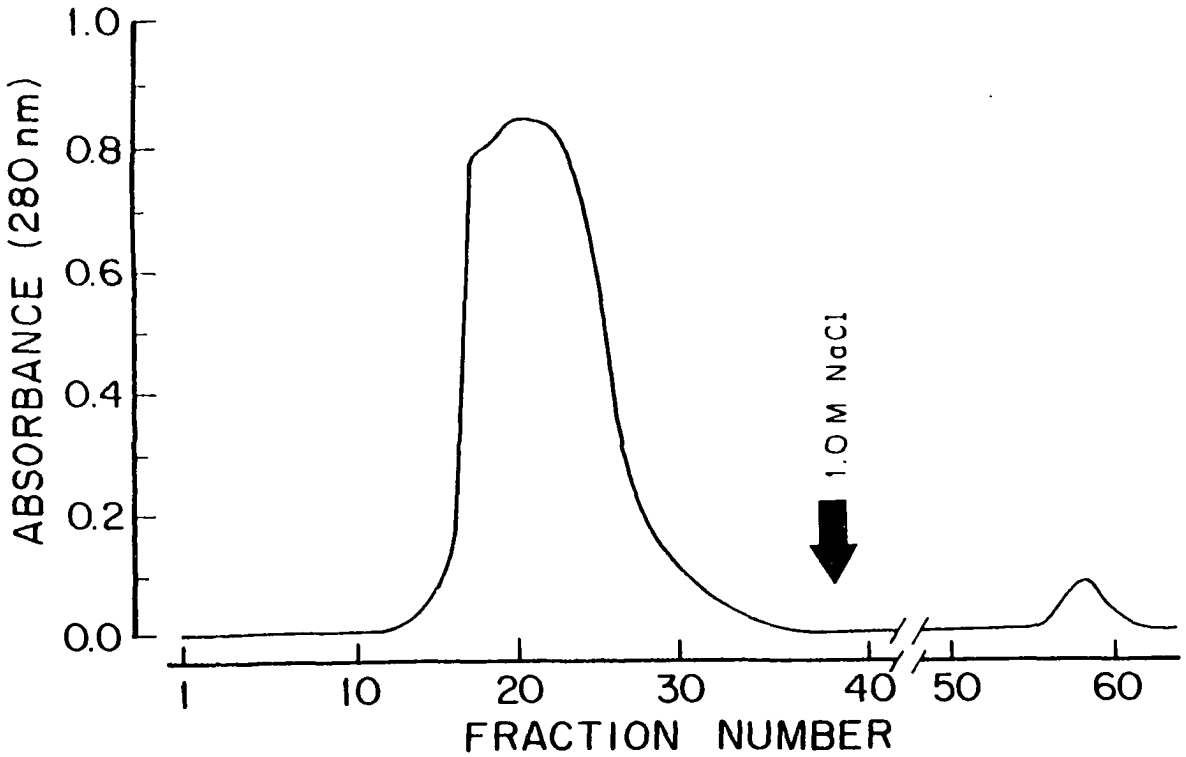

Figure 4-5. Heparin affinity chromatograph of neuroblastoma membrane extract. Unbound proteins were removed with 0.15 M NaCl in Tris-HCl buffer, pH 7.2. Heparin binding proteins were eluted with 1.0 M NaCl in Tris-HCl buffer.

Table 4-4. Protein yield of heparin affinity purification of neuroblastoma membrane protein.

	Protein (mg)	Percentage Recovery
NB membrane extract	4.94	100
Heparin-unbound protein	1.08	21.9
Heparin-binding protein	0.40	8.10

NB: neuroblastoma cells.

4-6. SDS-polyacrylamide gel electrophoresis and western blot analysis of neuroblastoma protein

SDS-polyacrylamide 9.0% separating gels and 4% stacking gels were prepared following the Bio-Rad Mini-Protean II Dual Slab Cell Instruction Manual (See Appendix III).

Neuroblastoma membrane proteins were separated on SDS-gels using a Bio-Rad Dual Slab Cell (Bio-Rad Laboratories, Hercules, CA, USA) at a constant setting of 200 volts. For each run of gels, one gel was stained with Coomassie Brilliant Blue, while the other gel was used for a western blot assay.

On dot blot analysis, samples were blotted to Immobilon transfer membranes by applying a vacuum to a MilliBlot-S system (Millipore Corp., Bedford, IL, USA). For western blot experiments, proteins were first resolved on SDS-polyacrylamide gel electrophoresis, and then electrophoretically transferred to Millipore Immobilon membranes by using a Bio-Rad Semi-Dry Electroblotter. When the Immobilon membrane containing the transfered samples is incubated with an antibody against the ßAPP C-peptide, the antibody should bind the corresponding proteins. At the end of the western blot, a color complex will be developed at the location

of the antibody - protein interaction (See Appendix IV).

As shown in Figure 4-6, when the neuroblastoma membrane proteins were separated by SDS-PAGE, four major polypeptides were detected in western blots by an antibody against synthetic ßAPP C-terminal peptide. These four major polypeptide bands had molecular weights of 89, 76, 60, and 41 Kd (Figure 4-6, Lane C). The antibody to the C-terminus of ßAPP also detected several minor higher molecular weight polypeptide bands on the western blot. Anti-substance P and anti-Kunitz inhibitor antibodies did not recognize any bands on the blot, but the anti-C immunoreactive components were also immunoreactive with anti-ß peptide antibody (results not shown).

On a dot blot experiment, only the heparin-binding fraction showed immunoreactivity to an anti-C antibody. The heparin-binding fraction was further resolved as three major polypeptides with apparent molecular weight of 89, 60, and 41 Kd upon SDS-PAGE (Figure 4-6. Lane B). Among them the 89 and 41 Kd bands show anti-C immunoreactivity on western blot (Figure 4-6. Lane D). These two bands have identical molecular weights when compared with the western blot of the neuroblastoma

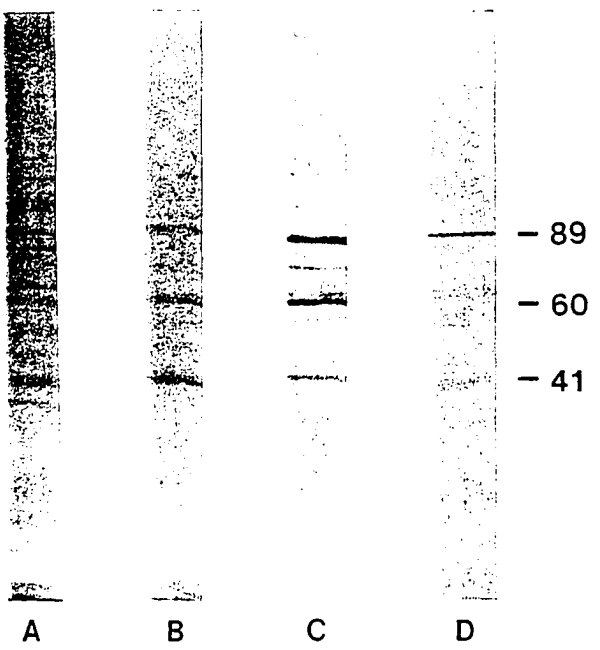

Figure 4-6. SDS-PAGE and western blot with antibody against the ßAPP C-terminal peptide.

Lane A: SDS-PAGE, NB membrane extract, Coomassie blue stain.

Lane B: SDS-PAGE, NB membrane heparin-binding fraction.

Lane C: Western blot, NB membrane extract.

Lane D: Western blot, NB membrane heparin-binding fraction.

membrane extract, which has two extra anti-C immunoreactive bands with molecular weights of 76 and 60 Kd.

4-7. Amino acid analyses of heparin-binding and heparin-unbound proteins

Both heparin-binding and unbound neuroblastoma membrane proteins were subjected to acid hydrolysis and amino acid analysis. About 0.1 ml of each fraction were separately lyophilized in a small hydrolysis test tube. Each tube was then put into a vial containing 0.5 ml of 6 N HCl. Together, they were subjected to a vacuum for 10 minutes on a Waters Pico-Tag Vacuum Station (Millipore Corp.) followed by a 110^{0}C incubation of 24 hours. The products were analyzed on a Beckman 6300 Amino Acid Analyzer (Beckman Instruments, Inc., Palo Alto, CA, USA).

Comparing the amino acid composition of neuroblastoma membrane heparin-binding protein with that of an unbound fraction, it appeared that most amino acids were present in both fractions in a similar ratio, while several polar amino acids were highly variable between the two fractions. Results in Table 4-5 indicate that the levels of tyrosine and serine in

Table 4-5. Amino acid analyses of neuroblastoma membrane heparin-binding and heparin-unbound proteins.

Amino Acid	Heparin-binding (%)	Heparin-unbound (%)	ßAPP last 100 residues (%)
Asp/Asn	9.79	9.23	8.00
Threonine	5.43	4.75	5.00
Serine	11.92	5.84	4.00
Glu/Gln	10.80	14.25	14.00
Proline	6.05	5.80	2.00
Glycine	8.86	7.77	8.00
Alanine	9.52	10.86	6.00
Valine	9.30	7.77	13.00
Isoleucine	3.62	3.30	6.00
Leucine	7.46	6.88	5.00
Tyrosine	2.05	1.09	4.00
Phenylanine	3.36	2.62	5.00
Lysine	6.11	11.79	7.00
Hisdidine	1.72	1.61	6.00
Arginine	2.99	5.39	2.00

the heparin-binding proteins were only about half of that in the heparin-unbound fraction, while lysine, arginine, and glutamic acid levels in heparin-binding proteins were about 50% to 100% more than in the heparin-unbound fraction. The fourth column of Table 4-5 compares the amino acid compositions of neuroblastoma membrane proteins with the last 100 residues at the C-terminus of ßAPP. When analyzing the experimental data, however, one should keep in mind that the neuroblastoma membrane heparin-binding fraction contains many proteins, and some of them may not be related to ßAPP or be immunoreactive to antibody against ßAPP C-peptide. The aspartic acid level in heparin-unbound (9.79%) and heparin-binding (9.23%) fractions were similar to the total of aspartic acid/asparagine in the last 100 residues of ßAPP (8.00%). The glutamic acid/glutamine level in the last 100 residues of ßAPP (14.00%) was close to that in heparin binding fraction (14.24%) and was significantly higher than that in the heparin-unbound fraction (10.80%). The serine level in C-terminal ßAPP (4.00%) was also much closer to that in the heparin-binding protein (5.84%) than that in the heparin-unbound fraction (11.92%). However, the heparin-binding fraction had higher levels of

positively charged amino acids. It contained 11.79% lysine and 5.39% arginine comparing to 7% lysine and 2% arginine at the last 100 residues of C-terminal ßAPP. These high lysine and arginine components may come from the non-anti-C immunoreactive proteins in the heparin-binding fraction. The negatively charged sulfate groups on heparin could attract positively charged free lysines and arginines as well as the positively charged proteins. Therefore, the heparin-binding fraction could contain proteins that had high lysine and arginine level and were not immunoreactive with anti-C antibody.

4-8. HPLC analysis of neuroblastoma heparin-binding protein.

The heparin-binding fraction of neuroblastoma membrane protein was further analyzed by reversed-phase HPLC on a 4.6x250 mm Vydac C4 column (The Separations Group, Hesperia, CA, USA) using an acetonitrile gradient of 20% to 80% in 0.1% (v/v) trifluoroacetic acid (TFA) at a flow rate of 1 ml/min. Protein absorbance was determined at 214 nm. Figure 4-7 shows the chromatographic profile where the heparin-binding fraction was separated by an acetonitrile gradient into two fractions. The first HPLC fraction consisted of

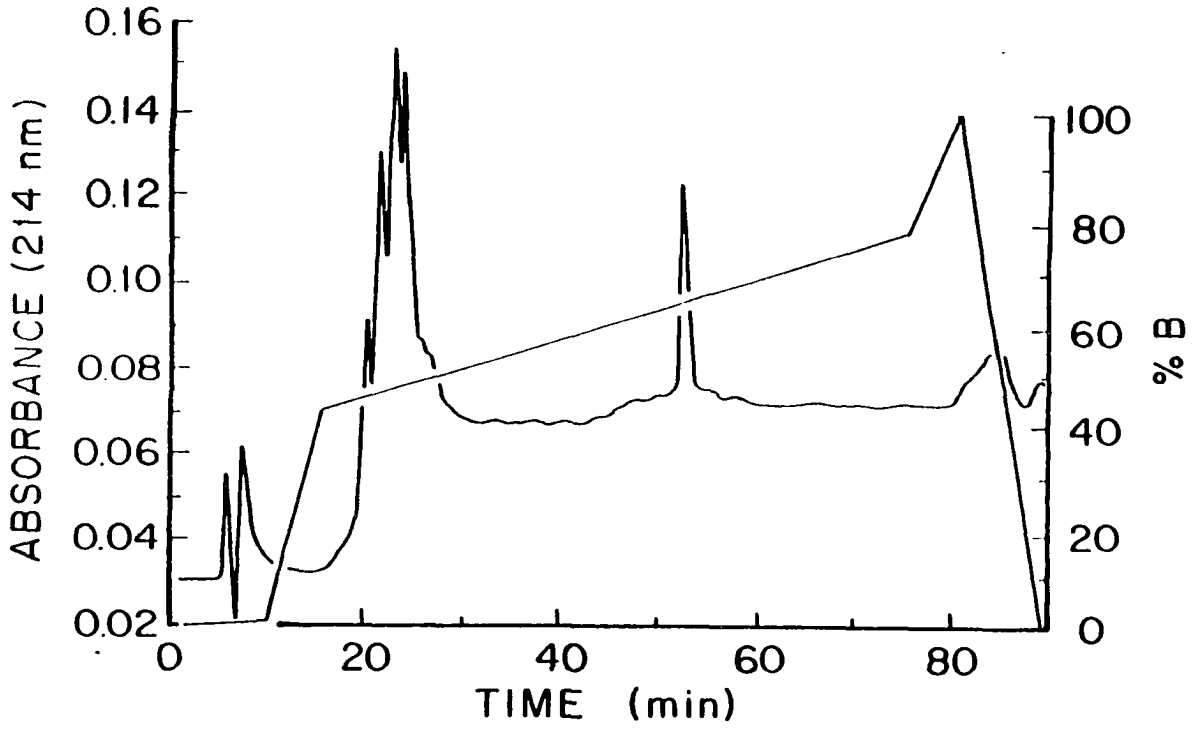

Figure 4-7. Reverse phase HPLC separation of neuroblastoma membrane associate heparin-binding proteins. 200 μg protein in 500 μl were injected into a Vydac C4 column. Buffer A: 20% acetonitrile in 0.1% TFA, Buffer B: 80% acetonitrile in 0.1% TFA. Flow rate is 1 ml/min.

several overlapping protein peaks with retention times ranging from 20 to 25 minutes. The second HPLC fraction contains one single peak with a retention time of 52.8 minutes. These fractions were tested on a dot blot analysis using an antibody against ßAPP C-peptide. Fraction 2 was cross-reactive with the antibody (result not shown).

4-9. Discussion

Brain tissue contains various heparin binding activities (Bladier *et al.*, 1989; Eloumami *et al.*, 1990; Jessell *et al.*, 1990). Human Alzheimer amyloid and the Alzheimer ß amyloid precursor protein have been observed over the years to be associated with glycosaminoglycans (Snow *et al.*, 1987; Glenner *et al.*, 1984). Since neuroblastoma cells can show different morphological forms depending on growth conditions (Gurwitz and Cunningham 1990), it is worthwhile to characterize their heparin-binding proteins and look for any relationship with the amyloid precursor protein.

Polypeptides of 41, 60, and 89 Kd have been purified from neuroblastoma cells using the heparin-binding purification protocol of Ceri *et al.* (1981).

Since the cells were washed free of medium before homogenization, these proteins are associated with the cells. Their presence in the 100,000g pellet indicates that they are bound to the cell membrane. In the heparin-binding fraction, the 41 and 89 Kd proteins were immunoreactive with antiserum to the carboxyl terminal of the ß amyloid precursor protein. The molecular weights of these polypeptides are lower than those reported for human fibroblasts where cross-reactive bands with molecular weights of 228 and 130 Kd were seen in SDS gels (Autilio-Gambetti *et al.*, 1988). However, the molecular weights of these two polypeptides fall in the range of cellular ßAPP fragments described by Dewji *et al.* (1990). We noted that several minor higher molecular weight bands in the total cell membrane homogenate were also immunoreactive. No anti-carboxyl terminal immunoreactive protein bands were seen in the heparin-unbound fraction. When we tested the heparin-binding fraction by dot blot analysis with an antibody to the ßAP region of ßAPP (anti-ßAPP$_{695}$ 597-624); a positive reaction was observed. This would indicate that the last 100 amino acids of ßAPP were present in these heparin-binding proteins and the fragment-generating

process occurred in the amino terminal half of the protein. Our identification of 89, 76, 60, and 41 Kd immunoreactive proteins from neuroblastoma cells supported the observations of Simpson *et al.* (1989). Using an antiserum raised to an extracellular domain (residues 556-566) of the ßAPP, they reported the presence of 70 and 88 Kd proteins in western blots of Alzheimer's disease, Down's syndrome and control human brains. In an experiment using the Triton X-100 soluble fraction of PC12 cells, they observed a pattern similar to what we observed in the NB41A3 cells.

Recently, Castro *et al.* (1990) proposed that ßAPP may function as part of a feedback control mechanism that modulates the production of nerve growth factors. It is possible that the presence or absence of different domains in the ß amyloid precursor protein dictate the metabolic pathway involved in its processing. Simpson *et al.* (1989) reported that the 88 Kd protein was reduced in three out of six brains with Alzheimer pathology and they suggest that an imbalance between pathways may lead to amyloid deposits. In our study, the anti-C immunoreactive components were not reactive with anti-Kunitz antibody, indicating they may not contain Kunitz proteinase inhibitor sequences.

Chapter 5

The Toxicity and Interaction of a Synthetic Amyloid ß1-40 Peptide with Mouse Neuroblastoma Cell Line NB41A3.

5-1. Introduction

Experimental studies have shown unexpected biological activities from the peptide products of degenerating neurons. Alzheimer ß amyloid peptides may have neurotrophic effects in rat neuronal hippocampal cultures (Araujo and Cotman, 1992; Whitson *et al.*, 1989; Whitson *et al.*, 1990; Yankner *et al.*, 1990b). At higher concentrations, neurotoxic effects have positively been observed in rat cells (Yankner *et al.*, 1990a; 1990b; 1989). The neurotoxicity of amyloid ß peptide is potentiated by nerve growth factor (Yankner *et al.*, 1990a) and, in turn, ß amyloid peptide may potentiate the toxicity of glutamate in cultured cortical neurons (Koh *et al.*, 1990; Mattson *et al.*, 1992). Amyloid ß peptide also increased neuronal susceptibility to injury by glucose deprivation (Copani *et al.*, 1991). Neurotoxicity has also been seen when SDS-insoluble amyloid fractions, called amyloid cores, isolated from Alzheimer Disease brains were injected into the rat brain (Frautschy *et al.*, 1991). At the

same time, Roher *et al.* (1991) have shown that isolated ß amyloid peptide reduces the survival of sympathetic neurons in culture. Recently, Kammesheidt *et al.* (1992) showed age related increases in the deposits of ß amyloid peptide immunoreactivity in transgenic mice expressing the carboxyl-terminal fragment of the Alzheimer amyloid precursor protein. The observation of abnormal appearing neurites in the CA2/3 region of the hippocampus of these transgenic mice supports the correlation between amyloidogenesis and specific neuropathology. Similarly, Cai *et al.* (1993) showed that human neuroblastoma cell line M17 transfected with a mutant ß amyloid precursor protein gene released 6 times more ß amyloid peptide into the medium.

Although these studies have implicated ß amyloid peptide in the neurodegenerative process, the mechanism of action is still unknown (Hardy and Higgins, 1992; Kosik, 1992; Mattson and Rydel, 1992a; Giordano *et al.*, 1994; Kowall, 1994). Besides excitotoxicity and alterations in calcium homeostasis (Koh *et al.*, 1990; Mattson *et al.*, 1992b; Hartmann *et al.*, 1994) other possible mechanisms of ß amyloid toxicity have been proposed in recent years, including membrane changes (Nitsch *et al.*, 1992; Arispe *et al.*, 1993), disruption

of cytoskeletal transport (Grundke-Iqbal *et al.*, 1986; Nukina *et al.*, 1992; Caputo *et al.*, 1992), complement activation (Rogers *et al.*, 1992), free radical generation (Hensley *et al.*, 1994), and local acute phase reaction (Abraham *et al.*, 1988; Griffin *et al.*, 1989).

Since primary brain neuronal cultures are difficult to establish and inefficient for large-scale screening procedures, we wished to determine if ßAP neurotoxicity could be assayed in other continuous neuronal cell lines using serum-free media. This chapter extends the ß amyloid peptide neurotoxicity studies to a cultured mouse neuroblastoma cell line NB41A3, and discusses the mechanism of neuroblastoma-ßAP interaction.

5-2. Amyloid ß1-40 peptide synthesis and cell culture

Synthetic ß1-40 peptide (See Section 3-4) was purified by gel filtration chromatography and HPLC (See Section 3-5). An amino acid analysis and a dot blot analysis were used to verify that the synthetic ß1-40 has the expected amino acid composition and immunoreactivity. Cultures of mouse neuroblastoma cells were obtained from ATCC and cultured in HL-1 medium

(Ventrex Laboratories, Inc., Portland, ME, USA) supplemented with 10% fetal calf serum (FCS), 2.5 mM glutamine, 50 units/ml penicillin and 50 μg/ml streptomycin (Sigma Chemical Co., St. Louis, MO, USA) in a 5% CO_2 humidified incubator.

After being washed with serum-free media, approximately 5000 cells were plated into each well of 24 well plates. Control cells were plated in FCS-free medium only, while experimental groups were plated in FCS-free medium with varying concentrations of the synthetic ß1-40 peptide. In the experiments designed to study the albumin effect, neuroblastoma cells were cultured in FCS-free medium with bovine serum albumin (BSA) concentrations ranging from 0 to 200 μg/ml. Quadruplicates of each assay were performed.

5-3. The interaction of ß1-40 with mouse neuroblastoma cells: a toxicity assay

Three different assays for ß1-40 toxicity were used:

1). Toxicity of synthetic ß1-40 was measured by observing changes in cell number. Twenty-four hours after plating the cells, 5 fields (0.708 mm^2 per field) were chosen from each well, and the

cell number in each field was counted using a x125 inverse phase microscope. A low number of cells compared to the control in the field indicates slow cell growth.

2). Cell growth was also evaluated by change in total cell protein. Six days after plating the cells, 1 ml of cell suspension was centrifuged. The resulting cell pellet was homogenized in one ml of PBS buffer. A 50 μl sample was assayed for protein using the Pierce BCA Microprotein Assay Kit (See Appendix II).

3). The release of a cytosolic enzyme, lactic dehydrogenase (LDH), by cells into the cell culture medium was used as an indicator of cell death. An Oxford LK-100 Cytotoxicity Assay Kit (Oxford Biomedical Research, Inc., Rochester Hill, MI, USA) was used in this assay. After centrifugation to remove cultured cells, 100 μl of conditioned media were mixed with 100 μl of LDH substrate, and incubated for one hour at room temperature. The reaction was stopped by adding 50 μl 1M HCl and the absorbance was measured at 492 nm. Because only a dead cell releases its cytosolic LDH into the medium, the amount of LDH

in the conditioned medium is proportional to the number of accumulated dead cells in the culture. This was denoted as LDH related to cell death (dLDH). When the cell culture was incubated with cell lysing reagent for 1 hour, all the cells in the culture should be lysed. Thus the detected LDH activity in the media is proportional to the total number of cells in the culture and is called tLDH. The difference between the tLDH and dLDH is the LDH released from the living cells (cLDH).

5-4. Cell growth curve

In order to examine if tLDH and dLDH truly reflect cell growth and cell death in the culture, a cell growth curve was developed using LDH data. Figure 5-1 shows that tLDH, an indicator of the total number of cells in the culture, increases rapidly within the first week, representing the rapid cell growth in the exponential phase. After day 6, tLDH release reaches a plateau, indicating a stationary phase. The cell protein assay, another indicator of the total number of cells in the culture, gives a similar curve to that of the tLDH (data not shown). The cell death-related LDH, dLDH, is low in the first 5 days of the culture, but it

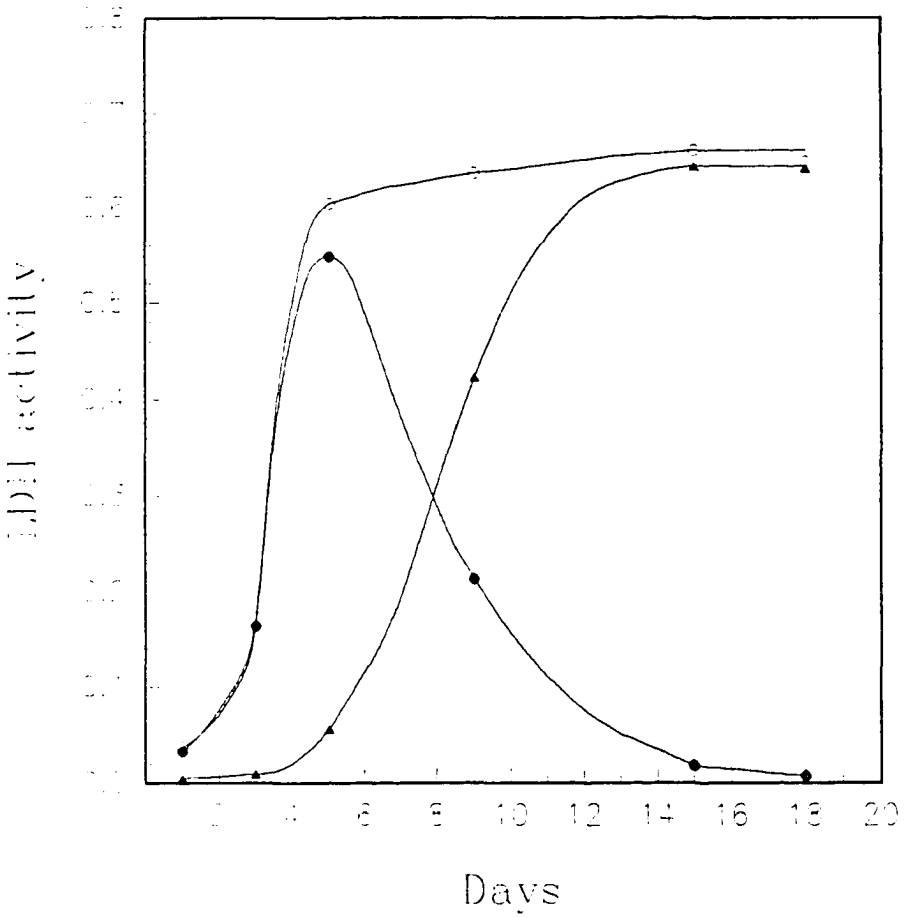

Figure 5-1. Cell growth measured by LDH activity. Cells were cultured in FCS-free medium.
▪ – ▪ tLDH; ▲ – ▲ dLDH; ● – ● cLDH.

rises rapidly after day 6 and eventually reaches the tLDH level at day 15, representing the cell death phase. The difference between tLDH and dLDH, which represents the number of living cells in the culture (cLDH), increases together with tLDH during the first 6 days when cells are in the exponential growth phase, and then decreases when cell death rate rises rapidly. This typical cell growth curve presented by the LDH data suggests that cells are in the exponential growth phase up to day 5, and that tLDH and dLDH could be used to evaluate cell growth and cell death in the cultures.

5-5. Amyloid ß peptide toxicity to neuroblastoma cells cultured in FCS-free medium

When cells were cultured in serum-free medium with 100 μg/ml BSA, different cell growth rates were observed at various ß1-40 peptide concentrations. The cell number counts indicated that there were more living cells in the group without ß1-40 peptide in the medium. Cell protein and tLDH were also lower in the ß1-40 treated groups. The higher the amyloid ß1-40 peptide concentrations, the lower the cell growth (as indicated by cell number) in the culture and the lower the cell protein and tLDH were (Figure 5-2). These data

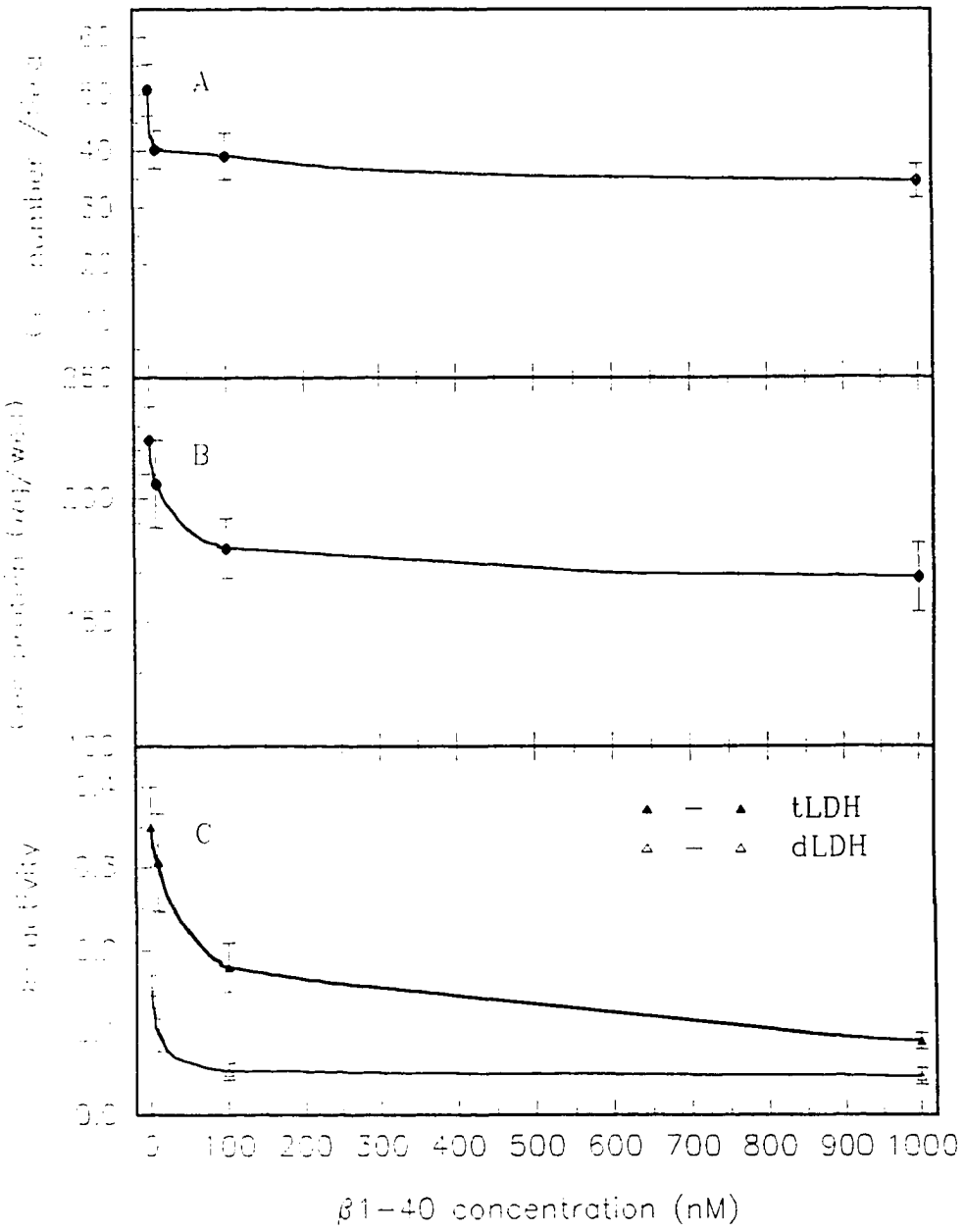

Figure 5-2. The effect of β1−40 on cultured neuroblastoma cells. High β1-40 concentrations lead to low cell growths. A: Cell number; B: Cell protein; C: LDH activity.

confirm the lower cell growth in the ß1-40 treated cells and suggest that ß1-40 has a toxic effect on cultured neuroblastoma cells. Surprisingly, the indicator of cell death, dLDH, is also lower in the ß1-40 treated cells than in the control group. The implications of lower cell death (dLDH) in ß1-40 treated cultures will be discussed later in this chapter in Section 5-8.

5-6. Bovine serum albumin stimulates neuroblastoma cell growth

In the absence of ß1-40 peptide, neuroblastoma cells were first cultured in a serum-free medium with varying BSA concentrations. Experimental data indicated that cells grew better in the presence of BSA. As shown in Figure 5-3, there was as much as a 20% increase in cell numbers and as much as 32% increase of cell protein in the groups where BSA was present.

A similar experiment was performed with 100 nM ß1-40 concentration. There was less overall cell growth in this experiment because of the addition of ß1-40 peptide. However, a similar cell growth - BSA concentration relationship was observed (Figure 5-3),

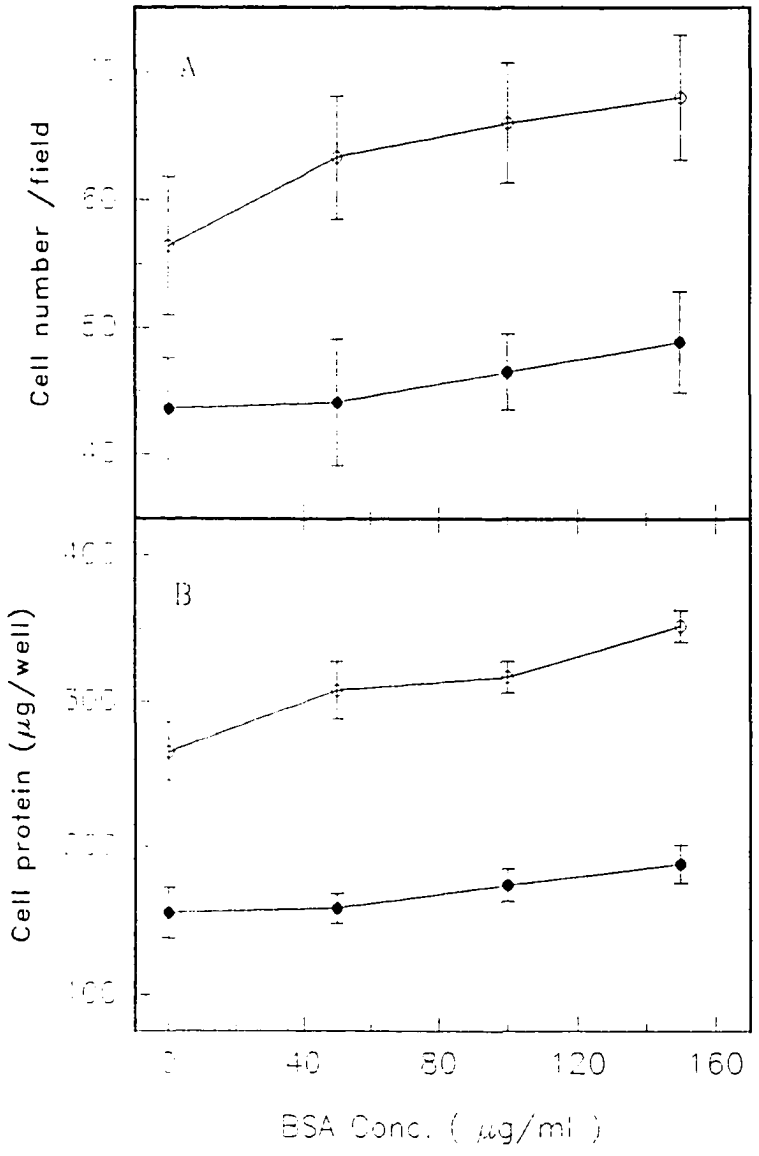

Figure 5-3. The effect of BSA on cell growth in cultures with or without β1-40 peptide treatment. A: Cell number count. B: Cell protein.
○ - ○ Without β1-40 treatment.
● - ● With 100 nM β1-40 peptide.

cell number increased up to 12% and total cell protein increased up to 21% in the presence of BSA.

At all tested BSA concentrations, BSA stimulated neuroblastoma cell growth despite ß1-40 peptides' presence. However, the trophic effect of BSA was less obvious when ß1-40 was added. In other words, the ß peptide toxicity might be larger in the presence of BSA.

5-7. The effect of BSA on ß1-40 toxicity

If ß amyloid peptide toxicity is evaluated as the percentage decrease of cell growth by comparing data from cultures with zero and 100 nM ß peptide treatment, then higher ß peptide toxicity was observed in the presence of BSA. For instance, a 35% cell growth decrease was observed by adding 100 nM ß1-40 peptide to the culture without BSA, while in the presence of 50 µg/ml BSA, 100 nM ß1-40 peptide inhibits cell growth by 42%. This suggests a possible interaction between BSA and ß1-40 peptide.

Two further experiments were conducted at various ß1-40 concentrations with: 1) no BSA and 2) a BSA concentration of 100 µg/ml. In both experiments, cell growth decreased with increasing ß1-40 concentrations,

indicating a dose-dependent toxic effect of amyloid ß1-40 peptide (Figure 5-4). However, when data from these two experiments were compared, it was observed that the ß1-40 inhibition of cell growth was higher in the BSA-containing cultures. It appeared that ß1-40 toxicity increased when BSA was present (Figure 5-4).

Neuroblastoma cells were also cultured at a constant ß1-40 concentration but varying BSA concentrations to examine the BSA - ß peptide interaction. Amyloid ß1-40 toxicity was calculated as percentage of cell growth inhibition by comparing cultures, which grew at the same BSA concentration, with or without ß peptide treatment. As shown in Figure 5-5, with increasing BSA concentrations, amyloid ß1-40 led to a higher percentage of cell growth inhibition, as indicated by both cell number and cell protein assay. This suggests BSA could potentiate the toxicity of amyloid ß1-40 peptide. The fact that BSA was able to bind to ß peptide (Vyas *et al.*, 1992) suggests that the interaction between the BSA and ß1-40 peptide may be related to the transport of ß1-40 into the cell or the solubility of ß1-40 peptide in the media.

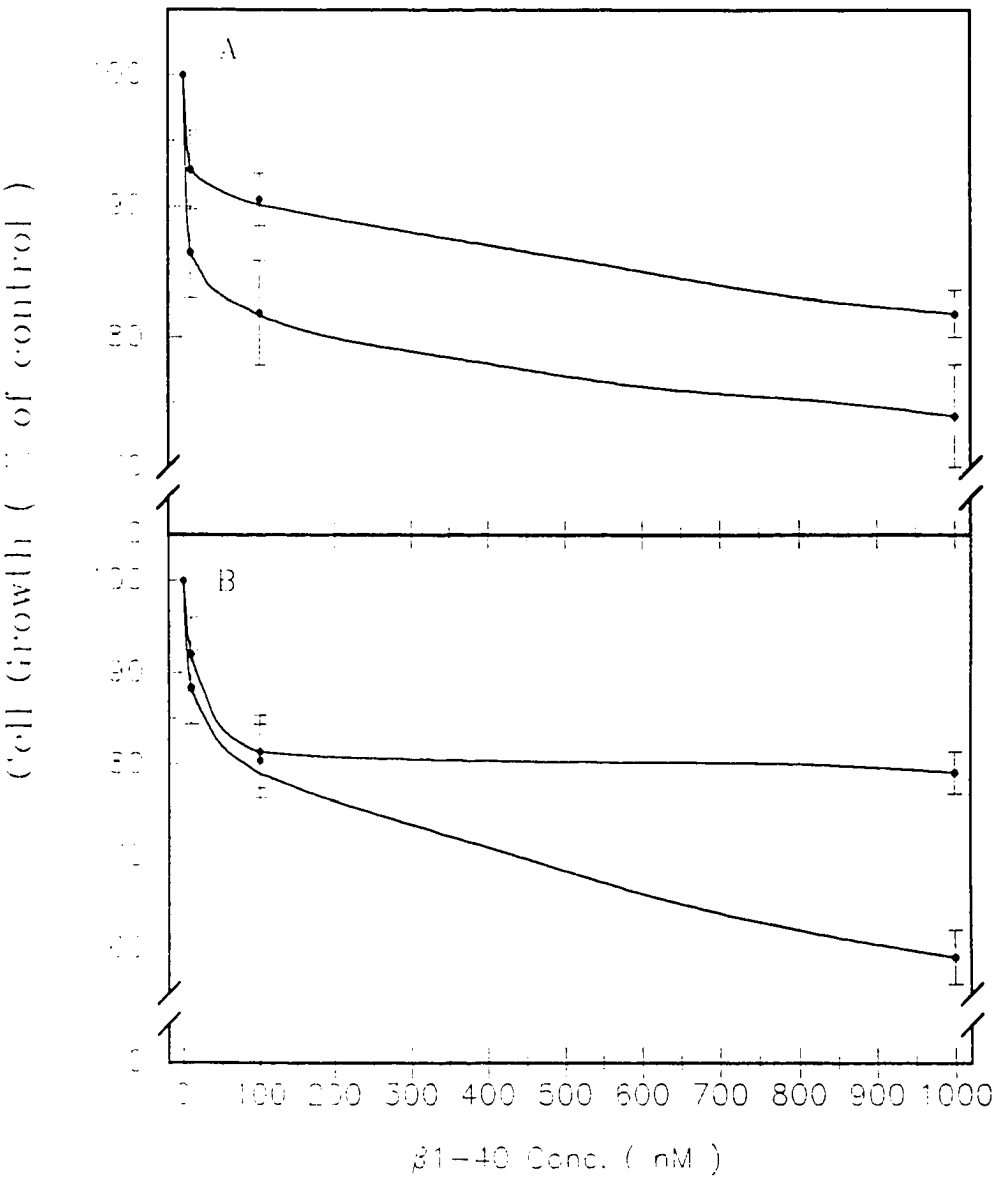

Figure 5-4. The effect of β1-40 on cell growth. The β1-40 induced cell growth inhibitions were compared at BSA=0 (· – ·) and BSA=100 μg/ml (• – •). Cell growth was measured by A: Cell number count; B: Cell protein. At the same β1-40 concentration, lower cell growth was observed for 100 μg/ml BSA groups.

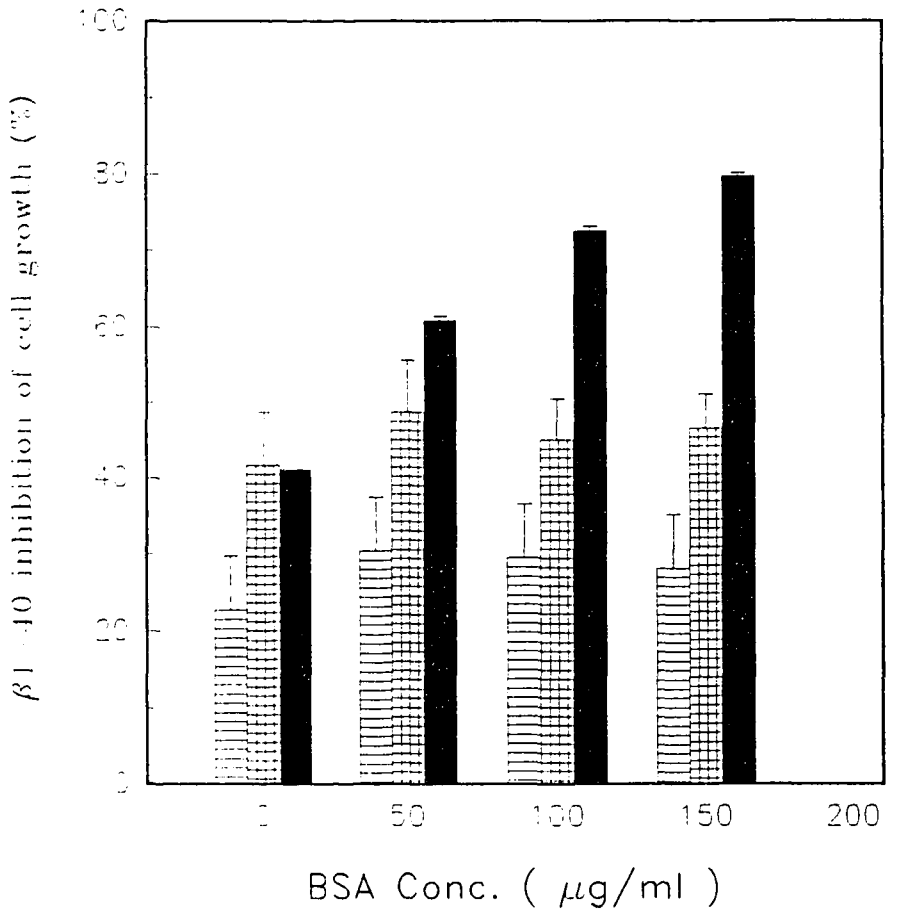

Figure 5-5. The effect of BSA on βAP induced cell growth inhibition. ▤, Cell number; ▦, Cell protein; ■, LDH activity. β1-40 concentration is 100 nM. In the presence of BSA, 100 nM β1-40 causes higher cell growth inhibition.

5-8. Mathematical models of ß1-40 toxicity Mechanism

The above experimental results indicate that cultured neuroblastoma cells grow more poorly in ß1-40 treated cultures. This "toxic effect" on cultured neuroblastoma cells could be caused by ß1-40 via: 1) inhibiting cell growth rate; 2) increasing cell death rate; or 3) some combination of each.

Since dLHD is an indicator of accumulated dead cells in the culture, the experimental data (Figure 5-2) showed that the ß1-40 treated cell culture has fewer dead cells than the control. The ß1-40 treated culture also has a smaller total number of cells growing. One valid hypothesis based on this observation is that ß1-40 toxicity in cultured neuroblastoma cells involves the inhibition of cell growth rate, rather than an increase in the cell death rate. This growth-inhibiting effect would not be observed in primary neuronal cultures where there is little or no growth of new cells.

5-8-1. Mathematical descriptions of the accumulated dead cells in control and in ß1-40 treated cultures

The neuroblastoma cell growth curve (Figure 5-1) indicates that the cultures were in their exponential growth phase from day 1 to day 5. The dLDH data representing accumulated dead cells in the cultures were obtained at day 5, falling in the range of exponential cell growth phase. During the exponential growth phase, the change of cell number can be expressed in the following first order differential equation:

$$\frac{dx}{dt} = \mu x$$

Where x is the cell number and μ is the instantaneous cell growth rate. Assuming the cell growth rate does not change with time (t) during the exponential cell growth phase, the cell number in the control group at any moment equals the solution of the first order differential equation

$$\frac{dx}{dt} = \mu x$$

$$\frac{dx}{x} = \mu dt$$

Assuming at t=0, $X(0)=X_0$

By integrating both sides of the equation, we get

$$\int_{X_0}^{X}\frac{dx}{x}=\int_0^t \mu dt$$

$$\ln\frac{X}{X_0}=\mu t$$

$$X=X_0 e^{\mu t}$$

Where X is the total cell number in the culture at time t, X_0 is the original cell number plated into the culture at t=0, $\mu>0$ is cell growth rate in the control group, and $t\geq 0$ is the time since the culture started.

Let A be the cell death rate in the control group and $A\leq 1$. If A does not change with time during the exponential cell growth phase, then at any moment, $AX_0e^{\mu t}$ cells are dying in the culture. The accumulated dead cells at time t (denoted by D), which corresponds to dLDH in the control culture, is the integration of $AX_0e^{\mu t}$ from time 0 to time t. That is

$$D=\int_0^t AX_0e^{\mu t}dt$$

$$D=\frac{AX_0}{\mu}(e^{\mu t}-1) \qquad A\leq 1$$

Because the same number of cells (X_0 cells) was plated into both control and ß1-40 treated groups at the beginning of the culture, then at any moment t, the cell number in a ß1-40 treated group, denoted by X_β, is the solution of the differential equation

$$\frac{dx}{dt}=vx$$

i.e.

$$\frac{dx}{x}=v\,dt$$

Where v is cell growth rate in ß1-40 treated culture. Integrate both sides of the equation, we get

$$\int_{X_0}^{X_\beta}\frac{dx}{x}=\int_0^t v\,dt$$

$$\ln\frac{X_\beta}{X_0}=vt$$

$$X_\beta=X_0e^{vt}$$

Where X_β is the cell number at time t, X_0 is the cell number at t=0, $v\geq 0$ is the cell growth rate in the ß1-40 peptide treated group.

Assume $B \leq 1$ is the cell death rate in a ß1-40 treated culture, and assume B does not change with time during the exponential cell growth phase. Thus, at any moment t, there would be BX_0e^{vt} cells dying. And the number of accumulated dead cells in ß1-40 treated cultures (denoted as D_β) is the integration of BX_0e^{vt} from time 0 to time t.

$$D_\beta = \int_0^t BX_0 e^{vt} dt$$

$$D_\beta = \frac{BX_0}{v}(e^{vt}-1) \qquad B \leq 1$$

Experimentally determined D and D_β values are derived from dLDH data in the control group and the ß1-40 treated culture, respectively. Starting with the same X_0, as shown in Figure 5-2, the observed dLDH in the control group (D) is higher than that in the ß1-40 treated group (D_β). Therefore, the function of $D-D_\beta$ is greater than zero, as determined experimentally. Theoretically, at the starting points of the cultures, no cells were dead. That is, when t=0, $D=D_\beta=0$. The experimentally determined D at0 day 1 is very close to zero (Figure 5-1).

5-8-2. Possible mechanisms of ß1-40 toxicity

The toxic effect of ß1-40 on cultured neuroblastoma cells could be caused: 1) by increasing cell death; 2) by inhibiting cell growth; or 3) by a combination these two mechanisms. The above three possibilities are discussed below.

A. First hypothesis: ß1-40 increases cell death rate but does not inhibit cell growth

Under this hypothesis, cells grow at the same rate in the control and the ß1-40 treated cultures, while the cell death rate is higher in the ß1-40 treated group than in the control group. That is, μ=v, and B>A. Now to examine whether the function $D-D_{\beta}$ follows the experimental observation, i.e. if $D-D_{\beta}\geq 0$.

$$D-D_{\beta}=X_0\frac{A}{\mu}(e^{\mu t}-1)-X_0\frac{B}{\nu}e(^{\nu t}-1) \qquad \mu=\nu \qquad A<B$$

$$D-D_{\beta}=\frac{X_0}{\mu}(e^{\mu t}-1)(A-B)$$

$$\because A<B, \qquad \therefore A-B<0, \qquad \because e^{\mu t}-1\geq 0 \qquad when \quad t\geq 0$$

$$\therefore D-D_{\beta}<0$$

That is

$$D<D_{\beta}$$

Under the hypothesis that ß1-40 peptides increases cell death rate but does not inhibit cell growth rate, dLDH in the control should be lower than dLDH in the ß1-40 treated culture. This is opposite to the experimental observation of a high dLDH in the control culture. Therefore, this hypothesis is not valid.

B. Second hypothesis: ß1-40 peptide inhibits cell growth rate but does not increase cell death rate in the culture

Under this assumption, the cell death rate is the same in both control and ß1-40 treated groups (A=B). However, the cell growth rate in ß1-40 treated culture is slower than in the control group (μ>v). Thus:

$$D-D_{\beta}=X_0\frac{A}{\mu}(e^{\mu t}-1)-X_0\frac{B}{v}(e^{vt}-1) \qquad \mu>v, \qquad A=B$$

$$D-D_{\beta}=X_0A[\frac{(e^{\mu t}-1)}{\mu}-\frac{(e^{vt}-1)}{v}]$$

$$D-D_{\beta}=X_0A(\frac{e^{\mu t}}{\mu}-\frac{e^{vt}}{v}-\frac{1}{\mu}+\frac{1}{v})$$

When t=0,

$$D-D_{\beta}=X_0A\left(\frac{1}{\mu}-\frac{1}{\nu}-\frac{1}{\mu}+\frac{1}{\nu}\right)=0$$

The first derivative of $D-D_{\beta}$ is needed to determine if $D-D_{\beta}\geq 0$. The first derivative of $D-D_{\beta}$ equals

$$(D-D_{\beta})'=\left[X_0A\left(\frac{e^{\mu t}}{\mu}-\frac{e^{\nu t}}{\nu}-\frac{1}{\mu}+\frac{1}{\nu}\right)\right]'$$

$$(D-D_{\beta})'=X_0A\left(\mu\frac{e^{\mu t}}{\mu}-\nu\frac{e^{\nu t}}{\nu}\right)$$

$$(D-D_{\beta})'=X_0A(e^{\mu t}-e^{\nu t})>0 \qquad when \qquad \mu>\nu, \qquad t>0$$

The first derivative of $D-D_{\beta}$ is greater than zero, indicating that the value of $D-D_{\beta}$ will rise with increasing time. At t=0, $D-D_{\beta}=0$. Therefore, at any time when t>0, $D-D_{\beta}$ is positive, the observation follows that dLDH in the control (D) is larger than the dLDH in the ß1-40 treated culture (D_{β}). The hypothesis that ß1-40 inhibits cell growth rate but does not increase cell death rate in the culture is supported by the experimental observation.

C. Third hypothesis: ß1-40 inhibits cell growth rate as well as increases cell death rate in the culture

In this case, not only do the cells grow more slowly, but also the cell death rate is higher in the ß1-40 peptide treated culture. That is, μ>v and A<B. Follow an analysis similar to the previous one, we find

$$D-D_\beta=X_0\frac{A}{\mu}(e^{\mu t}-1)-X_0\frac{B}{\nu}(e^{\nu t}-1)$$

$$D-D_\beta=X_0(\frac{Ae^{\mu t}}{\mu}-\frac{Be^{\nu t}}{\nu}+\frac{B}{\nu}-\frac{A}{\mu})$$

$$When\ t=0,\qquad D-D_\beta=X_0(\frac{A}{\mu}-\frac{B}{\nu}+\frac{B}{\nu}-\frac{A}{\mu})=0$$

Because A, B, μ, v are constants, when t is sufficiently big

$$D-D_\beta=X_0(\frac{Ae^{\mu t}}{\mu}-\frac{Be^{\nu t}}{\nu})$$

The first derivative of $D-D_\beta$ is needed to determine if $D-D_\beta$ is bigger or smaller than zero. It equals

$$(D-D_\beta)'=[X_0\frac{A}{\mu}(e^{\mu t}-1)-X_0\frac{B}{\nu}(e^{\nu t}-1)]'$$

$$(D-D_\beta)'=X_0(Ae^{\mu t}-Be^{\nu t})$$

Because X_0 is a positive real number, the factor $Ae^{\mu t}-Be^{\nu t}$ determines if $(D-D_\beta)'$ is positive or negative.

$$(D-D_\beta)'>0 \quad if \quad Ae^{\mu t}>Be^{\nu t}$$

Take the ln of both sides, we get

$$\ln(Ae^{\mu t})>\ln(Be^{\nu t})$$

$$\ln A+\mu t>\ln B+\nu t$$

That is

$$(\mu-\nu)t>\ln B-\ln A \qquad \mu>\nu \qquad B>A$$

And therefore,

$$(D-D_\beta)'>0 \quad if \quad t>\frac{\ln B-\ln A}{\mu-\nu}$$

We could also prove that

$$(D-D_\beta)'<0 \quad if \quad t<\frac{\ln B-\ln A}{\mu-\nu}$$

Combine above discussion,

$D-D_{\beta}=0$ when $t=0$

$D-D_{\beta}>0$ when t is sufficiently big

$(D-D_{\beta})'<0$ when $if\ t<\frac{\ln B-\ln A}{\mu-v}$

$(D-D_{\beta})'>0$ when $if\ t>\frac{\ln B-\ln A}{\mu-v}$

This means the value of $D-D_{\beta}$ starts at zero and decreases until time $t=(\ln B-\ln A)/(\mu-v)$. During this period, $D-D_{\beta}$ is negative (Figure 5-6). From the time $t=(\ln B-\ln A)/(\mu-v)$ $D-D_{\beta}$ starts to increase, eventually the value of $D-D_{\beta}$ becomes positive. Its biological meaning is that at the beginning of cell culture (t=0), dLDH in both control and ß1-40 treated groups is zero, and $D-D_{\beta}=0$. Then, during a period in which $D-D_{\beta}$ is negative, the dLDH in the control group (D) should be smaller than that in the ß1-40 treated culture (D_{β}). As time goes on, dLDH in the control eventually will be higher than that in the ß peptide treated group.

The dLDH assay, conducted at day 5, indicates that the dLDH in the control was higher than that in the ß1-40 treated culture. Both the 2nd and 3rd hypotheses are

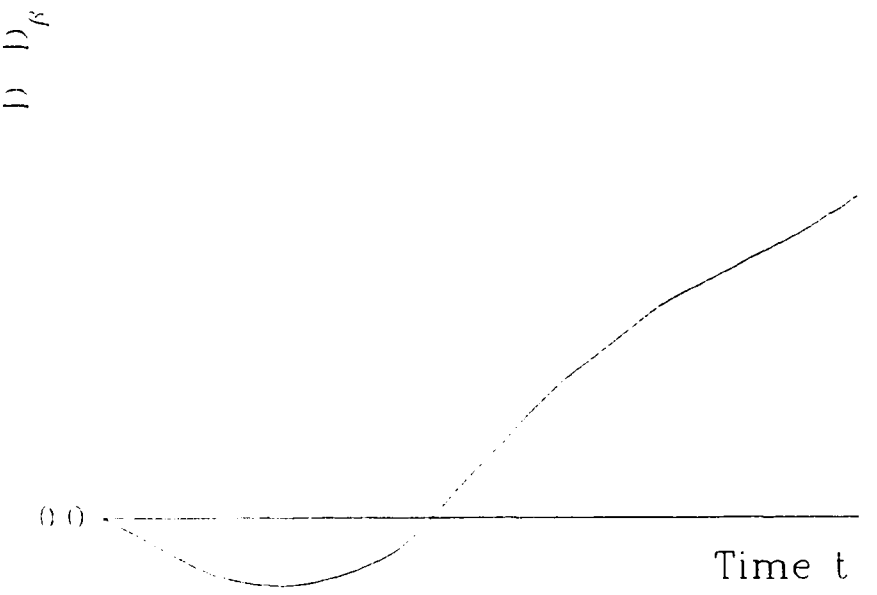

Figure 5-6. Demonstration of the function of D D_β in continuous cell culture. $D-D_\beta$ is below zero initially and then increases and becomes positive when time t is sffi-ciently big.

consistent with the observed dLDH data. It could be concluded that ß1-40's toxic effect on cultured neuroblastoma cells must involve the inhibition of cell growth rate. However, it may or may not involve any increase in cell death rate in the culture. This is important when considering ß peptide's toxic effects on continuously- growing cells. The inhibition of cell growth by ß peptide will not be observed in primary cell cultures, since these cells do not divide.

5-9. The interaction of ß1-40 with mouse neuroblastoma cells: a binding assay

In the previous sections, it has been demonstrated that the ß amyloid peptide affected growth of the cultured mouse neuroblastoma cells, suggesting a possible interaction of ß1-40 with cells. As of 1988, only one study using an immunohistochemical method has demonstrated the binding of ß amyloid to tissue (Allsop *et al.*, 1988). A peptide, ß8-17, was shown to bind to the vesicular elements of the pancreas and the adrenal gland. Allsop *et. al.* (1991) extended this study by showing specific binding of the ß8-17 peptides to rat cortical gray matter membranes. In their experiments, binding showed a clear dependence on time, temperature,

pH, and membrane concentration. In this section, the possibility of the ß amyloid peptide exerting its biological effects on neuroblastoma cells through a ligand - cell binding mechanism will be discussed.

5-9-1. Radioactive labeling of ß1-40 peptide

The chemical component of ^{125}I Bolton-Hunter Reagent (^{125}I-BHR) from New England Nuclear (NEN, Du Pont Co., Wilmington, DE, USA) is N-succinimidyl-3-(4-hydroxy-3-[^{125}I] iodophenyl) propionate. The reagent's active ester acylates primary amine groups as well as reacts with water. Thus, the amine groups of two lysine residues in ß1-40 peptide were radioactively labeled by reacting with ^{125}I-BHR (initial specific activity of 2200 Ci/mmole). In a NENSURE^{TM} vial, 250 μCi of reagent was provided in anhydrous benzene. Immediately prior to using ^{125}I-BHR for peptide labeling, the benzene was evaporated to dryness by inserting a needle through the septum as an intake for a gentle stream of dry air.

About 1 mg of ß1-40 peptide was dissolved in 50 μl 0.1 M borate (pH 8.5) - acetonitrile buffer (65:35 v/v). After the ^{125}I-BHR was air dried, ß peptide was added to the vial. The reaction was carried out at $4^{0}C$ overnight. At the end of the reaction, glycine was

added to reach the final concentration of 0.2 M. The amine group on the free glycine reacts with the excess unchanged ester on ^{125}I-BHR.

Gel filtration chromatography was used to separate labeled ß peptide from the glycine conjugate and hydrolysis products. A Sephadex G-25 column was equilibrated in 1% acetic acid before adding the reaction mixture to the top of the column. The column was then washed with 1% acetic acid. Forty fractions of 50 drops per tube were collected. Peptide components were monitored at a UV absorption of 252 nm. The radioactivity of each fraction was measured as counts per minute (cpm) on a Searle Automatic Gamma System, Model 1195. Figure 5-7 shows the separation of ^{125}I-labeled ß1-40 peptide from the glycine conjugate and hydrolysis products on a Sephadex G-25 column. The major UV peak was overlapped by a radioactivity peak which contained the radioactively labeled ß1-40 peptide. Fractions 4 - 12 in this peak were combined and used in the experiments.

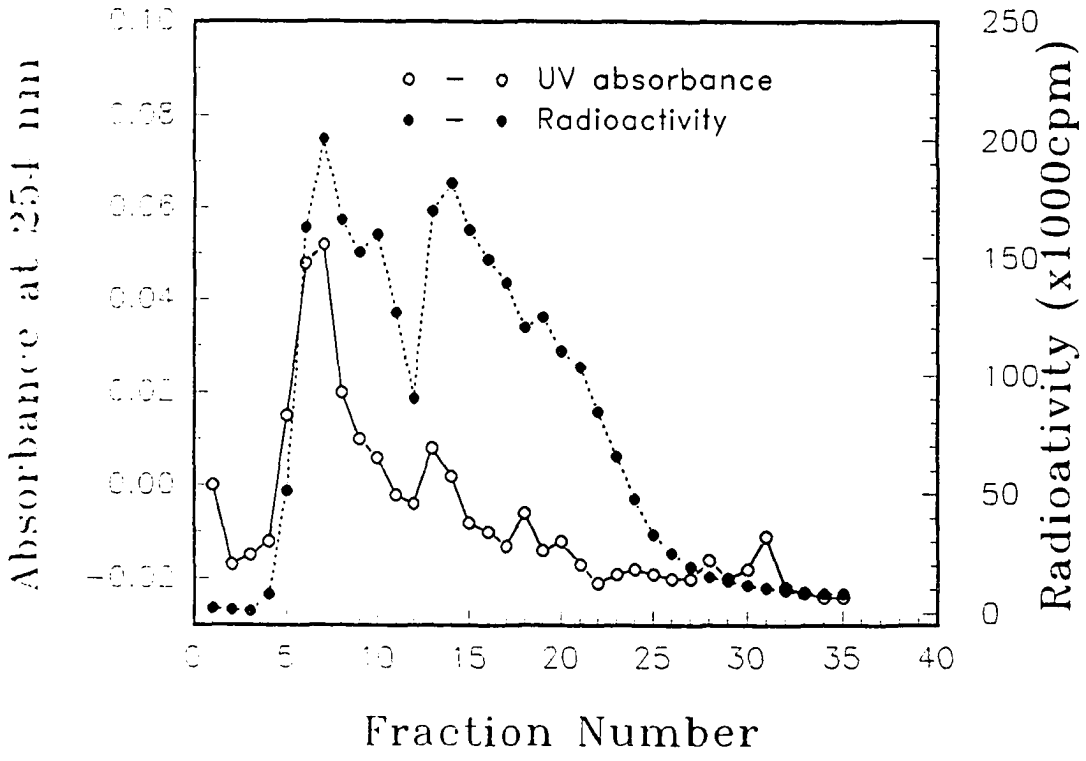

Figure 5-7. Gel filtration separation of radioactively labeled β1-40.

5-9-2. No specific neuroblastoma - ß peptide binding was observed in three hours incubations

About 10^6 cells were washed and plated with FCS-free cell culture medium in 25 cm^2 tissue flasks. After 3 days, neuroblastoma cells were then removed from the tissue culture flasks, resuspended in FCS-free medium in test tubes, and incubated with radioactively labeled ß1-40 peptide at room temperature for 5, 15, 30, or 60 minutes. Cells were collected by centrifugation and washed three times with fresh medium and the radioactivity measured on a Searle Automatic Gamma System. This provides a measure of the total binding of ß1-40 to neuroblastoma cells.

It was hypothesized that the non-labeled ß1-40 would compete with ^{125}I labeled peptides for the binding sites on cell surface and therefore block the specific interaction between cells and the ^{125}I-ß1-40. The addition of non-labeled ß1-40 would therefore reduce the binding measured by radioactivity. Thus the nonspecific binding of ß1-40 to neuroblastoma cells was determined with the addition of 5 times excess of non-labeled ß1-40 to the culture. The difference between the total and non-specific binding indicates the specific interaction of ß1-40 to neuroblastoma cells.

However, with incubation times of up to 60 minutes at room temperature, no specific binding of radioactively labeled ß1-40 to neuroblastoma cells was observed.

Since the shock of removing cells from the flasks may interrupt the cells' physiological condition and cause failure to detect neuroblastoma - ß peptide binding, in the next experiment, cells were first cultured at $37^{0}C$ for two days in FCS free medium containing 100 µg/ml BSA. Under a light microscope, cells were seen to grow into a smooth monolayer. Without physically interrupting cells, ^{125}I ß1-40 was added and cells were allowed to continue to grow at $37^{0}C$ for up to 3 hours. Samples were collected at incubation times of 0.5, 1.0, and 3 hours respectively and were washed three times with fresh cell culture medium before measuring the radioactivity. Again, specific binding of ß1-40 to neuroblastoma was not detected. These experimental results suggested that ß1-40 binding to neuroblastoma cells, if any, is weak and needs a relatively long incubation time or high concentrations of ß amyloid peptide.

5-9-3. Neuroblastoma - ß peptide binding was observed starting at the second day of incubation

Cells were cultured in FCS-free HL-1 medium with 100 μg/ml BSA at 37^{0}C. At replating, radioactively labeled ß1-40 was added to the cell culture at a concentration of 500 nM. Nonspecific binding was assayed in the presence of 7 fold excess of non-radioactive ß1-40 to block the specific interaction between neuroblastoma cells and ß1-40 peptides. Samples were taken each day from day one to day five. Cells were washed three times with fresh medium before determining the bound radioactivity. Specific binding was observed starting from day two (Figure 5-8). Binding increased along with cell growth at least up to day five in the cell culture. The ß peptide binding on cell surfaces was not dissociated by washing cells with 1% acetic acid in 0.5 M NaCl, suggesting the possibility of internalization of ß1-40 peptide into neuroblastoma cells.

5-9-4. Internalization of ß1-40 by neuroblastoma cells

Since it is not unusual for surface-bound peptide to be internalized by cells, a mild acid containing

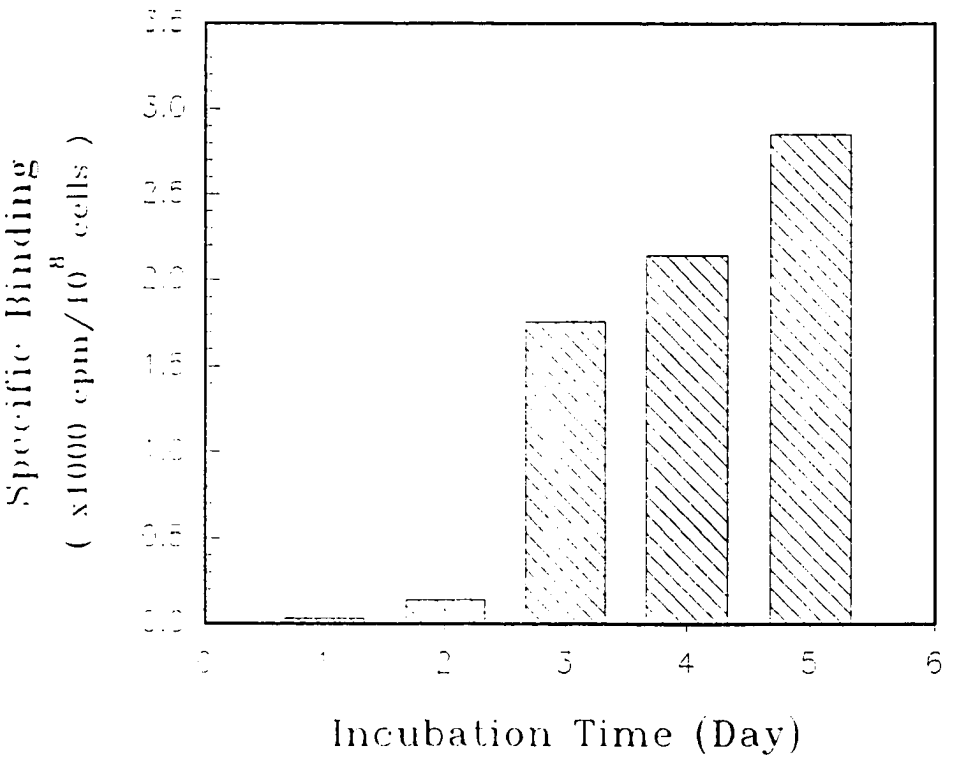

Figure 5-8. Time course of the neuroblastoma-β peptide interaction. Radioactively labeled β1-40 was added to the cell culture at day zero. Only specific binding is shown in this figure.

various NaCl concentrations was used to dissociate surface-bound peptide. Cells were either washed with fresh cell culture medium three times, or washed twice with medium and then washed a third time with 0.15 M to 1.0 M NaCl in 1% acetic acid (pH 4). The dissociation of surface-bound peptide by the acid and NaCl reduced the total as well as the non-specific binding. Specific binding was still observed after the dissociation of cell surface binding. Washing cells with higher concentrations of salt reduced more of the ß1-40 bound to the cell surface. Figure 5-9 shows that about 38.9% specific binding was retained by cells after a 0.15M NaCl/HAc wash, 36.1% and 34.7% specific binding survived 0.5 M and 1.0 M NaCl/HAc dissociation, respectively, indicating about one-third of the ß1-40 is internalized into the neuroblastoma cells.

5-9-5. Neuroblastoma - ß peptide interaction at peptide concentrations from 100 nM to 600 nM

Saturation studies were performed at $37^{0}C$ by incubating cells with ^{125}I labeled ß1-40 for 2 days from a concentration of 50 nM up to 600 nM. Figure 5-10 shows the neuroblastoma - ß1-40 interaction at ß1-40

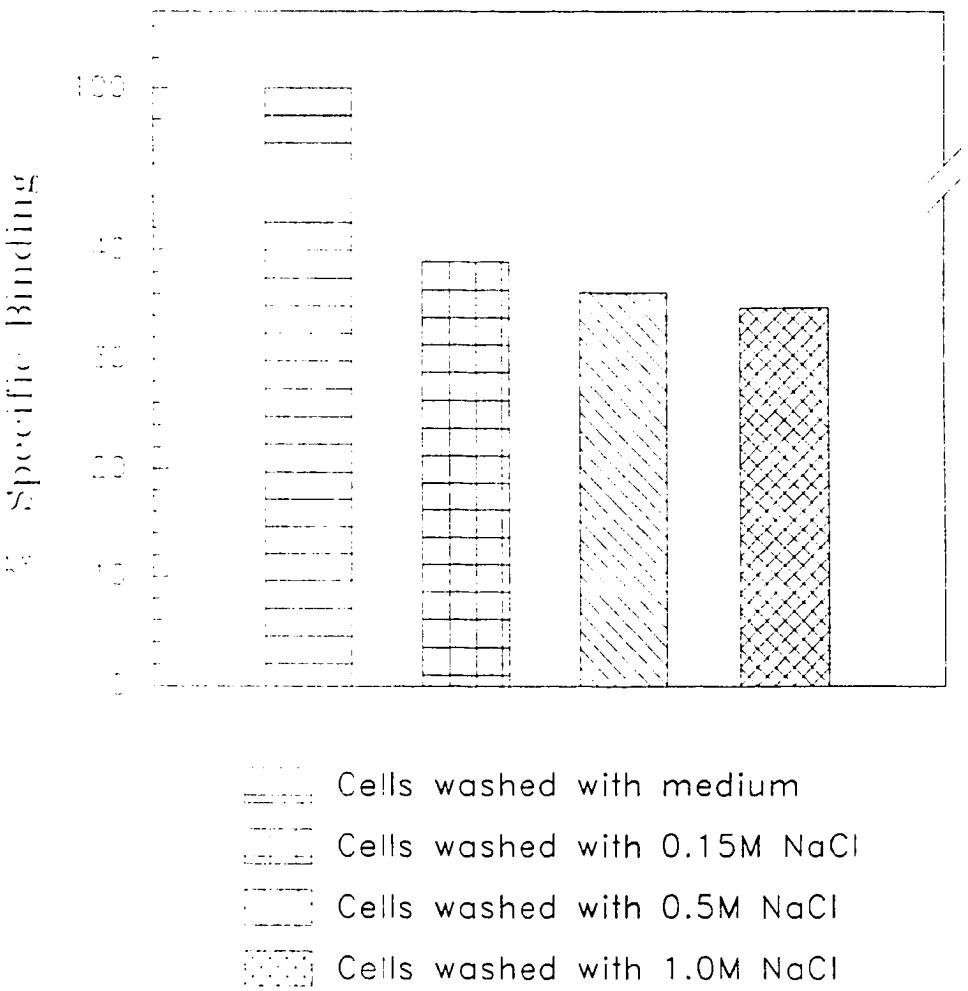

Figure 5-9. The specific binding of β1-40 with neuroblastoma cells under various conditions. Cells were washed with 1% acetic acid containing 0.15 M, 0.5 M, and 1.0 M NaCl, respectively, to dissociate binding on cell surface. The specific binding of cells washed with cell culture medium was taken as 100% and compared with that of cells washed with NaCl/HAc.

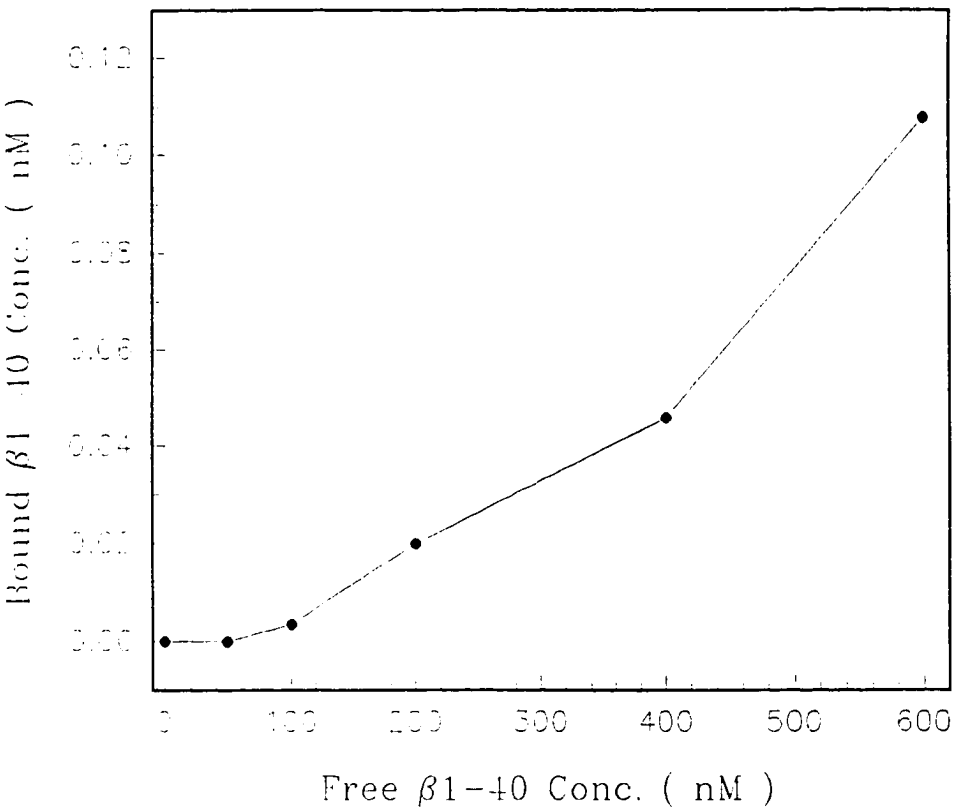

Figure 5-10. Neuroblastoma - β peptide binding at various β1-40 concentrations. About 0.02% of added ^{125}I-β1-40 was bound to neuroblastoma cells. There were 10^5 cells in each counting.

concentrations from 100 nM to 600 nM. Even though the binding was very weak, it was consistent in the five experiments. However, saturation was not reached in the neuroblastoma - ß1-40 binding assay. A possible explanation is that this is a complex interaction between the neuroblastoma cells and ß1-40 peptide, resulting from ß1-40 interacting with more than one type of protein, or one protein molecule interacting with more than one ß1-40 molecule. Also, since there is evidence that ß1-40 is internalized into the cells, cytoplasmic ß1-40 binding molecules could be present.

5-9-6. BSA enhances neuroblastoma - ß peptide interaction

It was shown in section 5-7 that bovine serum albumin (BSA) can stimulate neuroblastoma cell growth and also potentiate ß1-40 peptide toxicity on cultured neuroblastoma cells. In this binding assay, neuroblastoma cells were cultured in FCS-free medium at BSA concentrations equal zero or 100 µg/ml. Radioactively labeled ß1-40 was added to the culture at a concentration of 500 nM for 2 days. Nonspecific binding was measured in the presence of 3,500 nM of non-labeled ß1-40. Figure 5-11 shows that the specific

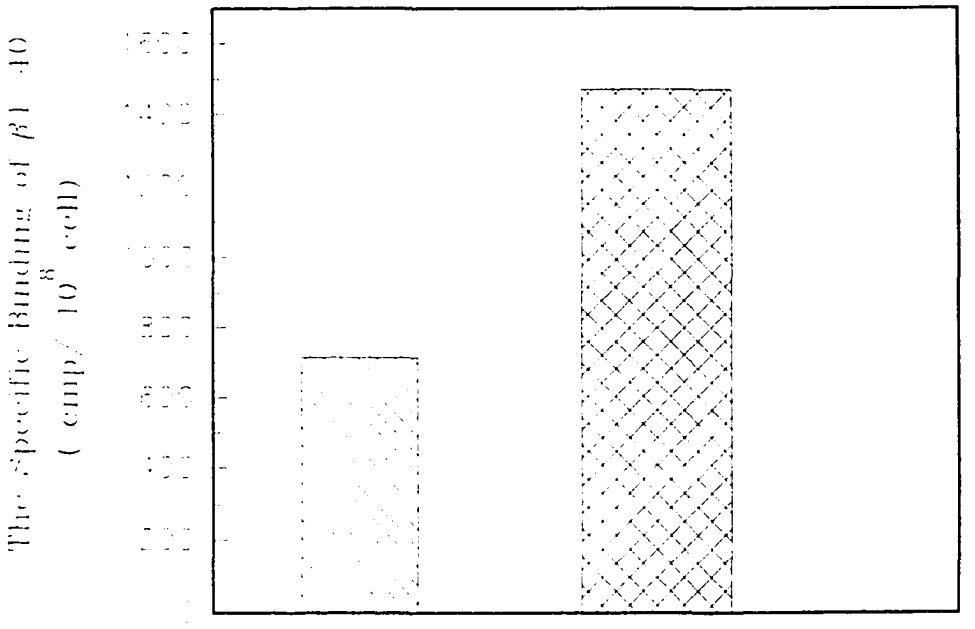

Figure 5-11. The effect of BSA on neuroblastoma - β peptide interaction. [ ], BSA concentration equals zero [ ], BSA concentration equals 100 μg/ml.

binding of ß1-40 to neuroblastoma was significantly higher at 100 μg/ml BSA than in BSA-free medium. This suggests that when BSA is present, the interaction between neuroblastoma cells and ß1-40 peptide is strengthened, which is consistent with the observation that BSA could potentiate amyloid ß1-40 peptide's neurotoxicity on cultured neuroblastoma cells.

5-10. Discussion

Since it has been proposed that amyloid precursor protein is processed to release a peptide ligand, such as a neuroendocrine hormone or growth factor, the biological activity of amyloid ß peptide has been widely investigated. Using the neuro-2A cell line, Breen *et al.*, (1991) suggested that ß amyloid precursor protein may mediate cell surface adhesion and neurite outgrowth. More recently, Ghiso *et al.*, (1992) reported that a C-terminal fragment of the ß amyloid precursor protein, which contains the ß amyloid peptide sequence, also promotes cell adhesion. They also demonstrated that the amino acid sequence RHDS (arginine-histidine-aspartate-serine; residues 5-8 of ß amyloid peptide) was responsible for the adhesion - promoting activity. The neurotoxicity of ß amyloid peptide was also

reported in many *in vitro* studies on primary neuronal cultures (Loo *et al.*, 1993; Forloni *et al.*, 1993; Pike *et al.*, 1992; Busciglio *et al.*, 1993). Fraser *et al.*, (1992) have investigated several analogues of ß amyloid peptide with respect to aggregation and fibril structure. They suggested that the aggregation state of the ß amyloid peptide, not just its ß-conformation, may be correlated with toxicity.

Using continuous cell lines, this study showed that ß amyloid peptide toxicity is a complex process involving the inhibition of cell growth. The experimental data indicate that neuroblastoma cell growth is better when BSA is present in the media. However the ß amyloid peptide toxicity, *i.e.* the inhibition of cell growth, also increased in the presence of BSA. This potentiation of the ß amyloid peptide toxicity on continuously growing cells may be explained by the interaction of ß amyloid peptides with other molecules. Amyloid ß peptides have been reported to bind complement C1q protein (Rogers *et al.*, 1992), ACT (Abraham *et al.*, 1988), lipoprotein E (Strittmatter *et al.*, 1993) and albumin (Vyas *et al.*, 1992). Amyloid peptide does not bind to the NK1 substance P receptor (Joslin *et al.*, 1991), but does bind to complement

proteins and membrane receptors (Arispe *et al.*, 1993; Rogers *et al.*, 1992). Joslin *et al.* (1991) showed that ß amyloid peptide binds to cultured liver cells as well as PC12 cells through the serpin protease inhibitor-enzyme complex receptor (SEC). Since the SEC receptor is involved in endocytosis, this may explain our observation that exogenous ß amyloid peptide is taken up by neuroblastoma cells. Cotman *et al.*, (1992) have suggested a threshold mechanism where, as neurons accumulate amyloid over time, they have a decreased ability to successfully overcome challenges.

The specific binding of the amyloid ß1-40 peptide to neuroblastoma cells was identified and the peptide was shown to be internalized into the cells. Amyloid may exert its biological activity by a complex mechanism including specific surface binding followed by internalization of the ß1-40 into the cell. In situations where a peptide ligand binds at a cell surface and the cell is able to internalize the peptide, the binding properties of the cell for that ligand are no longer simple. This internalization of the peptide opens the possibility that its effect on the neuropathogenesis of the disease is not limited to

cell surface-receptor mechanisms. The observation by Allsop *et al.* (1988) that ß7-18 staining was confined to cytoplasmic vesicles is also consistent with possible internalization. Many peptides act as autocrines, and it has been shown that receptors are found in vesicular elements of cells (Ottaway *et al.*, 1990; Posner *et al.*, 1985; Sussman *et al.*, 1983). These results support the idea that an amyloid fragment of the precursor protein can function as a ligand and interact with normal cellular metabolism. Kowall *et al.* (1991) showed that ß amyloid induced the expression of Alz-50 immunoreactive proteins in neurons. Also, exposure of hippocampal neurons to very low concentrations of ß amyloid peptide resulted in an induction of NGF receptors (Yankner *et al.*, 1990a). The ability to induce protein synthesis and the internalization of the peptide ligand might indicate a soluble intracellular receptor protein, similar to the steroid hormone receptors. Translocating proteins or factors may also be necessary for the complex to pass from the cytoplasm into the nucleus.

Chapter 6

Ultrastructural Study of ßAP - Neuroblastoma Interaction

Amyloid ß protein is a major proteinaceous component in senile plaque deposited in the Alzheimer's disease brain. The studies described in previous chapters investigated the neurotoxicity of ßAP to cultured neuroblastoma cells and discussed possible mechanisms of the interaction among neuroblastoma cells and ß1-40 peptide. However, the cellular location involved in the neuroblastoma - ß peptide interaction is still unknown. Using the techniques of transmission electron microscopy and immunocytochemistry, this chapter describes the study of the neuroblastoma - ß peptide interaction at the ultrastructural level.

6-1. Introduction

Currently the metabolism of ßAPP is of intense interest. Since the discovery that mutations in ßAPP can cause Alzheimer's disease, it is increasingly apparent that the formation and deposition of the ß amyloid protein plays a major role in the pathogenesis of Alzheimer's disease.

The previously reported pathway of cellular maturation of ßAPP results in the secretion of the extracellular domain of the transmembrane precursor protein into cerebrospinal fluid and into the medium of cultured cells (Palmert *et al.*, 1989, Weidemann *et al.*, 1989, Oltersdorf *et al.*, 1990). This ßAPP metabolism pathway is mediated by a proteolytic processing step which cleaves inside the ßAP region and thus the amyloidogenesis is precluded (Sisodia *et al.*, 1990; Esch *et al.*, 1990). However, the secretory route might only represent a minor metabolic pathway. An early study on ßAPP metabolism in Hela cells reported that only 30% of the initially labeled ßAPP was recovered in the conditioned medium, suggesting that the rest of ßAPP is rapidly degraded in the cells (Weidemann *et al.*, 1989). Meanwhile, ßAPP immunoreactivity was located in the Golgi / endoplasmic reticulum system (Caporaso *et al.*, 1994), endosomal vesicles (Dyrks *et al.*, 1993), and in secondary lysosomes in certain pyramidal cell bodies of the neocortex and hippocampus (Benowitz *et al.*, 1989). It has also been shown that full-length and degradative fragments of ßAPP are present in a lysosome-enriched subcellular fraction (Haass *et al.*, 1992). Therefore, a second ßAPP

processing pathway through the endosome / lysosome system has been suggested (Caporaso *et al.*, 1992; Benowitz *et al.*, 1989; Cole *et al.*, 1989; Haass *et al.*, 1992).

The lysosomotropic drug, chloroquine, has been used in the study of the ßAPP lysosome pathway. Chloroquine is a weak base that is taken up by cells where it is concentrated in and neutralized by the acidic organelle, the lysosome. The elevated pH of this organelle results in the inhibition of its acid-dependent hydrolyase activity. In cultured rat neuroendocrine PC12 cells, it was reported that only a small fraction of ßAPP molecules was targeted for secretion, whereas the majority of ßAPP molecules were degraded in a chloroquine-sensitive compartment. It was also reported that chloroquine exerted inhibitory effects on the degradation of mature full-length ßAPP molecules as well as the carboxyl-terminal fragments of ßAPP, suggesting a ßAPP processing pathway involving acidic organelles such as endosomes or lysosomes. The amyloid protein precursor was rapidly proteolyzed in lysosomes, since ßAPP could be seen in these structures only when lysosomal proteolysis was inhibited by chloroquine (Caporaso *et al.*, 1992).

Using a serine and thiol protease inhibitor leupeptin, which interrupts lysosomal protein degradation, one *in vivo* study of neuronal processing of ßAPP showed the accumulation of the neuronal lysosomes in treated rat brains. These lysosomes, which contained ßAPP fragments of apparent molecular weight 8.9-15 Kd, could be labeled by antisera to the cytoplasmic, transmembrane, and extracellular domains of ß amyloid precursor protein (Hajimohammadreza *et al.*, 1994). This *in vivo* model confirmed that neurons can process ßAPP via a lysosomal pathway and that neuronal lysosomes *in vivo* contain both N-terminal and potentially amyloidogenic C-terminal fragments of ßAPP.

Cell culture models used to explore the intracellular processing of ßAPP *in vitro* have also identified a lysosomal/endosomal pathway which produces a complex set of ßAPP C-terminal fragments containing the complete ß amyloid sequence, indicating the endosomal / lysosomal system might be the site for generation of ßAPP fragments that preserve intact ßAP region and thus contribute to the pathology of Alzheimer's disease (Golde *et al.*, 1992). In another *in vitro* study, Knops *et al.* (1992) analyzed the metabolic pathway of maturation of APP_{751} in a stably transfected

293 cells. In the presence of the lysosomal cysteine protease inhibitors, they found that the co-treatment of the inhibitor-treated cells with chloroquine completely blocked the generation of ßAPP fragments but did not significantly affect ßAPP maturation or secretion. This result indicated the non-secretory pathway of ßAPP degradation was mediated by a cysteine protease in an intracellular acidic compartment.

Nordsted *et al.* (1993) recently reported the identification of ßAPP in clathrin-coated vesicles (CCVs), which are responsible for the trafficking of many proteins to the endosomal compartment, including the transport of plasma membrane receptors and of proteins destined for lysosomes (Brodsky 1988). Specific sequence of Asparagine-Proline-X-Tyrosine (NPXY, where X represents any amino acid) have been identified as the signal of targeting cell-surface proteins to the CCVs that bud off the plasma membrane (Chen *et al.*, 1990). Since the cytoplasmic domain of ßAPP contains a NPXY (amino acid 759-762 of $ßAPP_{770}$) motif known to mediate clathrin coated pit internalization, it is possible that ßAPP could be reinternalized from the cell surface like a variety of receptors. Haass *et al.* (1992) and Koo *et al.* (1994)

showed the reinternalization of ßAPP by labeling cell-surface protein with biotin or radioactively labeled antibody.

The above studies provide a picture of the ßAPP metabolism pathway: full length ßAPP molecules reach the cell surface after maturation, where they can either be cleaved to release soluble ßAPP fragments into the medium or reinternalized to lysosomes, providing a substrate containing the intact ßAP region to lysosomal proteases. However, these studies all focused on the ß amyloid precursor protein. Few ultrastructural studies have been performed to understand the metabolic pathway and the internalization of the ß amyloid protein. Since the interaction of ß peptide with cultured neuroblastoma cells and the possible internalization of synthetic ß1-40 peptide have been demonstrated in Chapter 5, we look forward to studying the cellular locations which are responsible for the ß peptide metabolism and the ß peptide internalization at the ultrastructural level.

6-2. Ultrastructural study

In the ultrastructural study, control neuroblastoma cells were cultured in FCS-free HL-1

medium, while ß peptide treated cells were cultured in the same medium with the addition of 2 μM ß1-40 peptide. Cells were fixed in Karnovsky's solution containing 1% paraformaldehyde, 1.25% glutaraldehyde in 0.1 M cacodylate buffer (pH 7.2) and 2% O_sO_4. Cells were embedded in Epon 812 resin and stained with 7% uranyl acetate and 0.1% lead citrate (See appendix V). In the immunocytochemistry study, cells were fixed with a lower glutaraldehyde concentration (1%) and embedded in LR White. The ultrathin sections on formvar coated nickle grids were then processed through an immunocytochemistry staining procedure (See Appendix VI).

The ultrastructural of control neuroblastoma cells is shown in Figure 6-1 and Figure 6-2. They show a large nucleus surrounded by a double nuclear membrane; and a cytoplasm rich in cellular organelles, such as mitochondria, Golgi apparatus, lysosomes, and other small cellular vesicles. Small dark stained particles are seen in Golgi associated vesicles. Figure 6-3 details the structure of mitochondria, lysosome (Figure 6-3A), Golgi apparatus, and centriole (Figure 6-3B) in control cells.

Figure 6-1. A neuroblastoma cell cultured in FCS-free medium demonstrating normal cellular structure. N, nucleus; M, mitochondria; G, Golgi apparatus; L, lysosome. Original magnification, x 7,000.

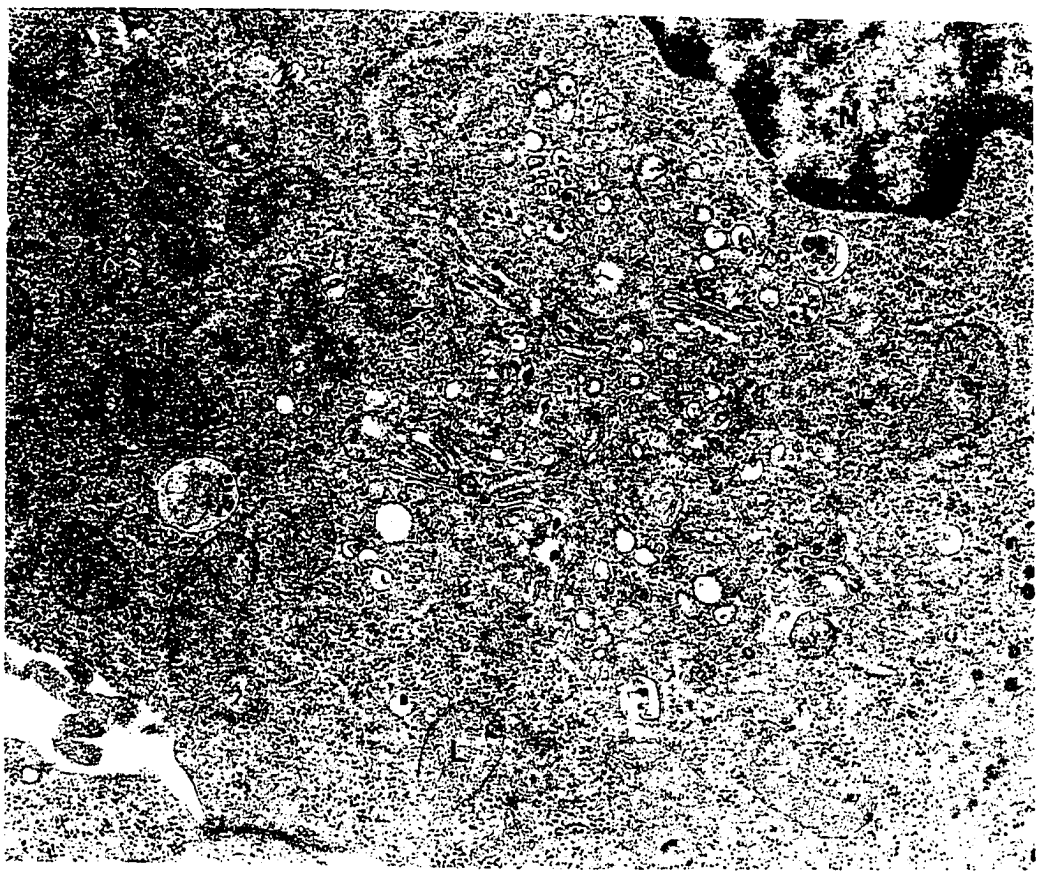

Figure 6-2. A control cell demonstrating cellular organelles. The cytoplasm is rich in Golgi system (G). N, nucleus; L, lysosome. Original magnification, x 12,000.

Figure 6-3. A control cell. A: Demonstrating structure of mitochondria (M) and lysosome (L). Original magnification x 30,000. B: Demonstrating structure of Golgi apparatus (G) and centriole (C). Original magnification, x 20,000.

Neuroblastoma cells treated with 2 μM ß1-40 peptide have similar cellular structure and organelles. Figure 6-4 and Figure 6-5 show the ultrastructural of ß1-40 treated cells with nucleus, mitochondria, endoplasmic reticulum, and Golgi system. The electron opaque structure shown in Figure 6-5 occasionally appears in both control and ß1-40 treated neuroblastoma cells. However, nuclear damage was noticed only in ß1-40 treated cells. Figure 6-6A shows the darkly stained electron dense particles in the nucleus followed by a trail of light stained space starting from the edge of the nucleus. These dark stained particles also appeared in the expanded perinuclear cisternal space (Figure 6-6B), which is known to be associated with endoplasmic reticulum, and in a vesicle connected with nuclear membrane (Figure 6-7), indicating this anomalous staining might enter the nucleus from the cytoplasm and cause nuclear damage .

In the immunocytochemistry study, cells were fixed in a low glutaraldehyde concentration and embedded in LR White to increase the labeling level. Peptide ß1-40 on ultrathin sections was then stained with gold particles. Control cells had a low labeling signal, which is not surprising since ßAPP was reported to be

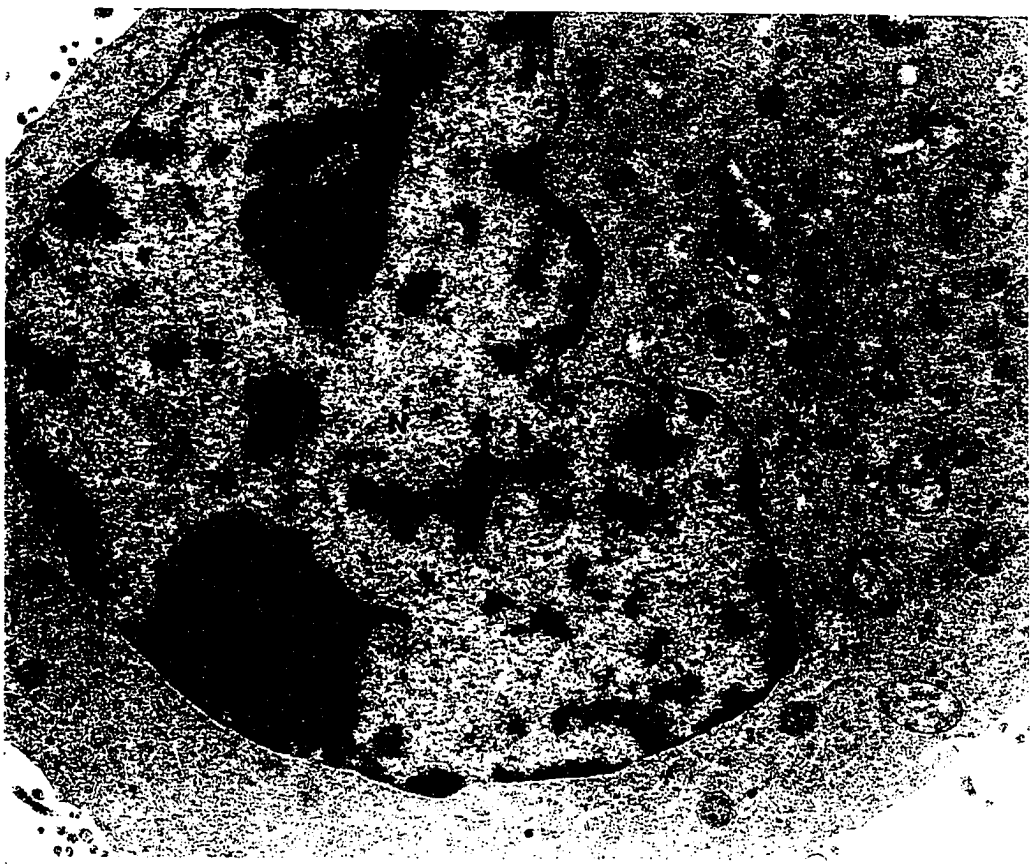

Figure 6-4. A neuroblastoma cell cultured in FCS-free medium containing 2 μM ß1-40 peptide. N, nucleus; M, mitochondria, L, lysosome, Original magnification, x 7,000.

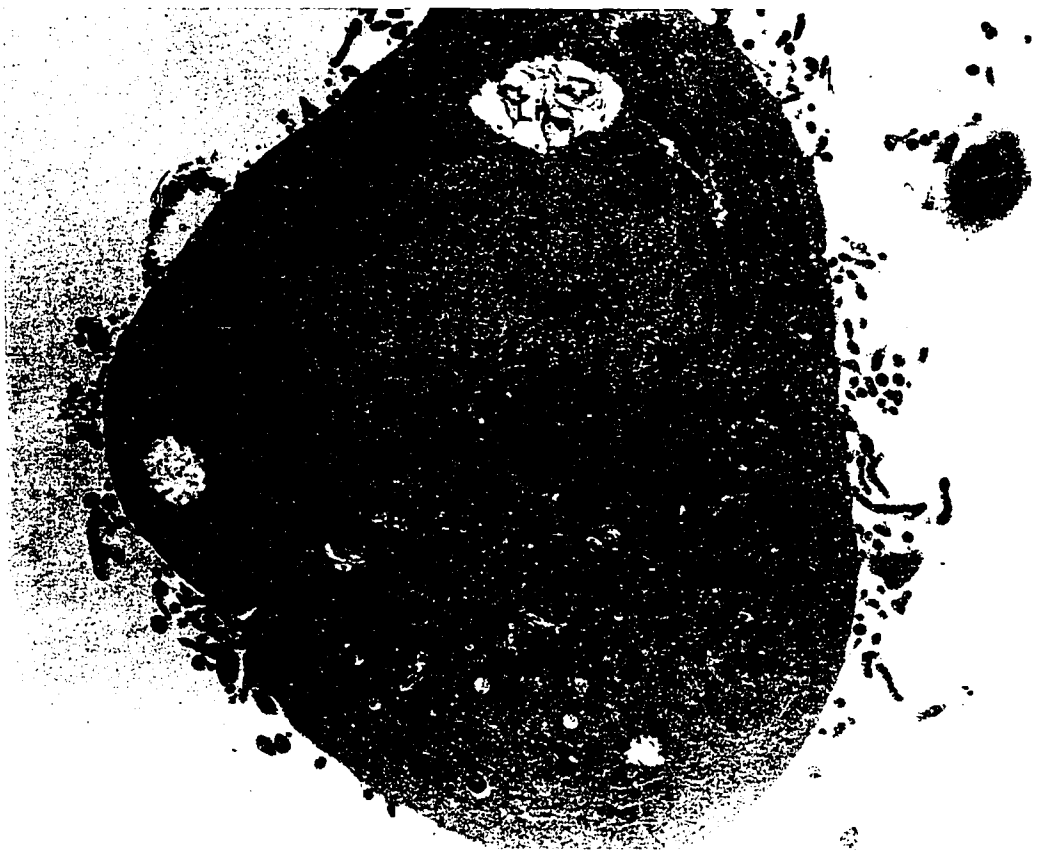

Figure 6-5. A ß1-40 treated neuroblastoma cell. Light stained structure is suspected to be lipofuscin (Li). Original magnification, x 4,400.

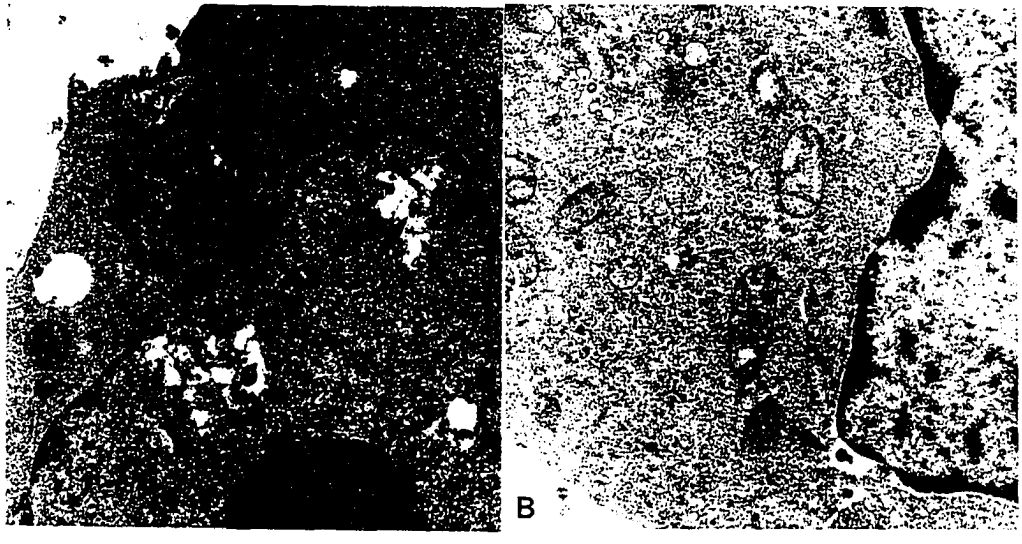

Figure 6-6. Nuclear damage in cells treated with ß1-40 peptide. A: The dark stained particles (arrow) is surrounded by a trail of light stained space in the nucleus. B: The dark stained particle also appears in the expanded perinuclear cisternal space (arrow). Original magnification of both photos, x 12,000.

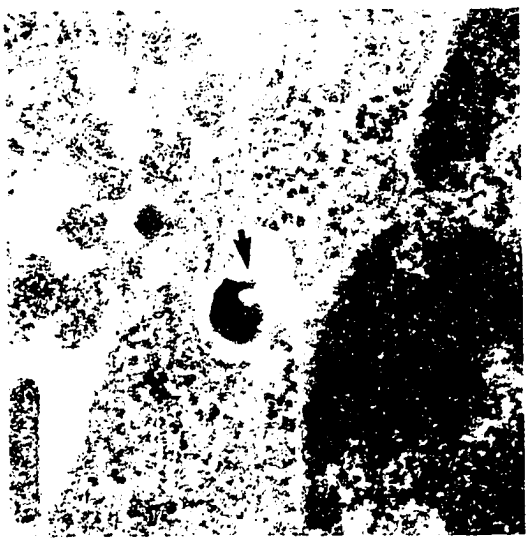

Figure 6-7. Nuclear damage in a ß1-40 treated cell, showing dark stained particle (arrow) in a vesicle connected with nuclear membrane.

rapidly degraded in the cell (Caporaso *et al.*, 1992). The ß1-40 treated cells generally had higher labeling than control cells, suggesting that ß1-40 treated cells obtain their anti-ß immunoreactivity from the cell culture medium. Figure 6-8 shows part of a ß1-40 treated cell. In this picture, the cellular membrane system seems to be associated with the cell surface. The gold labeling along the membrane close to cell surface suggests the internalization of ß peptide. However, the cellular locations of ß peptide processing were not determined. The immunocytochemistry technique will need improvement to provide more conclusive information about ß peptide internalization and its cellular metabolic locations.

6-3. Discussion

The ß amyloid protein is the major component in senile plaques in the AD brain. The recent findings that a familial form of AD is associated with genetic mutations within the amyloid precursor protein (Chartier-Harlin *et al.*, 1991; Goate *et al.*, 1991; Murrell *et al.*, 1991), and that cells expressing a mutant ßAPP found in familial AD secrete significantly

Figure 6-8. Immunocytochemistry of a ß1-40 peptide treated cell, demonstrating gold particles located along cell-surface-related cellular membrane system (arrow). Original magnification, x30,000.

higher amounts of ßAP (Cai *et al.*, 1993; Citron *et al.*, 1992), strongly support the hypothesis that ßAP accumulation *in vivo* may contribute to the progression of Alzheimer's disease.

The ß amyloid protein neurotoxicity has been addressed *in vivo* by injecting isolated AD plaque cores (Frautschy *et al.*, 1991) or synthetic ßAP (Kowall *et al.*, 1991) into rat brain, and *in vitro* by direct addition of ßAP to primary neuronal cultures (Koh *et al.*, 1990; Pike *et al.*, 1993; Yankner *et al.*, 1990a, 1990b). In all of these experimental systems ßAP was toxic to nerve cells.

Although there is now considerable evidence that ßAP can be cytotoxic to neuronal cells, little is known of the mechanism of ßAP neurotoxicity. It has been suggested that at least one pathway of ßAP toxicity results in free radical damage. It should be noted that control experiments are very important. Under serum-free growth conditions the effect of growth factors need to be further defined. Until these experiments are performed, alternate hypotheses involving indirect mechanisms of ßAP toxicity are possible. Using both primary central nervous system cultures and clonal cell lines, it is shown that antioxidants such as vitamin E

(Behl *et al.*, 1992; 1994a) protect cells from ßAP toxicity. Amyloid ß protein causes increased levels of H_2O_2 and lipid peroxides to accumulate in cells. The H_2O_2 degrading enzyme catalase protects cells from ßAP toxicity.

The process of cell death has been divided experimentally into two distinct pathways, necrosis and apoptosis. Necrosis and apoptosis differ from each other morphologically and biochemically. Apoptosis is an active process of self destruction. The main morphological characteristics of cells undergoing apoptosis are nuclear condensation and marginated chromatin, followed by the formation of apoptotic bodies. In the next stages the cells shrink and there is membrane ruffling and blebbing, cellular fragmentation, and cell death. The key observation is that throughout the whole process most intracellular organelles remain intact. Necrosis, the other principal pathway of cell death, is usually the result of a dramatic cell injury. Unlike the multistep apoptosis process, necrosis represents the rapid collapse of internal cell homeostasis initiated by massive cell damage. Necrotic cell increase in size due to cell swelling and have immediate organelle damage. This is

followed by chromatin clumping and the breakdown of the plasma membrane. There are inconsistent reports that ßAP induces necrosis (Behl *et al.*, 1994b) or apoptosis (Forloni *et al.*, 1993; Loo *et al.*, 1993). Loo *et al.* (1993) observed the characteristics of apoptosis in neuronal primary culture, including membrane blebbing, compaction of nuclear chromatin, and internucleosomal DNA fragmentation. Behl *et al.* (1994b), however, reported ultrastructural damages to Golgi apparatus, mitochondria, and other membrane systems within the cytoplasm, followed by total collapse of the cytoplasm and cell lysis. Both of these studies used high ßAP concentrations, (higher than 20 μM ßAP), that caused immediate cellular damage and cell death. Our experiment used a relatively low ßAP concentration. The ßAP treated cells had intact cellular organelles after exposure to 2 μM ß1-40 peptide for three days, but showed less organelle structure. Some nuclear damage was noticed as dark stained particles entered the nucleus presumably through nuclear membrane and cause nuclear damage. It is important to perform more intensive immunocytochemistry studies including serial sections to get a better picture of where the peptide is binding. The NB41A3 have a irregular topology which

leave precise interpretation difficult without a serial view. Using immunocytochemistry techniques, further research effort will be directed toward the study of ßAP toxicity and its cellular metabolic pathway.

Chapter 7

Conclusions and the potential for Further Development of NB41A3 Cell as a Model

Since the discovery that mutations in ßAPP can cause Alzheimer's disease, it is increasingly apparent that the formation of the ß amyloid protein deposits plays a major role in the pathogenesis of Alzheimer's disease. It is reported that ß amyloid precursor protein is expressed in a variety of tissues. However, ß amyloid deposits have only been observed in the brain. How the ß amyloid protein is generated in the brain and how ßAP affects neuronal cells are major focuses of current research. An easy to manipulate and interpret model system is needed to unravel the complexities of Alzheimer's disease at the molecular level.

A neuronal cell line, mouse neuroblastoma NB41A3, is targeted as a possible model system in this research and the processing of ßAPP and ßAP - cell interaction were investigated.

Immunoreactivity to the carboxyl terminal of ßAPP detected among the membrane fraction of neuroblastoma cells indicated that the ßAPP was produced in these

cells as a membrane protein. The ßAPP C-terminal immunoreactivity was also observed in the conditioned medium, demonstrating that the ßAPP C-terminal fragments were generated and secreted during the cellular processing of the ßAPP (Chapter 4). This could be one metabolic pathway of generating ß amyloid protein from its precursor.

The facts that mutations in ßAPP are sufficient to cause Alzheimer's disease (Goate *et al.*, 1991; Murrell *et al.*, 1991; Chartier-Harlin *et al.*, 1991) and that cells expressing a mutant ßAPP found in familial Alzheimer's disease secrete significantly higher amounts of ßAP (Citron *et al.*, 1992; Cai *et al.*, 1993) strongly suggest that ßAP contributes to the pathogenesis of Alzheimer's disease. Based on the observations in this research that the synthetic ß1-40 peptide negatively affects cultured neuroblastoma cells as judged by decreasing cell numbers, decreasing cell protein, and release of a cytosolic enzyme (lactic dehydrogenase), it can be hypothesized that the secreted ßAP-bearing fragments also have a toxic effect on these cultured cells (Chapter 5). Injecting isolated Alzheimer's disease amyloid plaque cores (Frautschy *et al.*, 1991) or synthetic ß peptide (Kowall *et al.*, 1991)

into rat brains caused brain damages, indicating ßAP neurotoxicity *in vivo*. These facts suggest that the deposits of ß amyloid protein in the Alzheimer's disease is partially responsible for the destruction of nutrites, thereby contributing to the formation of neuritic plaques and to neuronal death.

The mechanism of ßAP - cell interaction is still a controversial subject. One of the possible mechanisms of the ßAP - cell interaction might be through ßAP - cell surface binding. To investigate this possibility, a synthetic ß1-40 peptide was labeled with radioactive ^{125}I Bolton-Hunter Reagent. These specific binding between radioactively labeled ß1-40 peptide and neuroblastoma cells was observed. Washing cells with dissociation buffer did not abolish the specific binding, suggesting internalization of the ß1-40 peptide into the cells. The above study (Zhao *et al.*, 1991b) was among the first demonstrations of the binding of Alzheimer's ß amyloid protein to cell surfaces and of the ßAP internalization. Haass *et al.* (1992) and Koo *et al.* (1994) later showed the internalization of ß amyloid precursor protein into the cells. Thus, reinternalization of secreted ßAP-bearing fragments might be possible.

As described above, a picture of the ßAPP metabolic pathway has been proposed: full length ßAPP molecules reach cell surface after maturation as a membrane protein (Kang *et al.*, 1987), they are cleaved to release ßAPP fragments into the cerebrospinal fluid or into the medium of cultured cells (Palmert *et al.*, 1989; Weidemann *et al.*, 1989; Oltersdorf *et al.*, 1990), the ßAPP fragments are then reinternalized into the cells (Haass *et al.*, 1992; Koo *et al.*, 1994) where they have a toxic effect and cause cellular damage. Although little is known about the mechanism of ßAP intracellular neurotoxicity, it has been suggested that ßAP toxicity is a result of free radical attack on the cellular membrane system. Amyloid ß protein has been observed to cause increased levels of H_2O_2 and lipid peroxides to accumulate in cells. Antioxidant vitamin E and the H_2O_2 degrading enzyme, catalase, were reported to protect cells from ßAP toxicity (Behl *et al.*, 1992; 1994a). In an effort to extend these studies, ßAP effects at the ultrastructural level were investigated (Chapter 6). We observed nuclear damage and some light stained structure similar to lipofuscin in ß1-40 peptide treated cells. This observation supports the free radical hypothesis.

The studies described in this dissertation contribute to the knowledge of the ßAPP processing and of the ßAP toxicity. These studies also demonstrate that NB41A3 cell provides a practical *in vitro* model for studying the mechanism of Alzheimer's disease and amyloid toxicity.

References

Abraham C.R., Selkoe D.J., and Potter H., 1988, Immunocytochemical identification of the serine protease inhibitor α_1-antichymotrypsin in the brain amyloid deposits of Alzheimer's disease. *Cell* **52,** 487-501.

Allsop D., Wong C.W., Ikeda S-I., Landon M.; Kidd M., and Glenner G.G., 1988, Immunohistochemical evidence for the derivation of a peptide ligand from the amyloid ß-protein precursor of Alzheimer disease. *Proc. Natl. Acad. Sci. USA* **85,** 2790-2794.

Allsop D., Yamamoto T., Kametani F., Miyazaki N., and Ishii T., 1991, Alzheimer amyloid ß/A4 peptide binding sites and a possible "APP-secretase" activity associated with rat brain cortical membranes. *Brain Res.* **551,** 1-9.

Araujo D.M. and Cotman C.W., 1992, ß-amyloid stimulates glial cells *in vitro* to produce growth factors that accumulate in senile plaques in Alzheimer's Disease. *Brain Res.* **569,** 141-145.

Arispe N., Rojas E., and Pollard H.B., 1993, Alzheimer disease amyloid ß-protein forms calcium channels in bilayer membranes: Blockade by tromethamine and aluminium. *Proc. Natl. Acad. Sci. USA* **90,** 567-571.

Atherton E., Fox H., Harkiss D., Logan C.J., Sheppard R.C., and Williams B.J., 1978, A mild procedure for sold phase peptide synthesis: use of fluorenylmethoxy-carbonylamino acids. *J. Chem. Soc. Chem. Commun.* **13,** 537-539.

Autilio-Gambetti L., Morandi A., Tabaton M., Schaetzle B., Kovacs D., Perry G., Greenberg B. and Gambetti P., 1988, The amyloid precursor protein of Alzheimer disease is expressed as a 130 kDa polypeptides in various cultured cell types. *FEBS Lett.* **241,** 94-98.

Barany M., Chang Y.C., Arus C., Rustan T., and Frey W.H., 1985, Increased glycerol-3-phosphorylcholine in post-mortem Alzheimer's brain. *Lancet* **1,** 517.

Behl C., Davis J., Cole G.M., and Schubert D., 1992, Vitamin E protects nerve cells from amyloid ß protein toxicity. *Biochem. Biophys. Res. Commun.* **186,** 944-950

Behl C., Davis J.B., Lesley R., and Schubert D., 1994a, Hydrogen peroxide mediates amyloid ß protein toxicity. *Cell* **77,** 817-827.

Behl C., Davis J. B., Klier F.G., and Schubert D., 1994b, Amyloid ß peptide induces necrosis rather than apoptosis. *Brain Res.* **645,** 253-264.

Benowitz L.I., Rodriguez W., Paskevich P., Mufson E.J., Schenk D., and Neve R.L., 1989, The amyloid precursor is concentrated in neuronal lysosomes in normal and Alzheimer's disease subjects. *Exp. Neurol.* **106,** 237-250.

Bladier D., Joubert R., Avellana-Adalid V. Kemeny J-L., Doinel C., Amouroux J. and Caron M., 1989, Purification and characterization of a galactoside-binding lectin from human brain. *Arch. Biochem. Biophys.* **269,** 433-439.

Blusztajn J.K., Gonzalez-Coviella I.L., Logue M., Growdon J.H., and Wurtman R.J., 1990, Levels of phospholipid catabolic intermediates, glycero-phosphocholine and glycerophosphoethanolamine, are elevated in brains of Alzheimer's disease but not of Down's syndrome patients. *Brain Res.* **536,** 240-244.

Breen K.C., Bruce M., and Anderton B.H., 1991, Beta amyloid precursor protein mediates neuronal cell-cell and cell-surface adhesion. *J. Neurosci. Res.* **28,** 90-100.

Brenda D.S., Hilbich C., Multhaup G., Salbaum M., Beyreuther K., and Seeburg P.H., 1988, Alzheimer's disease amyloidogenic glycoprotein: expression pattern in rat brain suggests a role in cell contact. *EMBO J.* **7,** 1365-1370.

Brodsky F.M., 1988, Living with clathrin: its role in intracellular membrane traffic. *Science* **242,** 1396-1402.

Busciglio J., Yeh J., and Yankner B.A., 1993, ß-amyloid neurotoxicity in human cortical culture is not mediated by excitotoxins. *J. Neurochem.* **61,** 1565-1568.

Buxbaum J.D., Gandy S.E., Cicchetti P., Ehrlich M.E., Czernik A.J., Fracasso P., Ramabhadran T.V., Unterbeck A.J., and Greengard P., 1990, Processing of Alzheimer ß/A4 amyloid precursor protein: modulation by agents that regulate protein phosphorylation. *Proc. Natl. Acad. Sci. USA* **87,** 6003-6006.

Cai X.D., Golde T.E., and Younkin S.G., 1993, Release of excess amyloid ß-protein from a mutant amyloid ß-protein precursor. *Science* **259,** 514-516.

Caporaso G.L., Gandy S.E., Buxbaum J.D., and Greengard P., 1992, Chloroquine inhibits intracellular

degradation but not secretion of Alzheimer ß/A4 amyloid precursor protein. *Proc. Natl. Acad. Sci. USA* **89,** 2252-2256.

Caporaso G.L., Takei K., Gandy S.E., Matteoli M., Mundigl O., Greengard P., and DeCamilli P., 1994, Morphologic and biochemical analysis of the intracellular trafficking of the Alzheimer ß/A4 amyloid precursor protein. *J. Neurosci.* **14,** 3122-3138.

Caputo C.B., Sygowski L.A., Scott C.W., and Sobel I.R.E., 1992, Role of *tau* in the polymerization of peptides from ß-amyloid precursor protein. *Brain Res.* **597,** 227-232.

Castro M, Marks C.B., Nilsson B. and Anderson S., 1990, Does the Kunitz domain from the Alzheimer's amyloid ß protein precursor inhibit a kallikrein responsible for post-translational processing of nerve growth factor precursor? *FEBS Lett.* **267,** 207-212.

Ceri H., Kobiler D. and Barondes S. H., 1981, Heparin-inhibitable lectin. *J. Biol. Chem.* **256,** 390-394.

Chang C.D. and Meienhofer J. 1978, Solid phase peptide synthesis using mild base cleavage of N^{α}-fluorenylmethyloxycarbonyl amino acids, exemplified by a synthesis of dihydrosomatostatin. *Int. J. Pept. Protein Res.* **11,** 246-249.

Chartier-Harlin M.C., Crawford F., Houlden H., Warren A., Hughes D., Fidani L., Goate A., Rossor M., Roques P., Hardy J., and Mullan M., 1991, Mutations at codon 717 of the ß-amyloid precursor protein gene cause Alzheimer's disease. *Nature,* **353,** 844-846.

Chen W-J, Goldstein J.L., and Brown M.S., 1990, NPXY, a sequence often found in cytoplasmic tails, is required for coated pit-mediated internalization of the low density lipoprotein receptor. *J. Biol. Chem.* **265,** 3116-3123.

Citron M., Oltersdorf T., Haass C., McConlogue L., Hung A.Y., Seubert P., Vigo-Pelfrey C., Lieberburg I.,

and Selkoe D.J., 1992, Mutation of the ß-amyloid precursor protein in familial Alzheimer's disease increases ß-protein production. *Nature*, **360,** 672-764.

Cole G.M., Huynh T.V., and Saitoh T., 1989, Evidence for lysosomal processing of amyloid ß-protein precursor in cultured cells. *Neurochem. Res.* **14,** 933-939.

Cole. G. J. and Glaser L., 1986, Heparin-binding domain from N-CAM is involved in neural cell-substratum adhesion. *J. Cell Biol.* **102,** 403-412.

Copani A., Koh J-Y, and Cotman C.W., 1991, ß-amyloid increases neuronal susceptibility to injury by glucose deprivation. *NeuroReport* **2,** 763-765,

Corder E.H., Saunders A.M., Strittmatter W.J., Schmechel D.E., Gaskell P.C., Small G.W., Roses A.D., Haines J.L., and Pericak-Vance M.A., 1993, Gene dose of apolipoprotein E type 4 allele and the risk of Alzheimer's disease in late onset families. *Science* **261,** 921-923.

Cotman C.W., Cummings B.J., and Whitson J.S., 1991, The role of misdirected plasticity in plaque biogenesis and Alzheimer's disease pathology. In *Growth factors and Alzheimer's disease*. Hefti F., Brachet P., Will B., and Christen Y. (Eds.), Springer-Verlag, Berlin, pp.222-232.

Cotman C.W., Pike C.J., and Copani A., 1992, ß-amyloid neurotoxicity : a discussion of *in vitro* findings. *Neurobiol. Aging* **13,** 587-590.

Cunningham D.D. and Gurwitz D., 1989, Proteolytic regulation of neurite outgrowth from neuroblastoman cells by thrombin and protease nexin-1. *J. Cell Biochem.* **39,** 55-64.

Dewji N.N., Shelton E.R., Adler M.J., Chan H. W., Seegmiller J.E., and Coronel C., 1990, Processing of Alzheimer's disease-associated ß amyloid precursor pretein. *J. Mol. Neurosci.* **2,** 19-27.

Dyrks T., Dyrks E., Monning U., Urmoneit B., Turner J., and Beyreuther K., 1993, Generation of ßA4 from

the amyloid protein precursor and fragments thereof. *FEBS Lett.* **335,** 89-93.

Dyrks T., Weidemann A., Multhaup G., Salbaum J.M., Lemaire H-G, Kang J., Muller-Hill B., Masters C.L., and Beyreuther K., 1988, Identification, transmembrane orientation and biogenesis of the amyloid A4 precursor of Alzheimer disease. *EMBO J.* **7,** 949-957.

Eloumami H., Bladier D., Caruelle D., Courty J., Joubert R. and Caron M., 1990, Soluble heparin-binding lectins from human brain: purification, specificity and relationship to an heparin-binding growth factor. *Int. J. Biochem.* **22,** 539-544.

Esch F.S., Keim P.S., Beattie E.C., Blacher R.W., Culwell A.R., Oltersdorf T., McClure D., and Ward P.J., 1990, Cleavage of amyloid ß peptide during constitutive processing of its precursor. *Science* **248,** 1122-1124.

Flood J.F., Morley J.E., and Roberts E., 1991, Amnestic effects in mice of four synthetic peptides

homologous to amyloid ß protein from patients with Alzheimer disease. *Proc Natl. Acad. Sci. USA* **88,** 3363-3366.

Forloni G., Chiesa R., Smiroldo S., Verga L., Salmona M., Tagliavini F., and Angeretti N., 1993, Apoptosis mediated neurotoxicity induced by chronic application of ß amyloid fragment 25-35. *NeuroReport*, **4,** 523-526.

Fraser P.E., Duffy L.K., O'Malley M.B., Nguyen J., Inouye H., and Kirschner D.A., 1991, Morphology and antibody recognition of synthetic ß-amyloid peptides. *J. Neurosci. Res.* **28,** 474-485.

Fraser P.E., Nguyen J.T., Inouye H., Surewicz W.K., Selkoe D.J., Podlisny M.B., and Kirschner D.A., 1992, Fibril formation by primate, rodent, and Dutch-hemorrhagic analogues of Alzheimer amyloid ß-protein. *Biochemistry*. **31,** 10716-10723.

Frautschy S.A., Baird A., and Cole G.M., 1991, Effects of injected Alzheimer ß-amyloid cores in rat brain. *Porc. Natl Acad. Sci. USA* **88,** 8362-8366.

Fukuchi K-I, Kamino K., Deeb S.S., Smith A.C., Dang T., and Martin G.M., 1992, Overexpression of amyloid precursor protein alters its normal processing and is associated with neurotoxicity. *Biochem. Biophys. Res. Commun.* **182,** 165-173.

Gabuzda D., Busciglio J., and Yankner B.A., 1993, Inhibition of ß-amyloid production by activation of protein kinase C. *J. Neurochem.* **61,** 2326-2329.

Games D., Khan K.M., Soriano F.G., Keim P.S., Davis D.L., Bryant K., and Lieberburg I., 1992, Lack of Alzheimer pathology after beta amyloid protein injection in rat brain. *Neurobiol. Aging* **13,** 569-576.

Ghiso J., Rostagno A., Gardella J.E., Liem L., Gorevic P.D., and Frangione B., 1992, A 109-amino-acid C-terminal fragment of Alzheimer's disease amyloid precursor protein contains a sequence, -RHDS-, that promotes cell adhesion. *Biochem. J.* **288,** 1053-1059.

Giordano T., Pan J.B., Monteggia L.M., Holzman T.F., Snyder S.W., Krafft G., Ghanbari H., and Kowall N.W., 1994, Similarities between ß amyloid peptides 1-40 and 40-1: effects on aggregation, toxicity *in vitro*, and injection in young and aged rats. *Exp. Neurol.* **125,** 175-182.

Glenner G.G. and Wong C.W., 1984, Alzheimer's disease: initial report of the purification and characterization of a novel cerebrovascular amyloid protein. *Biochem. Biophys. Res. Commun.* **120,** 885-890.

Glenner G.G., Wong C.W., Quaranta V., and Eanes E.D., 1984, The amyloid deposit in Alzheimer's disease: their nature and pathogenesis. *Appl. Pathol.* **2,** 357-369.

Goate A., Chartier-Harlin M-C., Mullan M., Brown J., Crawford F., Fidani L., Giuffra L., Haynes A., Irving N., James L., Mant R., Newton P., Rooke K., Roques P., Talbot C., Pericak-Vance M., Roses A., Williamson R., Rossor M., Owen M., and Hardy J., 1991, Segregation of a missense mutation in the

amyloid precursor protein gene with familial Alzheimer's disease. *Nature*, **349,** 704-706.

Golde T.E., Estus S., Younkin L.H., Selkoe D.J., Younkin S.G., 1992, Processing of the amyloid protein precursor to potentially amyloidogenic derivatives. *Science* **255,** 728-730.

Goldgaber D., Lerman M.I., McBride O.W., Saffiotti U., and Gajdusek D.C., 1987, Characterization and chromosomal localization of a cDNA encoding brain amyloid of Alzheimer's disease. *Science*, **235,** 877-880.

Gorevic P.D., Goni F., Pons-Estel B., Alvarez F., Peress N.S., and Frangione B., 1986, Isolation and partial characterization of neurofibrillary tangles and amyloid plaque core in Alzheimer's disease: immunohistological studies. *J. Neuropathol. Exp. Neurol.* **45,** 647-664.

Griffin W.S.T., Stanley L.C., Ling C., White L., MacLeod V., Perrot L.J., White C.L.III, and Araoz C., 1989, Brain interleukin-1 and S-100

immunoreactivity are elevated in Down syndrome and Alzheimer disease. *Proc. Natl. Acad. Sci. USA* **86,** 7611-7615.

Grundke-Iqbal I., Iqbal K., Tung Y-C, Quinlan M., Wisniewski H.M., and Binder L.I., 1986, Abnormal phosphorylation of the microtubule-associated protein *tau* in Alzheimer cytoskeletal pathology. *Proc. Natl. Acad. Sci. USA* **83,** 4913-4917.

Gurwitz D. and Cunningham D.D., 1990, Neurite outgrowth activity of protease nexin-1 on neuroblastoma cells requires thrombin inhibition. *J. Cell Physiol.* **142,** 155-162.

Haass C., Koo E.H., Mellon A., Hung A.Y., and Selkoe D.J., 1992, Targeting of cell-surface ß-amyloid precursor protein to lysosomes: alternative processing into amyloid-bearing fragments. *Nature* **357,** 500-503.

Hajimohammadreza I., Anderson V.E.R., Cavanagh J.B., Seville M.P., Nolan C.C., Anderton B.H., and Leigh P.N., 1994, ß-amyloid precursor protein fragments

and lysosomal dense bodies are found in rat brain neurons after ventricular infusion of leupeptin. *Brain Res.* **640,** 25-32.

Hamos J.E., DeGennaro L.J., and Drachman D.A., 1989, Synaptic loss in Alzheimer's disease and other dementias. *Neurology* **39,** 355-361.

Hardy J.A. and Higgins G.A., 1992, Alzheimer's Disease: The amyloid cascade hypothesis. *Science* **256,** 184-185.

Hartmann H., Eckert A., and Muller W.E., 1994, Apolipopotein and cholesterol affect neuronal calcium signalling: the possible relationship to ß-amyloid neurotoxicity. *Biochem. Biophys. Res. Commun.* **200,** 1185-1192.

Hayashi M., Schlesinger D.H., Kennedy D.W., and Yamada K. ., 1980, Isolation and characterization of a heparin-binding domain of cellular fibronectin. *J. Biol. Chem.* **255,** 10,017-10,020.

Hensley K., Carney J.M., Mattson M.P., Aksenova M., Harris M., Wu J.F., Floyd R.A., and Butterfield D.A., 1994, A model for ß-amyloid aggregation and neurotoxicity based on free radical generation by the peptide: relevance to Alzheimer disease. *Proc. Natl. Acad. Sci. USA* **91,** 3270-3274.

Hilbich C., Kisters-Woike B., Reed J., Masters C.L., and Beyreuther K., 1991, Aggregation and secondary structure of synthetic amyloid ßA4 peptides of Alzheimer's disease. *J. Mol. Biol.* **218,** 149-163.

Hughes R.C., 1983, *Glycoproteins*. Chapman and Hall, London.

Jarrett J.T. and Lansbury Jr. P.T., 1992, Amyloid fibril formation requires a chemically discriminating nucleation event: studies of an amyloidogenic sequence from the bacterial protein OsmB. *Biochemistry* **31,** 12345-12352.

Jessell T.M., Hynes M.A., and Dodd J., 1990, Carbohydrates and carbohydrate-binding proteins in

the nervous sytem. *Annu. Rev. Neurosci.* **13,** 227-255.

Joachim C.L., Duffy L.K., Morris J.H., and Selkoe D.J., 1988, Protein chemical and immunocytochemical studies of meningovascular ß-amyloid protein in Alzheimer's disease and normal aging. *Brain Res.* **474,** 100-111.

Johnson S.A., McNeill T., Cordell B., and Finch C.E., 1990, Relation of neuronal APP-751/APP-695 mRNA ratio and neuritic plaque density in Alzheimer's disease. *Science*, **248,** 854-857.

Joslin G., Krause J.E., Hershey A.D., Adams S.P., Fallon R.J., and Perlmutter D.H., 1991, Amyloid ß-peptide, substance P, and bombesin bind to the serpin-enzyme complex receptor. *J. Biol. Chem.* **266,** 21897-21902.

Kammesheidt A., Boyce F.M., Spanoyannis A.F., Cummings B.J., Ortegon M., Cotman C., Vaught J.L., and Neve R.L., 1992, Deposition of ß/A4 immunoreactivity

and neuronal pathology in transgenic mice expressing the carboxyl-terminal fragment of the Alzheimer amyloid precursor in the brain. *Proc. Natl. Acad. Sci. USA* **89,** 10857-10861.

Kang J., Lemaire H-G, Unterbeck A., Salbaum J.M., Masters C.L., Grzeschik K-H, Multhaup G., Beyreuther K., and Muller-Hill B., 1987, The precursor of Alzheimer's disease amyloid A4 protein resembles a cell-surface receptor. *Nature* **325,** 733-736.

Kawabata S., Higgins G.A., and Gordon J.W., 1991, Amyloid plaques, neurofibrillary tangles and neuronal loss in brains of transgenic mice overexpressing a C-terminal fragment of human amyloid procursor protein. *Nature*, **354,** 476-478.

Kitaguchi N., Takahashi Y., Tokushima Y., Shiojiri S., and Ito H., 1988, Novel precursor of Alzheimer's disease amyloid protein shows protease inhibitory activity. *Nature*, **331,** 530-532.

Klagsbrun M. and Shing Y., 1985, Heparin affinity of anionic and cationic capillary endothelial cell gorwth factors: analysis of hypothalamus-derived growth factors and fibroblast growth factors. *Proc. Natl. Acad. Sci. USA* **82,** 805-809.

Knops J., Lieberburg I., and Sinha S., 1992, Evidence for a nonsecretory, acidic degradation pathway for amyloid precursor protein in 293 cells. *J. Biol. Chem.* **267,** 16022-16024.

Koh J-Y, Yang L.L., and Cotman C.W., 1990, ß-amyloid protein increases the vulnerability of cultured cortical neurons to exocitotoxic damage. *Brain Res.* **533,** 315-320.

Koo E.H. and Squazzo S.L., 1994, Evidence that production and release of amyloid ß-protein involves the endocytic pathway. *J Biol. Chem.* **269,** 17386-17389.

Kosik K.S., 1992, Alzheimer's Disease: a cell biological perspective. *Science* **256,** 780-783.

Kowall N.W., Beal M.F., Busciglio J., Duffy L.K., and Yankner B.A., 1991, An *in vivo* model for the neurodegenerative effects of ß amyloid and protection by substance P. *Proc Natl. Acad. Sci. USA* **88,** 7247-7251.

Kowall N.W., McKee A.C., Yankner B.A., and Beal M.F., 1992, *In Vivo* neurotoxicity of Beta-amyloid [ß(1-40)] and the ß(25-35) fragment. *Neurobiol. Aging* **13,** 537-542.

Kowall N.W., 1994, Beta amyloid neurotoxicity and neuronal degeneration in Alzheimer's disease. *Neurobiol. Aging* **15,** 257-258.

Loo D.T., Copani A., Pike C.J., Whittemore E.R., Walencewicz A.J., and Cotman C.W., 1993, Apoptosis is induced by ß-amyloid in cultured central nervous system neurons. *Proc. Natl. Acad. Sci. USA* **90,** 7951-7955.

Lundt B.F., Johansen N.L., Voelund A., and Markussen J., 1978, Removal of t-butyl and t-butoxycarbonyl

protecting groups with trifluroacetic acid. *Int. J. Pept. Protein Res.* **12,** 258-268.

Masliah E., Terry R.D., DeTeresa R.M., and Hansen L.A., 1989, Immunohistochemical quantification of the synapse-related protein synaptophysin in Alzheimer's disease. *Neurosci. Lett.* **103,** 234-239.

Masliah E., Terry R.D., Alford M., DeTeresa R., and Hansen L.A., 1991, Cortical and subcortical patterns of synaptophysin-like immunoreactivity in Alzheimer's disease. *Am. J. Pathol.* **138,** 235-246.

Masters C.L., Simms G., Weinman N.A., Multhaup G., McDonald B.L., and Beyreuther K., 1985a, Amyloid plaque core protein in Alzheimer disease and Down syndrome. *Proc. Natl. Acad. Sci. USA* **82,** 4245-4249.

Master C.L., Multhaup G., Simms G., Pottgiesser J., Martins R.N., and Beyreuther K., 1985b, Neuronal origin of a cerebral amyloid: neurofibrillary tangles of Alzheimer's disease contain the same

protein as the amyloid of plaque cores and blood vessels. *EMBO J.* **4,** 2757-2763.

Mattson M.P. and Rydel R.E., 1992a, ß-amyloid precursor protein and Alzheimer's disease: The peptide plot thickens. *Neurobiol. Aging* **13,** 617-621.

Mattson M.P., Cheng B., Davis D., Bryant K., Lieberburg I., and Rydel R.E., 1992b, ß-amyloid peptides destabilize calcium homeostasis and render human cortical neurons vulnerable to excitotoxicity. *J. Neurosci.* **12,** 376-389.

May P.C. Gitter B.D., Waters D.C., Simmons L.K., Becker G.W., Small J.S., and Robison P.M., 1992, Beta-amyloid peptide *in vitro* toxicity: Lot-to-lot variability. *Neurobiol. Aging* **13,** 605-607.

Merrifield R.B., 1963, Solid phase peptide synthesis I. The synthesis of a tetrapeptide. *J. Am. Chem. Soc.* **85,** 2149-2154.

MilliGen/Biosearch 9050 Peptide Synthesizer Operator's Mannal. 1991, MilliGen/Biosearch, Division of Millipore, Burlington, MA, USA.

Mita S., Sadlock J. Herbert J. and Schon E.A., 1988, A cDNA specifying the human amyloid ß precursor protein (AßPP) encodes a 95-kDa polypeptide. *Nucleic Acids Res*. **16,** 9351.

Mitsuhashi M., Akitaya T., Turk C.W., and Payan D.G. 1991, Amyloid ß-protein substituent peptides do not interact with the substance P receptor expressed in cultured cells. *Mol. Brain Res*. **11,** 177-180.

Murrell J., Farlow M., Ghetti B., and Benson M.D., 1991, A mutation in the amyloid precursor protein associated with hereditary Alzheimer's disease. *Science* **254,** 97-99.

Nishimoto I., Okamoto T., Matsuura Y., Takahashi S., Okamoto T., Murayama Y., and Ogata E., 1993,

Alzheimer amyloid protein precursor complexes with brain GTP-binding protein G_o. *Nature* **362,** 75-79.

Nitsch R.M., Blusztajn J.K., Pittas A.G., Slack B.E., Growdon J.H., and Wurtman R.J., 1992, Evidence for a membrane defect in Alzheimer disease brain. *Proc. Natl. Acad. Sci. USA* **89,** 1671-1675.

Noguchi S., Murakami K., Yamada N., Payami H., Kaye J., Heston L.L., Bird T.D., and Schellenberg G.D., 1993, Apolipoprotein E genotype and Alzheimer's disease. *Lancet*. **342,** 737-738.

Nordstedt C., Caporaso G.L., Thyberg J., Gandy S.E., and Greengard P., 1993, Identification of the Alzheimer ß/A4 amyloid precursor protein in clathrin-coated vesicles purified from PC 12 cells. *J. Biol. Chem.* **268,** 608-612.

Nukina N., Kanazawa I., Mannen T., and Uchida Y., 1992, Accumulation of amyloid precursor protein and ß-protein immunoreactivities in axons injured by cerebral infarct. *Gerontology* **38,** (suppl 1), 10-14.

Oltersdorf T., Ward P.J., Henriksson T., Beattie E.C., Neve R., Lieberburg I., and Fritz L.C., 1990, The Alzheimer amyloid precursor protein. Identification of a stable intermediate in the biosynthetic / degradative pathway. *J. Biol. Chem.* **265,** 4492-4497.

Ottaway C.A., 1990, The effect of ligand internalization on cellular binding studies of peptide ligands. In *Neuropeptides and immunopeptides: messengers in a neuroimmune axis.* O'Dorisio M.S. and Panerai A. (Eds.), Annals of the New York Academy of Sciences, New York, pp.45-59.

Palmert M.R., Podlisny M.B., Witker D.S., Oltersdorf T., Younkin L.H., Selkoe D.J., and Younkin S.G., 1989, The ß-amyloid protein precursor of Alzheimer disease has soluble derivatives found in human brain and cerebrospinal fluid. *Proc Natl. Acad. Sci. USA* **86,** 6338-6342.

Pardridge W.M., Vinters H.V., Yang J., Eisenberg J., Choi T.B., Tourtellotte W.W., Huebner V., and Shively J.E., 1987, Amyloid angiopathy of Alzheimer's disease: amino acid composition and partial sequenc of a 4,200-dalton peptide isolated from cortical microvessels. *J. Neurochem.* **49,** 1394-1401.

Patterson D., Gardiner K., Kao F-T., Tanzi R., Watkins P., and Gusella J.F., 1988, Mapping of the gene encoding the ß-amyloid precursor protein and its relationship to the Down syndrome region of chromosome 21. *Proc Natl. Acad. Sci. USA* **85,** 8266-8270.

Pericake-Vance M.A., Bebout J.L., Gaskell P.C., Yamaoka L.H., Hung W.Y., Alberts M.J., Walker A.P., Bartlett R.J., Haynes C.A., Welsh K.A., Earl N.L., Heyman A., Clark C.M., and Roses A.D., 1991, Linkage studies in familial Alzheimer disease: evidence for chromosome 19 linkage. *Am. J. Hum. Genet.* **48,** 1034-1050.

Pettegrew J.W., Panchalingam K., Moossy J., Martinez J., Rao G., and Boller F., 1988a, Correlation of phosphorus-31 magnetic resonance spectroscopy and morphologic findings in Alzheimer's disease. *Arch. Neurol.* **45,** 1093-1096.

Pettegrew J.W., Moossy J., Withers G., McKeag D., and Panchalingam K., 1988b, ^{31}P nuclear magnetic resonance study of the brain in Alzheimer's disease. *J. Neuropathol. Exp. Neurol.*, **47,** 235-248.

Pike C.J., Walencewicz A.J., Glabe C.G., and Cotman C.W., 1991, *In vitro* aging of ß-amyloid protein causes peptide aggregation and neurotoxicity. *Brain Res.* **563,** 311-314.

Pike C.J., Cummings B.J., and Cotman C.W., 1992, ß-amyloid induces neuritic dystrophy *in vitro*: similarities with Alzheimer pathology. *NeuroReport*, **3,** 769-772.

Pike C.J., Burdick D., Walencewicz A.J., Glabe C.G., and Cotman C.W., 1993, Neurodegeneration induced

by ß-amyloid peptides in vitro: the role of peptide assembly state. *J. Neurosci.* **13,** 1676-1687.

Podlisny M.B., Stephenson D.T., Frosch M.P., Lieberburg I., Clemens J.A., and Selkoe R.J., 1992, Synthetic amyloid ß-protein fails to produce specific neurotoxicity in monkey cerebral cortex. *Neurobiol. Aging* **13,** 561-567.

Ponte P., Gonzalez-DeWhitt P., Schilling J., Miller J., Hsu D., Greenberg B., Davis K., Wallace W., Leiberburg I., Fuller F., and Cordell B., 1988, A new A4 amyloid mRNA contains a domain homologous to serine proteinase inhibitors. *Nature* **331,** 525-527.

Posner B.I., Khan M.N., and Bergeron J.J.M., 1985, Receptor-mediated uptake of peptide hormones and other ligands. In *Polypeptide hormone receptors.* Posner B.I. (Ed.), Marcel Dekker, Inc., New York pp.61-90.

Quon D., Wang Y., Catalano R., Scardina M., Murakami K., and Cordell B., 1991, Formation of ß-amyloid protein deposits in brains of transgenic mice. *Nature*, **352,** 239-241.

Rogers J., Cooper N.R., Webster S., Schultz J., McGeer P.L., Styren S.D., Civin W.H., Brachova L., Bradt B., Ward P., and Lieberburg I., 1992, Complement activation by ß-amyloid in Alzheimer disease. *Proc. Natl. Acad. Sci. USA* **89,** 10016-10020.

Roher A.E., Ball M.J., Bhave S.V., and Wakade A.R., 1991, ß-amyloid from Alzheimer disease brains inhibits sprouting and survival of sympathetic neurons. *Biochem. Biophys. Res. Commun.* **174,** 572-579.

Saitoh T., Sundsmo M., Roch J.M., Kimura N., Cole G., Schubert D., Oltersdorf T., and Schenk D.B., 1989, Secreted form of amyloid ß protein precursor is involved in the growth regulation of fibroblasts. *Cell* **58,** 615-622.

Schellenberg G.D., Bird T.D., Wijsman E.M., Moore D.K., Boehnke M., Bryant E.M., Lampe T.H., Nochlin D., Sumi S.M., 1988, Absence of linkage of chromosome 21q21 markers to familial Alzheimer's disease. Science, **241,** 1507-1510.

Schellenberg G.D., Bird T.D., Wijsman E.M., Orr H.T., Anderson L., Nemens E., White J.A., Bonnycastle L., Weber J.L., Alonso M.E., Potter H., Heston L.L., and Martin G.M., 1992, Genetic linkage evidence for a familial Alzheimer's disease locus on chromosome 14. *Science*, **258,** 668-671.

Schmechel D.E., Saunders A.M., Strittmatter W.J., Crain B.J., Hulette C.M., Joo S.H., Pericak-Vance M.A., Goldgaber D., and Roses A.D., 1993, Increased amyloid ß-peptide deposition in cerebral cortex as a consequence of apolipoprotein E genotype in late-onset Alzheimer disease. *Proc. Natl. Acad. Sci. USA* **90,** 9649-9653.

Schubert D., Schroeder R., LaCorbiere M., Saitoh T., and Cole G., 1988, Amyloid ß protein precursor is

possibly a heparin sulfate proteoglycan core protein. *Science* **241,** 223-226.

Schubert D., LaCorbiere M., Saitoh T., and Cole G., 1989, Characterization of an amyloid precursor protein that binds heparin and contains tyrosine sulfate. *Proc. Natl. Acad. Sci. USA* **86,** 2066-2069.

Scott G.K., 1992, Proteinases and proteinase inhibitors as modulators of animal cell growth. *Comp. Biochem. Physiol.* **103B,** 785-793.

Selkoe D.J., Podlisny M.B., Joachim C.L., Vickers E.A., Lee G., Fritz L.C., and Oltersdorf T., 1988, ß-amyloid precursor protein of Alzheimer's disease occurs as 110 to 135-kilodalton membrane-associated proteins in neural and nonneural tissues. *Proc. Natl. Acad. Sci. USA* **85,** 7341-7345.

Simpson J., Bladon C.M., Yates C.M., and Harmar A.J., 1989, An antiserum to the extracellular domain of the Alzheimer amyloid precursor recognizes 70 and 88 kDa brain proteins. *FEBS Lett.* **257,** 238-240.

Sisodia S.S., Koo E.H., Beyreuther K., Unterbeck A., and Price D.L., 1990, Evidence that ß-amyloid protein in Alzheimer's disease is not derived by normal processing. *Science* **248,** 492-495.

Smith R.P., Higuchi D.A., and Broze G.J. Jr., 1990, Platelet coagulation factor XI_a-inhibitor, a form of Alzheimer amyloid precursor protein. *Science* **248,** 1126-1128.

Snow A.D., Willmer J., and Kisilevsky R., 1987, Sulfated glycosaminoglycans in Alzheimer's disease. *Hum. Pathol.* **18,** 506-510.

Snow A.D. and Wight T.N., 1989, Proteoglycans in the pathogenesis of Alzheimer's disease and other amyloidoses. *Neurobiol. Aging* **10,** 481-497.

St. George-Hyslop P.H., Tanzi R., Polinsky R.J., Haines J.L., Nee L., Watkins P.C., Myers R.H., Feldman R.G., Pollen D., Drachman D., Growdon J., Bruni A., Foncin J-F., Salman D., Frommelt P., Amaducci L., Sorbi S., Piacentini S., Stewart G.D., Hobbs W.J., Conneally P.M., and Gusella J.F., 1987, The

genetic defect causing faimilial Alzheimer's disease maps on chromosome 21. *Science* **235,** 885-890.

Strittmatter W.J., Saunders A.M., Schmechel D., Pericak-Vance M., Enghild J., Salvesen G.S., and Roses A.D., 1993, Apolipoprotein E: high-avidity binding to ß-amyloid and increased frequency of type 4 allele in late-onset familial Alzheimer disease. *Proc. Natl. Acad. Sci. USA* **90,** 1977-1981.

Sussman K.E., Pollard H.B., Leitner J.W., Nesher R., Adler J., and Cerasi E., 1983, Differential control of insulin secretion and somatostatin-receptor recruitment in isolated pancreatic islets. *Biochem J.* **214,** 225-230.

Tam J.P., 1988, Acid deprotection reactions in peptide synthesis. In *Macromolecular sequencing and synthesis: Selecccted methods and applications.* David H. (Ed.), Schlesinger, Alan R. Liss, Inc., New York. pp.153-184.

Tanaka S., Nakamura S., Ueda K., Kameyama M., Shiojiri S., Takahashi Y., Kitaguchi N., and Ito H., 1988, Three types of amyloid protein precursor mRNA in human brain: their differential expression in Alzheimer's disease. *Biochem. Biophys. Res. Commun.* **157,** 472-479.

Tanzi R.E., St. George-Hyslop P.H., Haines J.L., Polinsky R.J., Nee L., Foncin J-F, Neve R.L., McClatchey A.I., Conneally P.M., and Gusella J.F., 1987, The genetic defect in familial Alzheimer's disease is not tightly linked to the amyloid ß-protein gene. *Nature*, **329,** 156-157.

Tanzi R.E., McClatchey A.I., Lamperti E.D., Villa-Komaroff L., Gueslla J.F., and Neve R.L., 1988, Protease inhibitor domain encoded by an amyloid protein precursor mRNA associated with Alzheimer's disease. *Nature*, **331,** 528-530.

Terry R. and Katzman R., 1983, Senile dementia of the Alzheimer type: defining a disease. In *The Neurology of Aging*. Katzman R. and Terry R. (Eds.), Philadelphia: F.A. Davis, pp. 51-84.

Vyas S., Zhao X., Luick T.J., and Duffy L.K., 1992, ß-amyloid peptides, aluminum and albumin. In *Treatment of Dementias*. Meyer E.M., Simpkins J.W., Yamamoto J., and Crews F.T. (Eds.), Plenum Press, New York, pp.503-513.

Waudelen C.V., Zeikus R., and Tsou D., 1989, Cleavage, deprotection and isolation of peptides after Fmoc synthesis. *Chemistry Update*. MilliGen/Biosearch, Division of Millipore.

Weidemann A., Konig G., Bunke D., Fischer P., Salbaum J.M., Masters C.L., and Beyreuther K., 1989, Identification, biogenesis, and localization of precursors of Alzheimer's disease A4 amyloid protein. *Cell* **57,** 115-126.

Whitson J.S., Selkoe D.J., and Cotman C.W., 1989, Amyloid ß-protein enhances the survival of hippocampal neurons *in vitro*. *Science* **243,** 1488-1490.

Whitson J.S., Glabe C.G., Shintani E., Abcar A., and Cotman C.W., 1990, ß-amyloid protein promotes neuritic branching in hippocampal cultures. *Neurosci. Lett.* **110,** 319-324.

Wirak D.O., Bayney R., Ramabhadran T.V., Fracasso R.P., Hart J.T., Hauer P.E., Hsiau P., Pekar S.K., Scangos G.A., Trapp B.D., and Unterbeck A.J., 1991, Deposits of amyloid ß protein in the central nervous system of transgenic mice. *Science* **253,** 323-325.

Yankner B.A., Dawes L.R., Fisher S., Villa-Komaroff L., Oster-Granite M.L., and Neve R.L., 1989, Neurotoxicity of a fragment of the amyloid precursor associated with Alzheimer's disease. *Science* **245,** 417-420.

Yankner B.A., Caceres A., and Duffy L.K., 1990a, Nerve growth factor potentiates the neurotoxicity of ß-amyloid. *Proc. Natl. Acad. Sci. USA* **87,** 9020-9023.

Yankner B.A., Duffy L.K., and Kirschner D.A., 1990b, Neurotrophic and neurotoxic effects of amyloid ß-

protein: reversal by tachykinin neuropeptides. *Science* **250,** 279-282.

Yankner B.A. and Mesulam M.M., 1991, ß-amyloid and the pathogenesis of Alzheimer's disease. *The New Engl. J. Med.* **325,** 1849-1857.

Yankner B.A., 1992, Commentary and perspective on studies of ß-amyloid neurotoxicity. *Neurobiol. Aging* **13,** 615-616.

Zabel B.U., Salbaum J.M., Multhaup G., Masters C.L., Bohl J., and Beyreuther K., 1987, Sublocation of the gene for the precursor of Alzheimer's disease amyloid A4 protein on chromosome21. *Cytogenet. Cell Genet.* **46,** 725-726.

Zhao X, Schoenheit C., and Duffy L.K., 1991a, A heparin-binding protein from neuroblastoma cells: immunological comparison to ß-amyloid precursor protein. *Comp. Biochem. Physiol.* **100A,** 715-718.

Zhao X. and Duffy L.K., 1991b, On the interaction of a synthetic Alzheimer ß-amyloid peptide with NB41A3 cells. *Neurosci. Res. Commun.* **9,** 159-166.

Zhao X., Valantas J.A., Vyas S., and Duffy L.K., 1993, Comparative toxicity of amyloid ß-peptide in neuroblastoma cell lines: effects of albumin and physalaemin. *Comp. Biochem. Physiol.* **106C,** 165-170.

Appendices

Appendix I. Cell Culture Media

Cells *in vivo* exist in and react to a complex set of nutritional, hormonal, and stromal influences. If a cell is to survive or proliferate when removed from an animal and placed in culture, the medium must carry out the functions previously served by the complicated external *in vivo* environment of the cell. The media originally used for the growth of mammalian cells were based on biological fluid such as plasma and embryonic extracts. However, such chemically undefined media suffer from many disadvantages including batch variation and vulnerability to contamination.

Eagle's minimum essential medium (EMEM) is a chemically defined medium which contains a minimum number of components shown to be essential for cell growth. The components of the formulation include a complex mixture of salts, carbohydrates, amino acids, and vitamins. Dulbecco's modified Eagle's medium (DMEM) has higher concentrations of amino acid and vitamins than Eagle's medium as well as additional nonessential amino acids and added ferric

nitrate. Ham's F12 medium is another chemically defined medium with a complex composition including various trace elements (Table I-1).

Most cultured cells, however, will not survive or exhibit optimal phenotypic properties for long periods of time in basal culture medium alone, and require serum supplementation. This reflects additional requirements for growth factors, hormones, transport proteins, and trace elements. One of the most effective serum supplements for cell growth is fetal calf serum because of its high content of embryonic growth factors. Serum is a complex heterogeneous mixtures of proteins, hormones, growth factors, lipids, and other known and unknown factors, whose concentrations could vary greatly depending on the donor and the particular batch used. It could introduce variability in experimental results.

Therefore, the use of chemically defined serum-free media for cultured cells has many advantages. The combination of F12 and DMEM (1:1) has been the basis of the development of some serum-free formulations. Factors most commonly added to

Table I-1. Chemical components of DMEM and F12*

Component (mg/l)	DMEM	F12
Amino acids		
L-Alanine		8.9
L-Arginine	84.0	211.0
L-Asparagine		15.0
L-Aspartic acid		13.3
L-Cysteine	62.6	35.1
L-Glutamic acid		14.7
L-Glutamine**	584.0	146.0
Glycine	30.0	7.5
L-Histidine	42.0	21.0
L-Isoleucine	105.0	3.9
L-Leucine	105.0	13.1
L-Lysine	146.0	36.5
L-Methionine	30.0	4.5
L-Phenylalanine	66.0	5.0
L-Proline		34.5
L-Serine	42.0	10.5
L-Threonine	95.0	11.9
L-Tryptophan	16.0	2.0

Table I-1. Continued

Component (mg/L)	DMEM	F12
L-Tyrosine	103.8	7.8
L-Valine	94.0	11.7
Vitamins		
B-12		1.4
Biotin		0.007
Choline chloride	4.0	14.0
Folic acid	4.0	1.3
Inositol	7.2	18.0
Niacinamide		0.04
Nicotinamide	4.0	
D-Pantothenic acid	4.0	0.5
Pyridoxal	4.0	
Pyridoxine		0.06
Riboflavin	0.4	0.04
Thiamine	4.0	0.3
Inorganic salts		
Calcium chloride	200.0	33.2
Copper sulfate		0.0025
Iron nitrate	0.1	

Table I-1. Continued

Component (mg/L)	DMEM	F12
Iron sulfate		0.83
Magnesium chloride		57.2
Magnesium sulfate	97.7	
Potassium chloride	400.0	223.6
Sodium chloride	6400.0	7599.0
Sodium phosphate	125.0	142.0
Zinc sulfate		0.9
Other		
D-Glucose	4500.0	1802.0
Hypoxanthine		4.8
Linoleic acid		0.084
Lipoic acid		0.2
Putrescine		0.16
Sodium pyruvate		110.0
Thymidine		0.7

* Formulations are from Bottenstein 1992.

** Glutamine is added immediately prior to use.

chemically defined media base are polypeptide hormone insulin, the iron-transport protein transferrin, and the trace element selenium. The other components vary depending on the cell type.

Serum-free formulations have been found suitable for many *in vitro* cell growth studies. A rat neuroblastoma B104 cell has been shown to successfully grown in DMEM/F12 (1:1) with supplement of 5 μg/ml insulin, 5 μg/ml transferrin, 30 nM sodium selenite, and 20 nM progesterone (Bottenstein *et al.*, 1979a; 1979b). In this study for culturing mouse neuroblastoma NB41A3 cells, the commercially available serum-free medium HL-1 was used. Supplied by Ventrex (Ventrex Laboratories, Inc., Portland, ME, USA), HL-1 is a DMEM/F12 basal medium with supplement of insulin, transferrin, testosterone, sodium selenite, and fatty acids. HEPES (N-2-hydroxyethyl piperazine-N'-2-ethanesulfonic acid) is used as buffering system and phenol red is used as a pH indicator in the medium. HL-1 medium contains less than 50 μg/ml total protein and does not contain albumin, serum, or growth factors such as EGF, FGF, PDGF, estrogen, and progesterone. Table I-2 shows the components added in the HL-1 medium.

Table I-2. HL-1 serum-free medium*

Component	Concentrations
Insulin (bovine source)	15 μg/ml
Transferrin (human source)	10 μg/ml
Testosterone	
Ethanolamine	
Sodium Selenite	
Variety of fatty acids	
HEPES	15 mM
Biocarbonate	2.2 g/L
Glucose	6 g/L
Phenol Red	

* From Ventrex technical notes. All other additives are proprietary.

References

Bottenstein J.E., 1992, Environmental influences on cells in culture. In *Practical Cell Culture Techniques*. *Neuromethods*. Boulton A.A., Baker G.B., and Walz A.(Eds.), Humana Press. New Jersey, pp.66-67.

Bottenstein J., Hayashi I., Hutchings S., Masui H., Mather J., McClure D.B., Ohasa S., Rizzino A., Sato G., Serrero G., Wolfe R., and Wu R., 1979a, The growth of cells in serum-free hormone supplemented media. *Methods Enzymol*. **58,** 94-109.

Bottenstein J.E. and Sato G.H., 1979b, Growth of a rat neuroblastoma cell line in serum-free supplemented medium. *Proc. Natl. Acad. Sci. USA* **76,** 514-517.

Bulter M., 1992, In *Cell Culture Labfax*. Butler M. and Dawson M. (Eds.), Bios Scientific Publishers, Academic Press. Chapter 6-7.

Appendix II. Micro BCA Protein Determination

The Micro BCA protein assay is a highly sensitive method for protein determination. When protein is placed in an alkaline condition containing Cu^{2+}, a color complex can form between the peptide bounds of the protein and the copper atoms. This is the well-known Biuret Reaction. When bicinchoninic acid (BCA) is introduced in this system, it greatly increases the sensitivity of the protein assay. This method is also compatible with commonly encountered biochemical reagents, such as 1% Triton X-100, SDS, and sodium phosphate buffer.

II-1. Preparation of Working Reagent.

The Micro BCA Protein Assay Reagent (Pierce, Rockford, IL) is supplied in three separate bottles:

Micro Reagent A (MA) contains sodium carbonate, sodium bicarbonate, and sodium tartrate in 0.2 N NaOH.

Micro Reagent B (MB) contains 4% BCA in water.

Micro Reagent C (MC) contains 4% cupric sulfate, pentahydrate in water.

To prepare the Micro Working Reagent, mix:

2 parts of MC and 48 parts of MB.

Then, add 50 parts of MA.

This Working Reagent is stable for one day at room temperature.

II-2. Standard Protocol of Micro BCA Protein Assay.

A. Prepare a set of protein standards of concentration ranging from 0 to 20 μg per milliliter in the same diluent as in the unknown samples.

B. Pipette 1.0 ml of each standard or unknown protein into the appropriately labeled test tube. For blanks, use 1.0 ml of diluent.

C. Add 1.0 ml Working Reagent to each tube. Mix well.

D. Incubate all tubes at 60^{0}C for 60 minutes.

E. Cool all tubes to room temperature. Measure the absorbance at 562 nm of each tube.

F. Prepare the standard curve by plotting the net absorbance at 562 nm vs. protein concentration. Using this standard curve, determine the protein concentration for each unknown protein sample.

References

Micro BCA Protein Assay Reagent Instruction. Pierce Co., Rockford, IL, U.S.A.

Smith P.K., Krohn R.I., Hermanson G.T., Mallia A.K., Gartner F.H., Provenzano M.D., Fujimoto E.K., Goeke N.M., Olson B.J., and Klenk D.C., 1985, Measurement of protein using bicinchoninic acid. *Anal. Biochem.* **150,** 76-85.

Appendix III. SDS-Polyacrylamide Electrophoresis

III-1. Stocking Solutions

A. 30% Acrylamide/bis

Acrylamide 87.6 g

N'N'-bis-methylene-acrylamide 2.4 g

Make to 300 ml with distilled water. Filter and store at 4^0C in the dark (30 days maximum).

B. 1.5 M Tris-HCl, pH 8.8

Tris base 27.23 g

Add 80 ml distilled water

Adjust to pH 8.8 with 1 N HCl. Make to 150 ml with distilled water and store at 4^0C.

C. 0.5 M Tris-HCl, pH 6.8

Tris base 6 g

Add 60 ml distilled water

Adjust to pH 6.8 with 1 N HCl. Make to 100 ml with distilled water and store at 4^0C.

D. 10% SDS

Dissolve 10 g SDS with gentle stirring and bring to 100 ml with distilled water.

E. SDS-PAGE Sample Buffer

Distilled water	4.0 ml
0.5 M Tris-HCl, pH 6.8	1.0 ml
Glycerol	0.8 ml
10% (w/v) SDS	1.6 ml
2-ß-mercaptoethanol	0.4 ml
0.05% (w/v) bromophenol blue	0.2 ml
Total	8.0 ml

Dilute the sample at least 1:4 with sample buffer, and heat at 95^{0}C for 4 minutes.

F. 5x Electrode (Running) Buffer, pH 8.3

Tris base	9.0 g
Glycine	43.2 g
SDS	3.0 g

Make to 600 ml with distilled water. Store at 4^{0}C.

Dilute 60 ml 5x stock with 240 ml distilled water for one electrophoretic run.

III-2. 9.0% Separating Gel Preparation, pH 8.8

Distilled water	4.85 ml
1.5 M Tris-HCl, pH 8.8	2.5 ml
10% SDS	100 µl
30% Acrylamide/bis	3.0 ml
*10% Ammonium persulfate (fresh daily)	50 µl
**TEMED	5 µl
Total	10 ml

*To make the 10% ammonium persulfate solution, dissolve 100 mg Ammonium Persulfate in one ml distilled water.

**TEMED: N,N,N',N'-Tetramethylethylenediamine.

III-3. 4.0% Stacking Gel Preparation, pH 6.8

Distilled water	6.1 ml
0.5 M Tris-HCl, pH 6.8	2.5 ml
10% (w/v) SDS	100 µl
Acrylamide/bis (30% stock)	1.3 ml

Degas for 15 minutes at room temperature

10% ammonium persulfate (fresh daily)	50 µl
TEMED	10 µl
Total	10 ml

III-4. Running Conditions

The power condition for optimal resolution is 200 volts, constant voltage setting.

III-5. Coomassie Blue Staining of the Gel

Stain the gel for half an hour with 0.1% Coomassie blue R-250 in 40% methanol and 10% acetic acid. Destain the gel with 40% methanol, 10% acetic acid to remove background.

The sensitivity of protein detection is in the microgram range.

Reference

Mini-Protean II Dual Slab Cell Instruction Manual. Bio-Rad Laboratories, Richmond, CA, USA.

Appendix IV. Western Blot Protocol

A. Resolve proteins on SDS-PAGE

B. Blot proteins on Immobilon transfer membrane using a Bio-Rad semi-dry electroblotter. Set power supply at 230 mA. Bloting time is 2 hours.

C. Block non-specific binding sites on the membrane with 5% dry milk in 10 mM phosphate, 150 mM NaCl, 0.05% tween 20, pH 7.2 at 4^{0}C overnight.

D. Wash the membrane 3x10 minutes with 10 mM phosphate, 150 mM NaCl (PBS) containing 0.05% tween 20.

E. Incubate the membrane with primary antibody for 2 hours at room temperature.

   Dilute the antibody against the synthetic ßAPP C-peptide 1:50 with PBS buffer containing 0.05% tween 20 and 3% bovine serum albumin (BSA).

F. Wash the membrane 3x10 minutes with 0.05% tween 20 in PBS.

G. Incubate the membrane with the secondary antibody for 2 hours at room temperature.

Dilute anti-rabbit IgG-peroxidase conjugates 1:500 with PBS containing 0.05% tween 20 and 3% BSA.

H. Wash the membrane 3x10 minutes with 0.05% tween 20 in PBS.

I. Develop a color complex.

To prepare substrate solution, mix:

2.5 mg DAB (3,3'-diaminobenzidine) and 40 μl 3% H_2O_2 in 10 ml PBS.

Incubate the membrane with substrate solution.

Stop the enzyme-substrate reaction by washing the membrane with distilled water.

Reference

Bjerrum O.J. and Heegaard N.H.H. (Eds.), 1988, *CRC handbook of immunoblotting of proteins. Volume I, Technical descriptions*. CRC Press, Inc. Florida.

Appendix V. Ultrastructure Study Protocol

V-1. Cell Culture

Control mouse neuroblastoma NB41A3 cells were cultured in fetal calf serum-free HL-1 medium (Ventrex Laboratories, Inc., Portland, ME, USA). Amyloid ß peptide treated cells were cultured in the medium containing 2 μM ß1-40 peptide. In three days, cells grew into a smooth monolayer in the cell culture flask under light microscope. Floating dead cells were removed by decanting cell culture medium. Cells were then washed with PBS buffer containing 10 mM phosphate and 150 mM NaCl (pH 7.2).

V-2. Sample Preparing Protocol

A. Fixation

Fix cells with Karnovsky's fix (1% paraformaldehyde, 1.25% glutaraldehyde in 0.1 M cacodylate, 5% sucrose pH 7.2) for 2 hours at 4^0C.

Wash cells with 0.1 M cacodylate buffer 3x15 minutes.

Fix cells with 2% O_sO_4 for 1.5 hours at 4^0C.

B. Dehydration

30% ethanol	1x15 minutes
50% ethanol	1x15 minutes
70% ethanol	2x15 minutes
95% ethanol	2x15 minutes
100% ethanol	3x15 minutes
Propylene Oxide	3x15 minutes

C. Infiltration

1:3 Epon 812 : Propylene Oxide	1 hour
1:1 Epon 812 : Propylene Oxide	4 hour
3:1 Epon 812 : Propylene Oxide	overnight

D. Polymerization

To 20 ml Epon 812, add 0.3 ml DMP-30 immediately prior to use. Embed neuroblastoma cells in the Epon 812. Incubate at 58^{0}C for 48 hours. Sectioning.

E. Staining

Stain sections with 7% uranyl acetate in 50% methanol for 10 minutes.

Wash sections with distilled water for 1 minute.

Stain sections with 0.1% lead citrate for 10 minutes.

Wash sections with distilled water for 1 minutes.

Air dry.

Observe under transmission electron microscope.

References

Iron K., 1993, *Technical notes: fixation protocol*.

Newman G.R. and Hobot J.A., 1993, *Resin microscopy and on-section immunocytochemistry*. Springer-Verlag, Berlin.

Appendix VI. Immunocytochemistry Protocol

Mouse neuroblastoma cells were cultured in fetal calf serum-free HL-1 medium and handled as described in Appendix V. To increase the immunosensitivities, cells were fixed in 1% glutaraldehyde only, but not in O_sO_4. Cells were then partially dehydrated and embedded in LR White. The following describes the procedure in detail.

VI-1. Sample Preparing Protocol

A. Fixation

Fix cells with 1% glutaraldehyde in 0.1 M cacodylate, 5% sucrose (pH 7.2) for 1 hours at 4^0C.

Wash cells with 0.1 M cacodylate, 5% sucrose 3x15 minutes.

B. Dehydration

30% ethanol	1x15 minutes
50% ethanol	1x15 minutes
70% ethanol	1x15 minutes
70% ethanol	overnight

C. Infiltration

2:1 LR White : 70% ethanol	1 hour
LR White	1 hour

LR White overnight

D. Polymerization

Embed neuroblastoma cells in LR White. Incubate at 50^{0}C for 24 hours. Sectioning.

VI-2. Immunogold Staining

A. Wash sections with distilled water for 1 minutes.

B. Wash sections with 5% FCS in 10 mM phosphate, 150 mM NaCl, 0.1 M Glycine (PBS-Glycine buffer, pH 7.2) 3x1 minute.

C. Primary antibody incubation. Dilute rabbit anti-ßAP 1:10 with 5% FCS in PBS-Glycine buffer (pH 7.2). Incubate sections with anti-ßAP dilution for 1 hour.

D. Wash sections with 5% FCS in PBS-Glycine buffer (pH 7.2) 3x1 minute.

E. Wash sections with 1% FCS in PBS-Glycine buffer (pH 8.6) 3x1 minute.

F. Secondary antibody incubation. Dilute 15 nm gold conjugated goat anti-rabbit IgG (E-Y Laboratories, Inc., San Mateo, CA, USA) 1:10 with 1% FCS PBS-Glycine buffer (pH 8.6). Incubate sections with secondary antibody for 1 hour.

G. Wash sections with PBS (pH 7.2) 3x1 minute.

H. Wash sections with distilled water 3x1 minute. Air Dry.

I. Stain sections with 7% uranyl acetate in 50% methanol. Wash sections with distilled water for 1 minute.

J. Stain sections with 0.1% lead citrate. Wash sections with distilled water for 1 minute. Air dry.

K. Observe samples under transmission electron microscope.

References

Iron K., 1993, *Technical notes: fixation protocol.*

Iron K., 1993, *Technical notes: immunocytochemistry staining protocol.*

Newman G.R. and Hobot J.A., 1993, *Resin microscopy and on-section immunocytochemistry.* Springer-Verlag, Berlin.